KAPL, Inc.
Knolls Atomic Power Laboratory
Post Office Box 1072 Schenectady, N.Y. 12301-1072
Telephone (518) 395-4000 Facsimile (518) 395-4422

Bechtel Bettis, Inc.
Bettis Atomic Power Laboratory
P. O. Box 79
West Mifflin, PA 15122-0079

LOCKHEED MARTIN

BECHTEL

MDO-723-0046
January 31, 2006

B-MT(SPME)-23

The Manager
Schenectady Naval Reactors Office
United States Department of Energy
Schenectady, New York

The Manager
Pittsburgh Naval Reactors Office
United States Department of Energy
West Mifflin, Pennsylvania

Subject: Space Reflector Materials for a Prometheus Application

References:
(a) KAPL Letter MDO-723-0042, "Reflector and Shield Material Properties for Project Prometheus," dated November 2, 2005.
(b) NRPCT Letter B-SE(RE)-0003/SPP-67410-0013, "Project Prometheus Space Reactor Pre-conceptual Design Report," January 27, 2006.

Enclosures:
(1) Beryllium
(2) Beryllium Oxide
(3) Assessment of Alumina, Spinel and Magnesia as Reflector Materials
(4) Annotated Bibliography

Dear Sir:

This letter provides a summary of the Naval Reactors Prime Contractor Team (NRPCT) evaluation of potential reflector materials for a Prometheus application. Most of the information provided herein, including discussions of candidate materials, was developed in support of a future down-selection to allow focused materials development. The down-selection recommendation was not completed due to Prometheus program restructuring.

Summary:
The two materials studied in depth which appear to have the most promise in a Prometheus reflector application are beryllium (Be) and beryllium oxide (BeO). Three additional materials, magnesium oxide (MgO), alumina (Al_2O_3), and magnesium aluminate spinel ($MgAl_2O_4$) were also recently identified to be of potential interest, and may have promise in a Prometheus application as well, but are expected to be somewhat higher mass than either a Be or BeO based reflector.

Literature review and analysis indicates that material properties for Be are largely known, but there are gaps in the properties of BeO relative to the operating conditions for a Prometheus application. A detailed preconceptual design information document was issued providing material properties for both materials (Reference (a)). Beryllium oxide specimens were planned

to be irradiated in the JOYO Japanese test reactor to partially fill the material property gaps, but more testing in the High Flux Isotope Reactor (HFIR) test reactor at Oak Ridge National Laboratory (ORNL) was expected to be needed. A key issue identified for BeO was obtaining material for irradiation testing with an average grain size of ~5 micrometers, reminiscent of material for which prior irradiation test results were promising. Current commercially available material has an average grain size of ~10 micrometers. The literature indicated that improved irradiation performance could be expected (e.g., reduced irradiation-induced swelling) with the finer grain size material. Confirmation of these results would allow the use of historic irradiated materials test results from the literature, reducing the extent of required testing and therefore the cost of using this material.

Environmental, safety and health (ES&H) concerns associated with manufacturing are significant but manageable for Be and BeO. Although particulate-generating operations (e.g., machining, grinding, etc.) involving Be-bearing materials require significant controls, handling of clean, finished products requires only modest controls. Neither material was initially considered to be viable as a structural material, however, based on improved understanding of its unirradiated properties, Be should be evaluated due to having potentially acceptable structural properties in the unirradiated condition, i. e., during launch, when loads might be most limiting.

All three of the alternative materials are non-hazardous, and thus do not engender the ES&H concerns associated with use of Be or BeO. Aluminum oxide is a widely available ceramic material with well characterized physical properties and well developed processing practices. Although the densest (3.97 g/cm^3 versus Be: 1.85, BeO: 3.01, MgO: 3.58, and $MgAl_2O_4$: 3.60, all theoretical density), and therefore the heaviest, of all the materials considered for this application, its ease of fabrication, mechanical properties, availability and neutronic characteristics warrant its evaluation. Similarly, MgO is widely used in the refractory materials industry and has a large established manufacturing base while being lighter than Al_2O_3. Most of the commercially available MgO products incorporate additives or a second phase to avoid the formation of $Mg(OH)_2$ due to spontaneous reaction with ambient humidity. The hygroscopicity of MgO makes it a more difficult material to work with than Al_2O_3 or $MgAl_2O_4$. Magnesium aluminate spinel, although not as widely available as either Al_2O_3 or MgO, has the advantage of a density almost as low as MgO without being hygroscopic, and shares comparable neutronic performance characteristics in the reflector application.

Background:
Beryllium and BeO have been considered for and used in many nuclear applications, e.g., reflector/moderator, nuclear fusion applications including first wall protective armor, and solid breeding blankets. In a space reactor application, the reflector materials must be able to change the amount of fast neutron leakage when moved, as well as remain physically stable throughout life. Beryllium clearly has the advantage, relative to other candidate materials, in required nuclear properties to efficiently perform the function of a fast neutron reflector, namely, low neutron absorption, high neutron scattering, high atom density and a beneficial (n,2n) multiplication reaction. Beryllium also provides moderation (lowering fast neutron energies), which can be beneficial to reactor design. Commercial use of Be and prior Be research has characterized much of the Prometheus design space for the commercially available grades of Be (Brush Wellman grades S-65 and S-200F). In addition to the beneficial nuclear properties of the Be atom, BeO also provides a higher total atom density and inelastic scattering by oxygen, which increases the neutron moderation.

An important issue associated with BeO and Be manufacturing is ES&H concerns. Beryllium and BeO are hazardous materials causing lung disease and skin irritations in a fraction of the population. Inhaling particulate materials containing Be can cause a serious lung disease called chronic beryllium disease (CBD), and any handling of powders or processing, such as grinding

or machining, that produces fine particulate must be done with strict controls and appropriate personnel protective measures.

Aluminum oxide, MgO, and $MgAl_2O_4$ were also under consideration as reflector materials for the space nuclear power plant (SNPP) due to their wide availability, non-hazardous nature, well established vendor base and neutronic performance comparable to Be and BeO (for given reflector thickness). Although non-moderating, these materials have very similar performance characteristics as reflector materials to the Be based materials in this particular application. However, these materials would have a mass penalty associated with their use, which would need to be closely evaluated in the final reflector material selection. Additionally, these materials, especially MgO, have not been as extensively characterized with regard to irradiation behavior as have Be and BeO. The limited data available for alumina and spinel indicates that performance is probably acceptable, but substantial irradiation testing, and the associated expense, would be a necessary part of evaluation of these materials.

Discussion:
The Prometheus reflector design efforts primarily evaluated sliding reflectors, however drum reflectors were also considered in reactor concept studies. The assessments reported in this letter assume sliding reflectors, however, material findings should be generally applicable to both reactor control approaches. Prometheus reflector neutronic studies indicated that Be, BeO, MgO, Al_2O_3, and $MgAl_2O_4$ provided comparable reactor control for a comparable thickness reflector (Reference (b)). Highly enriched boron carbide ($^{11}B_4C$, 99.99%) was also shown to provide comparable reactor control compared to the other materials. However, due to the high costs associated with isotopic enrichment, material properties of $^{11}B_4C$ were not investigated. Depending on the reflector design, the reflector material may provide structural support (potentially lowering overall system complexity and mass), or may simply be incorporated into a reflector structure (i.e., canned and supported). Of the five materials considered, only Be may have structural properties that could potentially be exploited in a design (Enclosure 1), but this is considered unlikely. Although density is expected to be a key variable, detailed system design trades are needed to select the preferred reflector material. A summary of the candidate reflector materials is as follows.

Beryllium
Unirradiated and irradiated material properties are largely known and discussed in Enclosure 1. Beryllium is the lowest density candidate material (~1.85 g/cm^3) and has a melting point of ~1558 K. It can be considered for structural application, but is known to embrittle under irradiation to relatively low fast fluences (~$7.5x10^{20}$ n/cm^2 E>1 MeV, see Enclosure 1).

Beryllium Oxide
In addition to the external radial reflector, BeO was also evaluated as an axial reflector within the fuel element because of its very high melting point, ~2840 K. Following a detailed literature review and analysis, material property data gaps for these applications were identified (Enclosure 2). Most of the data available was from the 1950's and 1960's and were obtained from different grades of BeO (i.e., impurity content, processing and grain size) than those currently available commercially. The grain size of BeO is reported to strongly affect the irradiation properties (primarily swelling). A contract was placed with Brush Ceramic Products (BCP) to procure BeO specimens for material property testing. A significant part of this effort was to produce material with a nominal grain size of 5 microns as compared to their standard material BW-1000 which displays a nominal grain size of ~10 microns. Following three experimental runs the grain size was reduced to ~7 microns. Results of this contract are discussed in Enclosure 2. Specimens were planned to be tested at various fluences (1.3 – $5.1x10^{21}$ n/cm^2 (E>0.1MeV)) and temperatures (850K and 1050K) in the JOYO test reactor. Irradiation testing of BeO was also planned in the HFIR at ORNL. The focus of these irradiation

tests was to determine irradiation swelling, irradiated thermal conductivity and irradiated compressive strength. Irradiation swelling was identified as a key parameter in determining the viability of BeO as a reflector material (Reference (a)). Details of planned BeO irradiation testing are described in Enclosure 2.

A plan was developed with BCP to safely handle BeO test specimens intended for irradiation testing. This plan, described in Enclosure 2, included loose surface contamination limits, cleaning procedures, Be detection methods and packaging/shipping requirements for BeO test specimens. A key outcome from this planning was assurance that BeO specimens could be handled safely provided no actions were taken that would produce loose BeO particulate (e.g., no grinding, machining, etc.).

Aluminum Oxide

Aluminum oxide unirradiated material properties are well known and presented in Enclosure 3. Aluminum oxide is a well characterized material with a broad vendor base and is obtainable at low cost. It has a high melting point (~2343K), but limited irradiation data is available.

Magnesium Oxide

Magnesium oxide is a thoroughly studied refractory material (T_m ~3123K) with a large unirradiated material properties database. It has an established vendor base but most of the commercially available material needs an additive to prevent the reaction of MgO with atmospheric water. Magnesium oxide does have the lowest density of the non-moderating materials. Irradiated material properties are not well known. Material properties are summarized in Enclosure 3.

Magnesium Aluminate Spinel

Magnesium aluminate spinel is not as widely available commercially as MgO or Al_2O_3, but it is also a well characterized material. It is similarly refractory to MgO and Al_2O_3 with a melting point of ~2408K. Its primary advantage for this application is that it is just slightly heavier than MgO but it is non-hygroscopic. Knowledge of irradiated material properties is limited, and significant irradiation testing would be required. However, the limited irradiation data reported universally indicates that spinel is exceptionally stable in irradiation at elevated temperatures, lending credibility to its inclusion as a candidate for the reflector material. Material properties are described in Enclosure 3.

Enclosures 1 through 3 provide materials information on Be, BeO, and the alternate materials, Al_2O_3, MgO, and $MgAl_2O_4$, respectively. Enclosure 4 provides an annotated bibliography for reflector materials.

Conclusions:

Beryllium and BeO remain the leading candidate materials for a Prometheus reflector application, based primarily on the likelihood that they represent the lowest mass solutions. Recently identified alternate materials, Al_2O_3, MgO, and $MgAl_2O_4$ may be promising, less hazardous alternatives to Be and BeO, but require more evaluation, especially with regard to irradiation behavior. Their use will incur a mass penalty that must be traded off against the ES&H concerns with Be and BeO from both manufacturing and the potential for dispersion during inadvertent spacecraft re-entry. The latter is considered in more detail in Reference (b) and needs to be balanced against the total Be/BeO inventory on the spacecraft. Enriched $^{11}B_4C$ was also identified as a potential reflector material, but its material properties were not studied.

Material properties for Be and BeO were reviewed and are compiled in Enclosures 1 and 2, respectively, and should support future researchers' efforts to begin preconceptual designs of a space reactor reflector. Beryllium material properties are well characterized, but confirmatory testing may be required. However, further testing and probably grain size modification of BeO are still required, especially with regard to irradiation induced swelling, irradiated thermal conductivity and compressive strength. ES&H issues associated with Be containing materials were identified and addressed, including a process to clean BeO specimens and detect loose Be surface contamination. Safety issues were considered to be manageable.

Material properties and general availability of aluminum oxide, magnesium oxide and magnesium aluminate spinel have been compiled and are included in Enclosure 3. These oxides are good candidate materials for this application, but adequate characterization of irradiated material properties would require substantial testing, and the mass penalty associated with their use must be thoroughly evaluated.

Concurrence and Acknowledgement:
The Manager, Space Materials (Simonson), the Manager, Advanced Materials Technology (Hack) and the Manager, Reactor Nuclear Design (Gideon) concur with this letter.

NR Action Requested:
This submittal is for information. No NR action is requested.

Very truly yours,

James Nash, Engineer
Fuel and Shield Technologies
Space Materials, KAPL

B Campbell for L. Stimely per telecon 1/31/06
Laura Stimely, Engineer
Space Plant Materials Engineering
Space Materials, Bettis

B Campbell for V Munne per telecon 1/31/06
Vicente Munne, Senior Engineer
Space Plant Materials Engineering
Space Materials, Bettis

Approved by:

Brian Campbell, Manager
Fuel and Shield Technologies
Space Materials, KAPL

B Campbell for W. Ohlinger per telecon 1/31/06 12:30
Wayne Ohlinger, Manager
Space Plant Materials Engineering
Space Materials, Bettis

Enclosure 1 to MDO-723-0046/B-MT(SPME)-23:

Beryllium

Author:
James Nash

Reviewed by:
Barri Gurau

This Page is Intentionally Left Blank

Beryllium (Be) was considered to be an attractive, viable low mass reflector material. This assessment of Be provides information used in the consideration of Be for use in space nuclear reflector applications. Commercial grades of Be are discussed and work completed by the Naval Reactors Prime Contractor Team (NRPCT) is summarized. A literature review of material properties provides a pre-conceptual design basis for Be. Literature review and analysis indicates that material properties for Be are largely known. Furthermore, based on commercial use of Be in operating conditions similar to a Prometheus type reactor and known material properties, limited confirmatory testing of Be is expected to be required. The NRPCT judges that if temperatures are within Be material limits (not determined at this time), Be is competitive to beryllium oxide (BeO) as a reflector material based on mass, cost and fabricability.

1. Introduction

Beryllium (Be) has been considered for use in nuclear applications since the beginning of the nuclear era. There is a vast experience base with the use of Be in core, e.g., the Advanced Test Reactor (ATR) and the High Flux Isotope Reactor (HFIR) use Be as reflectors. Beryllium possesses many attractive features for use in a space reactor, especially as a reflector or moderator (Reference (a)):

- High neutron scattering cross section (σ_s = 6 b)
- Low thermal neutron absorption cross section (σ_a = 8 mb)
- High (n, 2n) neutron multiplication cross section ($\sigma_{n,2n}$ = 125 mb)
- Low atomic weight (9.012182 g/mol)
- Low density (1.85 g/cm^3)
- High atom density (0.123 atom/barn-cm)

The low thermal neutron cross section of Be minimizes the loss of neutrons while the high neutron scattering cross section minimizes the distance between scattering events (Reference (b)). Additionally, Be has been evaluated for nuclear fusion applications such as first wall protective armor and solid breeding blankets (Reference (c)). Research for use in these applications involved extensive testing of modern grade material (the same grade likely to be used in space reactor applications: S-65 structural grade Be from Brush Wellman). These efforts have largely characterized the unirradiated and irradiated properties of Be.

1.1 Beryllium Grades

Characterization of many different grades of Be is reported in the literature. This includes older Be grades produced in the 1950's, Russian grade Be, and the Be made today in the USA (Brush Wellman). The mechanical properties of Be tend to differ significantly from grade to grade. The main differences between the various grades of Be include the impurity content (primarily beryllium oxide, BeO) as a weight percent and processing method. The NRPCT focused on four grades of high purity Be available from Brush Wellman (Table 1).

Table 1: Brush Wellman Beryllium Grades (References (d) – (h))

Grade	S-65 (d)	S-65H (e)	S-200F (f)	S-200FH (g)
Processing	Vacuum Hot Press (VHP)	Hot Isostatic Press (HIP)	VHP	HIP
Be min wt%	99	99	98.5	98.5
BeO max wt%	1.0	1.0	1.5	1.5
Al max wt%	0.06	0.06	0.1	0.1
C max wt%	0.1	0.1	0.15	0.15
Fe max wt%	0.08	0.08	0.13	0.13
Mg max wt%	0.06	0.06	0.08	0.08
Si max wt%	0.06	0.06	0.06	0.06
% Theoretical Density (min)	99.0	99.7	99.0	99.7
Ave. Grain Size (microns) (h)	8.4	6.6	8.2	7.1

1.2 Impurities

Principle impurities include beryllium oxide (BeO), aluminum (Al), iron (Fe), silicon (Si) and magnesium (Mg). These impurities are usually introduced during the fabrication and processing of the material. At high temperatures BeO particles tend to inhibit grain growth which stabilizes the microstructure and limits creep – similar to dispersion strengthened alloys (Reference (i)). However, at lower temperatures the BeO particles behave as stress concentrators, increasing the chance of local failure (microcracks). Additionally, an increased BeO content significantly decreases the ductility of Be. The decreased ductility becomes more pronounced under irradiation at higher temperatures (Reference (a)).

Aluminum and Fe impurities are also an integral part of Be properties. Excess Al at the grain boundaries (impurities segregate to the boundaries in low melting, eutectic phases) is responsible for minimum ductility values at temperatures above the melting point of Al (923K). In addition, the material begins to fail intergranularly when under stress and above 923K (Reference (i)). It was determined that the upper content limit of Al to prevent intergranular failure was 200 weight ppm (Reference (i)). Iron in the Be will combine with the free Al. Because of this, it is critical to maintain a sufficient Fe content to combine with all free Al, preventing Al segregation to the grain boundaries (Reference (i)).

1.3 Processing and Fabrication

Variations in Be properties also arise from different processing methods used in fabrication such as cold pressing (CP), cold isostatic pressing (CIP), vacuum hot pressing (VHP), hot isostatic pressing (HIP), sintering, extrusion, plasma spraying and casting (Reference (j)). The four Be grades in Table 1 are either VHP or HIP material. VHP Be is fabricated by pressing Be powder in a cylindrical die, applying pressure from top and bottom rams while at an elevated temperature in vacuum. Mechanical properties tend to be more anisotropic with the longitudinal (parallel to pressing direction) properties generally lower than the transverse (perpendicular to pressing direction) properties. VHP Be generally has coarse BeO (0.1 – 0.5 μm) particles with a heterogeneous dispersion located at the Be grain boundaries (Reference (i)). HIP Be is fabricated by pressing Be powder in a sealed can within a

pressure vessel at elevated temperature. Pressure is applied uniformly from all directions by argon (Ar) gas. This results in nearly isotropic mechanical properties and is often used for complex, net shaped parts. HIP Be typically has fine BeO (0.05 – 0.1 µm) particles uniformly dispersed along the Be grain boundaries (Reference (i)). The microstructure of S-65 and S-200F Be is shown in Figure 1 (Reference (k)). Samples were taken from a billet consolidated from impact-ground powder. The polarized light micrographs (Figure 1) show equiaxed grains with particles of BeO. Bright areas are locations where BeO has "pulled-out" during metallographic preparation (Reference (k)).

The grain size of the Be is of some interest. Beryllium follows the Hall-Petch relationship, which states that the strength of the material is proportional to the inverse square root of the grain size. Consequently, smaller grain sizes result in higher strengths (Reference (h)). From Table 1 it is observed that HIP Be generally has a smaller average grain size than VHP Be and accordingly demonstrates higher strength (average VHP yield strength = 290 MPa and HIP yield strength = 354 MPa (Attachment A to Enclosure 2).

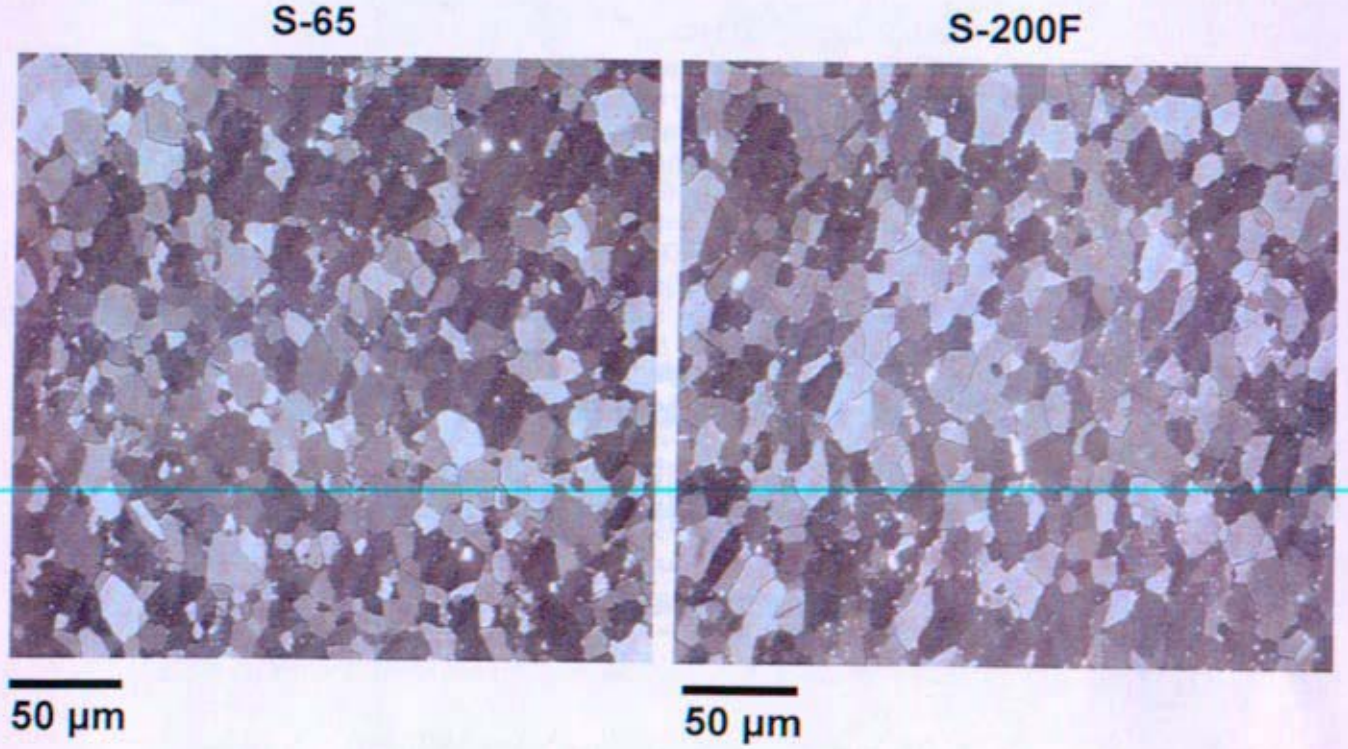

Figure 1: Microstructure of S-65 and S-200F Grade Be (Reference (k))

2. Work Done to Date

Attachment A to Enclosure 2 provides reflector material property information which supported pre-conceptual Prometheus reactor design efforts. Information provided in Attachment A was formally documented in Reference (l) which superceded prior reflector material property information issued in Reference (m)).

Attachment A to Enclosure 2 provides data and discussion of data sources where available, for the following Be properties:

- Composition, density, maximum use temperature, melting temperature
- Thermal conductivity
- Thermal expansion (mean and instantaneous)
- Specific heat
- Modulus of elasticity
- Emissivity
- Yield strength
- Ultimate tensile strength
- Poisson's ratio
- Irradiation swelling

A significant amount of literature review and analysis was performed as part of this effort. To the extent possible, available data, NRPCT-recommended equations and competing equations were provided. However, more work remains to be done, both in terms of literature review and data analysis to identify further data and recommend testing. The NRPCT judged the Attachment A material properties sufficient to support pre-conceptual design studies, but not final design studies.

Since the majority of the data presented in this attachment was obtained from open source literature, the measurement uncertainties in the data are not quantified. For example, it is commonly understood that the measurement uncertainty associated with thermocouples alone can be ± 0.5 to 1.0%. These and other uncertainties are not accounted for specifically in data presented herein. Statistical analysis and review included linear regression and curve-fitting techniques for the raw data, which provides some confidence, but is not a replacement for full understanding of the experiments. Therefore, the robustness of the data is questionable. Since the recommended equations were generated using all available data from the literature, additional data is required to validate these equations and relationships. Key references are included in the Annotated Bibliography in Enclosure 4.

3. Conclusions/Key Findings

- If design conditions (e.g., temperature conditions) allow the use of Be as a reflector material, it would be considered over BeO for the following reasons: potentially lower mass; likely lower cost overall; more simple to design with and fabricate.
- Beryllium has been studied on and off for several decades. Much of the data spans the expected Prometheus design space and is reported for modern grades of Be (S-65 and S-200F).
- Data and correlations are given for physical (density, melting temperature, maximum use temperature), elastic (elastic modulus, Poisson's ratio), thermal (thermal expansion, thermal conductivity, emissivity, specific heat) and mechanical (tensile yield strength, ultimate tensile strength) properties of Be.
- From the material property assessment (Attachment A to Enclosure 2), it was identified that minimal property testing (irradiated and unirradiated) is required for Be. This property assessment provides a preliminary design basis for the use of Be in space nuclear applications. Figure 2 provides a summary of the irradiation data available for Be and the estimated Prometheus operating conditions (fluence and temperature predictions for Prometheus are based on design assumptions that are subject to change based on final reactor design) (References (h) and (n)-(u)).
- Although no testing was proposed, the NRPCT planned to fund Oak Ridge National Laboratory (ORNL) to modify an existing laboratory to carry out thermal and mechanical

property measurements on irradiated space materials, potentially including Be. Attachment 7 to Enclosure 2 of Reference (v) describes the plan for the laboratory.

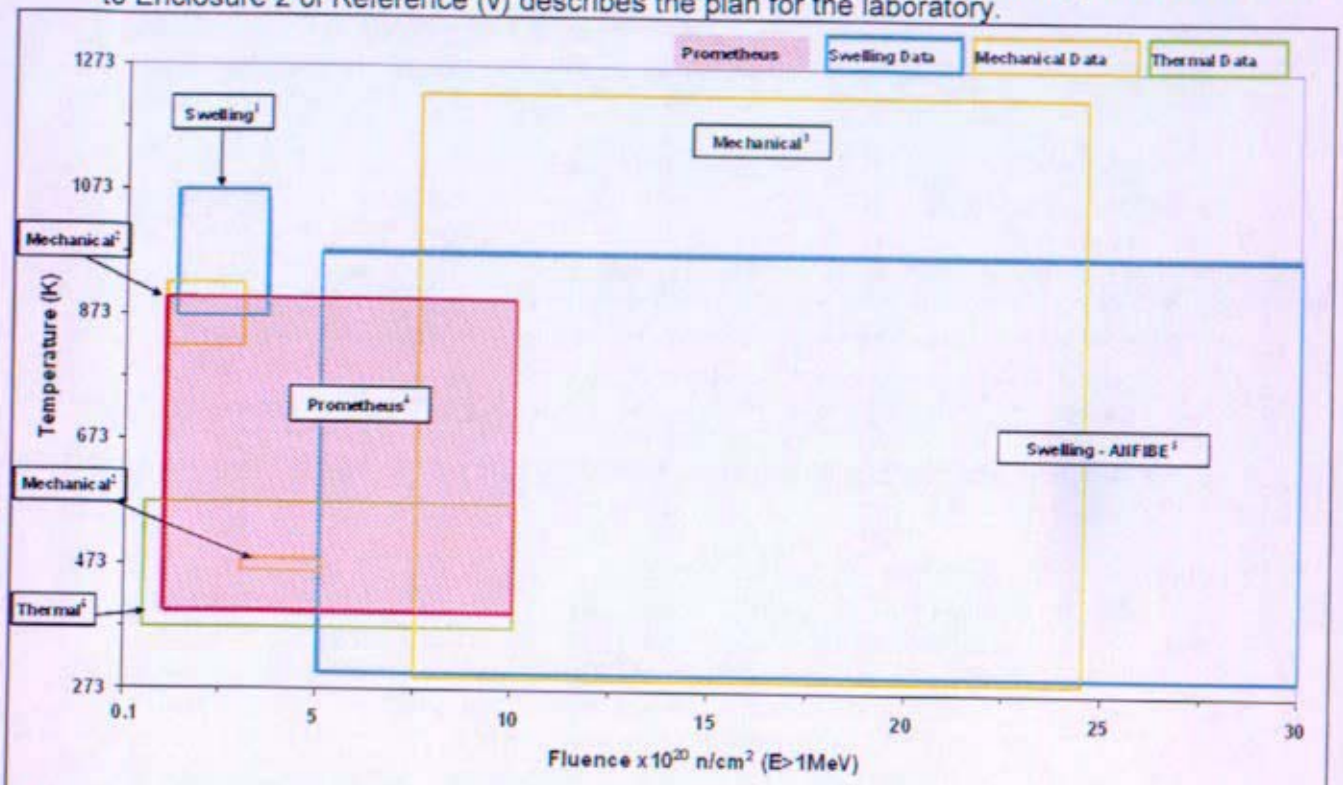

[1]J.M. Beeston (1970)
[2]B.S. Hickman (1966)
[3]B.S. Hickman (1966), M.F. Smith (1985), F. Moons (1996), R. Chaouadi (1997) and S.H. Goods (1997)
[4]KAPL Letter SPP-SRE-0020 (2005)
[5]M. Dalle Donne and F. Scaffidi-Argentina (1994)
[6]L.L. Snead (2004)

Figure 2: Existing Irradiated Be Thermal, Mechanical and Swelling Data with Prometheus Design Space (Reference (h) and (n)-(u))

4. Future Work

As identified in Attachment A to Enclosure 2 and Reference (l), limited confirmatory testing is required to validate correlations for irradiation swelling, thermal conductivity, mechanical properties and elastic properties.

5. References

(a) Dombrowski, D.E., E. Deksnis and M.A. Pick, "Thermomechanical Properties of Beryllium", Brush Wellman Report TR-1182, February 20, 1995.

(b) DOE Fundamentals Handbook, Nuclear Physics and Reactor Theory, DOE-HDBK-1019/1-93, January 1993.

(c) Khomutov, A., V. Barabash, V. Chakin, V. Chernov, D. Davydov, V. Gorokhov, H. Kawamura, B. Kolbasov, I. Kupriyanov, G. Longhurst, F. Scaffidi-Argentina and V. Shestakov, "Beryllium for Fusion Application – Recent Results", *J. Nucl. Mat.* **307-311** (2002) 630-637.

(d) Brush Wellman specification, S-65 Structural Grade Beryllium Block, Rev C, July 1, 1987.

(e) Brush Wellman specification, S-65H Structural Grade Beryllium Block, Rev A, October 5, 1998.

(f) Brush Wellman specification, S-200F Standard Grade Beryllium Block, Rev A, April 1, 1987.

(g) Brush Wellman specification, S-200FH Grade Beryllium, Rev B, December 12, 1990.

(h) Moons, F., L. Sannen, A. Rahn and J. Vande Velde, "Neutron Irradiated Beryllium: Tensile Strength and Swelling", *J. Nucl. Mat.*, **233-237** (1996) 823-827.

(i) Abeln, S.P., M.C. Mataya and R. Field, "Elevated Temperature Stress Strain Behavior of Beryllium Powder Product", Proceedings 2nd IEA International Workshop on Beryllium Technology for Fusion, Jackson Lake Lodge, WY, 6-8 September 1995, 57-105.

(j) Scaffidi-Argentina, F., G.R. Longhurst, V. Shestakov and H. Kawamura, "Beryllium R&D for Fusion Applications", *Fusion Eng. and Design*, **51-52** (2000) 23-41.

(k) Marder, J.M. and R. Batich, "Beryllium", *ASM Handbook, Volume 9, Metals Handbook*, ASM International, Materials Park, OH (1985) 389-391.

(l) KAPL Letter MDO-723-0042, "Reflector and Shield Material Properties for Project Prometheus", dated November 2, 2005.

(m) KAPL Letter SPP-67410-0004, "Space Power Program, Preliminary Reactor Design Basis, Revision 1, for NR Information", dated December 22, 2004.

(n) KAPL Letter SPP-SRE-0020, "Documentation of Fluence Values Given to Space Mechanical Reactor Engineering and Space Materials", dated October 18, 2005.

(o) Beeston, J.M., "Beryllium Metal as a Neutron Moderator and Reflector Material", *Nuclear Eng. and Design*, **14** (1970) 445-474.

(p) Hickman, B.S., "Radiation Effects in Beryllium and Beryllium Oxide", *Studies in Radiation Effects, Series A Physical and Chemical Volume 1*, (1966).

(q) Smith, M.F., R.D. Watson, J.B. Whitley and J.M. McDonald, "Thermomechanical Testing of Beryllium for Limiters in ISX-B and JET", *Fusion Technology*, **8** (1985) 1174-1183.

(r) Chaouadi, R., F. Moons and J.L. Puzzolante. 1997. "Tensile and Fracture Toughness Test Results of Neutron Irradiated Beryllium", Proceedings of the 3rd IEA International Workshop on Beryllium Technology for Fusion, Mito City, Japan, 22-24 October.

(s) Goods, S.H. and D.E. Dombrowski. 1997. "Mechanical Properties of S-65C Grade Beryllium at Elevated Temperatures", Proceedings of the 3rd IEA International Workshop on Beryllium Technology for Fusion, Mito City, Japan, 22-24 October.

(t) Dalle Donne, M., F. Scaffidi-Argentina, C. Ferrero and C. Ronchi, "Modeling of Swelling and Tritium Release in Irradiated Beryllium", *J. Nucl. Mat.*, **212-215** (1994) 954-960.

(u) Snead, L.L., "Low-Temperature Low-Dose Irradiation Effects on Beryllium", *J. Nucl. Mat.*, **326** (2004) 114-124.

(v) KAPL Letter MDO-723-0048, "The Evaluation of Lithium Hydride for Use in a Space Nuclear Reactor Shield, Including a Historical Perspective, for NR Information", dated December 9, 2005.

Enclosure 2 to MDO-723-0046/B-MT(SPME)-23:

Beryllium Oxide

Author:
James Nash

Reviewed by:
Barri Gurau

Beryllium oxide (BeO) was considered to be an attractive reflector for high temperature reflector applications (e.g., axial reflectors within the fuel pins) and possibly low temperature reflector applications (e.g., radial reflectors). This assessment of BeO provides information used in the consideration of BeO for use in space nuclear reflector applications. Commercial grades of BeO are discussed and work completed by the Naval Reactors Prime Contractor Team (NRPCT) is summarized. A literature review of material properties provides a pre-conceptual design basis for BeO. Beryllium oxide is less widely used in nuclear applications than beryllium (Be) and less data is available for modern grades of BeO. Material test recommendations (irradiated and un-irradiated) are provided based on gaps identified in the literature review and predicted operating conditions of Prometheus-type space reactors. Additionally, in an effort to improve irradiation performance of the material, experimental grain size reduction runs were performed on commercially available grades of BeO. The NRPCT had not concluded that BeO was more desirable than Be as a reflector material from either a mass, cost, fabricability or simplicity standpoint. The NRPCT judges that if temperatures are within the Be material limits (not determined at this time), Be is competitive to BeO as a reflector material based on mass, cost and fabricability.

1. Introduction

Most space reactor studies since the 1950's have assumed that beryllium oxide (BeO) would be used in situations where neutron reflection was necessary. Beryllium oxide has very low neutron absorption, high number density, is excellent at moderating fast flux (both due to low mass of Be and the inelastic scattering by oxygen), and has high temperature capability (T_{melt} = 2840K) due to the ceramic nature of BeO. Beryllium oxide actually improves upon the moderating capabilities of Be with a higher neutron scattering cross section and lower absorption cross section at the expense of density ($\rho_{BeO,\ theoretical}$ = 3.01 g/cm^3 vs. $\rho_{Be,\ theoretical}$ = 1.85 g/cm^3). In addition to the moderating capability of BeO, previous nuclear design studies were attracted to the high thermal conductivity of BeO. For example, at room temperature BeO conducts heat as well as aluminum metal.

1.1 Beryllium Oxide Grades

Brush Ceramic Products (BCP), a subsidiary of Brush Wellman, is the primary manufacturer of BeO in the United States. BCP has the capability of pressing and machining BeO in plates, bricks, rods and tubular geometries. Processing methods include dry pressing and isopressing of BeO ceramics. Currently, BCP has two commercial grades of BeO: Thermalox 995 and BW-1000. Table 1 shows that the main difference between the two BeO grades is grain size (References (a) and (b)). As discussed in later sections, the grain size of BeO is of particular importance to irradiation performance and strength of the material. Beryllium oxide is known to undergo anisotropic swelling, which in certain situations has led to macroscopic swelling (1-5%), and microcracking. It was experimentally determined that finer grain size material experiences less irradiation swelling than larger grain size material (Section 2.3).

Despite having more attractive nuclear properties than Be metal, BeO technology remains at about the same level of maturity achieved during the early 1970's. Effort is required to understand both unirradiated and irradiated properties for modern grades of BeO (Thermalox 995 and BW-1000).

Table 1: Material Properties Thermalox 995 vs. BW-1000 (Reference (a) and (b))

Property	Unit	Test Method	Thermalox 995	BW-1000
BeO content	Weight %	Spectrographic by difference	99.5 (min)	99.5 (min)
Nominal Density	g/cm^3 %theoretical	ASTM C-373	2.85 (95%)	2.85 (95%)
Hardness		ASTM E-18	60 min (Rockwell 45N)	60 min (Rockwell 45N)
Grain Size	microns	ASTM E-112	9-25 (15 typical)	9-12 (10 typical)
Flexural Strength	MPa	ASTM F-417	220 (min)	260 (min)
Thermal Conductivity	W/m-K (at T_{room})	Laser Flash	285	275
Mean Coefficient of Thermal Expansion	10^{-6} /°C	ASTM E-228	9.0 (T_{room} – 1273K)	9.0 (T_{room} – 1273K)

2. Work Done to Date

2.1 Brush Ceramic Products Technical Specification

In support of irradiation testing in the JOYO test reactor (Section 2.4), the NRPCT initiated a contract with BCP for test specimen fabrication. Attachment B is the Technical Specification for BeO Test Specimen Fabrication Rev. 12 dated 9/2/05 provided to BCP. In creating this specification, numerous variables were considered including sample fabrication, safety and handling concerns, experimental efforts and documentation.

Test specimen fabrication was the focus of this specification. For the specimen fabrication, decisions were made on processing routes, quality control, use of chamfers and sample identification methods. BCP utilizes multiple processing methods for BeO parts (isopressed and dry pressed are most common). Of these processing routes, isopressed BeO was selected because it provided the finest grain size material available (see Section 2.3 for grain size discussion). Attachment C is the BCP material data sheet for isopressed BeO and includes baseline property information and quality control information (BCP Visual Defect Criteria and Machined Dimensional Tolerances). Chamfers were specified for all BeO test specimens in an attempt to prevent cracking that could lead to inaccurate property test data. Specimen identifications were required for all irradiated test specimens. Based on requirements for irradiation test specimens, laser scribing was identified as the best option for BeO specimens. Sample identifications were to be laser scribed on all BeO specimens as indicated in the Attachment B. A small scale study at BCP was planned to establish the effect of laser scribing on material properties.

Because BeO is a hazardous material, capable of causing lung disease and skin irritation if improperly handled (proper safety and handling procedures are required (Section 2.2)). Special regulations were necessary for all BeO specimens destined for NRPCT facilities due to these health concerns. BCP, as well as other DOE facilities investigated (Y-12 and Los Alamos National Laboratory), have taken extensive measures to minimize these hazards including

protective equipment, engineered ventilation controls, air showers, training and administrative controls. A post machining process was developed with BCP to remove any post-fabrication loose particles, involving cleaning and bake out of the specimens. Swipe testing was proposed to evaluate if loose BeO contamination was present (and quantify the amount) on the specimens prior to shipment and special shipping and packaging requirements were established to prevent the generation of loose powder in transit.

Small scale research efforts were included in the specification. These include grain size reduction runs (Section 2.3) and material property testing (Section 2.6). As discussed in Section 2.3, grain size has a strong effect on the irradiated properties of BeO. This research effort was an attempt to reduce the grain size of standard BW-1000 material from 10 μm to 5 μm (nominally). Material property testing of BeO specimens was proposed to establish unirradiated properties of standard BW-1000 material and the new experimentally developed BeO with a reduced grain size (referred to as BW-1000K). Material properties were tested over a range of temperatures and included thermal expansion, specific heat, thermal diffusivity, density and compressive strength testing.

The specification for BeO test specimen fabrication also included detailed requirements for documentation. BCP was to provide manufacturing process documentation and material reports on BW-1000 and BW-1000K material. Manufacturing process documentation included chemical analysis, starting grain size, processing parameters, sintering protocol and machining instructions.

2.2 Cleaning Procedure for BeO Specimens

Inhaling particulate containing beryllium may cause a serious lung disease called chronic beryllium disease (CBD) in some individuals. Additionally, the International Agency for Research on Cancer (IARC) lists Be as a group 1 known human carcinogen (Reference (c)). As previously mentioned, BCP and other DOE facilities have taken extensive measures to control this hazard. To avoid potential health hazards at NRPCT facilities special cleaning, handling and packaging requirements were established for all BeO specimens prior to shipment. Loose BeO particulate is of greatest concern from a health and safety standpoint, therefore all processes generating powder (e.g. machining, grinding etc.) were completed by BCP at the BCP facility.

Current OSHA, DOE and KAPL airborne and surface control limits for Be work areas are summarized in Table 2 (References (d) and (e)). Based on these guidelines, the NRPCT planned to establish a surface contamination limit of 0.25 μg/100cm^2 for all BeO specimens (half of the KAPL administrative control level). A detailed cleaning procedure was established at BCP to ensure BeO particulate free specimens. Figure 1 shows this procedure and more details can be found in Reference (f). It should be noted that the cleaning process outlined below could introduce chemical contamination, which requires verification that there is no adverse affects on material performance. Figure 1 also shows that following cleaning a selected number of specimens will be swipe tested to verify specimens are below the proposed limit. Wet swipe testing of BeO specimens is a destructive test. Therefore, a statistically determined number of "sister" samples (samples cleaned and prepared identically to the final delivered samples) would be destructively tested to verify that the entire batch of cleaned specimens were free of loose BeO. BCP uses a wet benzylkonium chloride wipe to detect loose BeO. Benzylkonium chloride wipes are analyzed using the inductively coupled plasma (ICP) method with a detection limit of 0.2 μg of Be. Other surface swipe testing methods with similar detection limits were examined for use at NRPCT facilities (ChemTest® Be Swipes).

Table 2: Airborne and Surface Contamination Limits for Be

Airborne Limits	
2 $\mu g/m^3$	OSHA limit (d)
0.2 $\mu g/m^3$	DOE limit (e) BCP limit
Surface Limits	
0.2 $\mu g/100cm^2$	DOE release criteria (e)
0.25 $\mu g/100cm^2$	Proposed NRPCT control level (f)
0.5 $\mu g/100cm^2$	KAPL administrative control level
3.0 $\mu g/100cm^2$	DOE "housekeeping" limit (e)

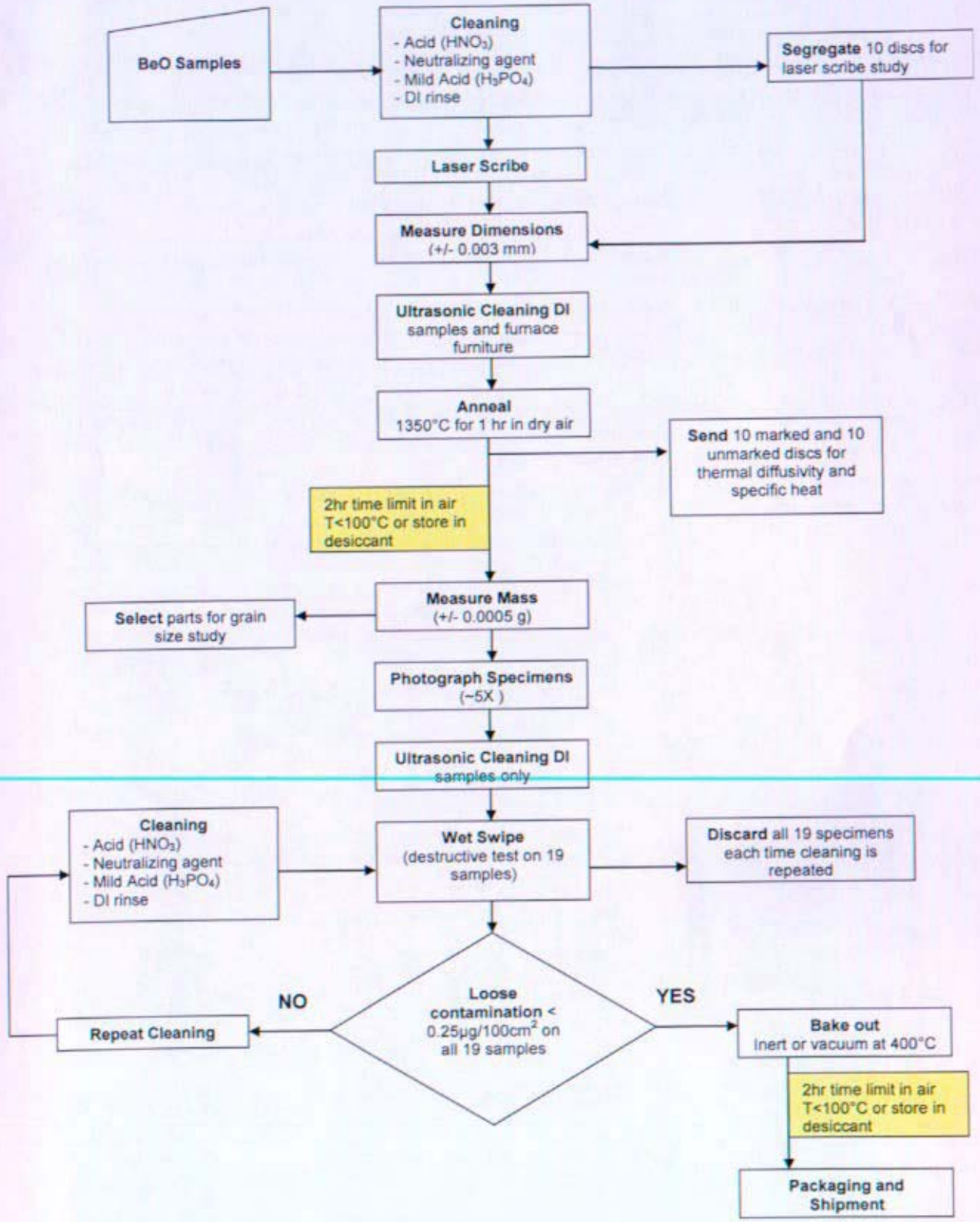

Figure 1: Post Machining Process for BeO Specimens at BCP

2.3 Grain Size Reduction Runs

Grain size of BeO is an important factor in irradiation performance of the material. Historical data indicates that finer grain size material swells less than larger grain size material (Reference (g)). Much of the data used for swelling correlations was obtained from fine grain size (nominally 5 µm) BeO specimens. In an effort to utilize historical data and minimize irradiation swelling, experimental efforts were taken to reduce the grain size of the BW-1000 material from 10 µm to 5 µm (nominal grain size). It should be noted that other variables may influence swelling (e.g. sintering aid composition and processing). Although this was acknowledged, it was not considered in detail early in the project and should be considered in future studies.

Beryllium oxide has a wurtzite crystal structure as shown in Figure 2 (Reference (h)). The anisotropy of the wurtzite crystal structure results in degradation of material properties during irradiation and promotes swelling. As shown in Figure 3, during low temperature irradiation (348 – 373K) the crystal structure expands nearly 30 times greater in the c direction than in the a direction (Reference (g)). This mismatch strains the crystal structure and can lead to swelling (>5%), microcracking and possibly disintegration of the BeO material. At higher temperatures (>1273K) the anisotropic crystal expansion is less and swelling occurs based on other mechanisms (Reference (i)). In some cases at low temperatures, severe microcracking and disintegration of BeO specimens was observed by Keilholtz for larger grain size material (>20 µm) (Reference (j)). Finer grain size BeO was observed to crack less and not disintegrate.

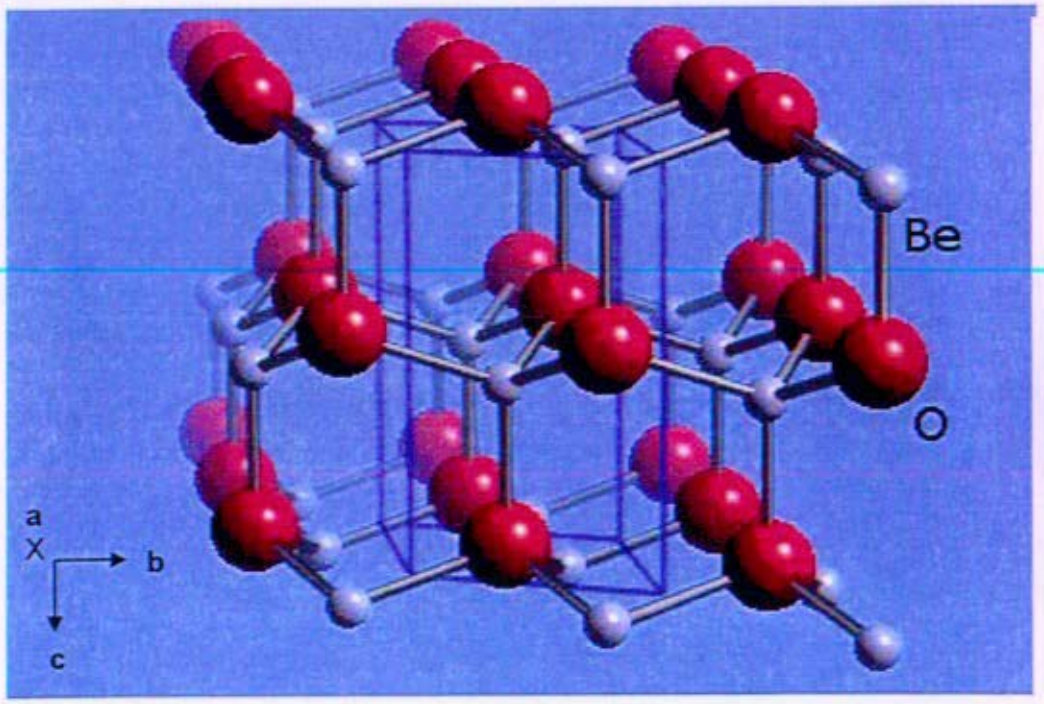

Figure 2: BeO Crystal Structure (Reference (h))

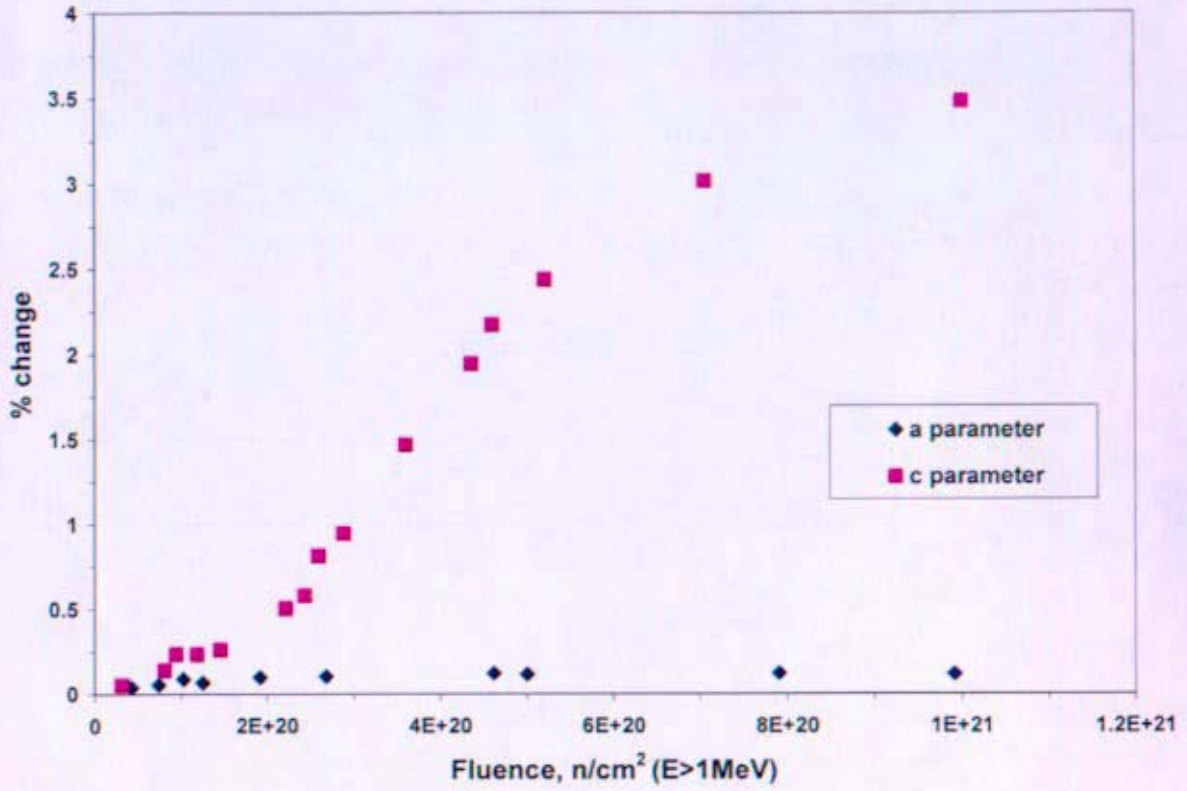

Figure 3: Lattice Parameter Change of BeO irradiated at 348 – 373K (Reference (g))

The Technical Specification for BeO Test Specimen Fabrication (Attachment B) instructed BCP to perform 3 sequential, experimental runs in an attempt to reduce the grain size of the BW-1000 material to 5 μm (referred to as BW-1000K material). With oversight, BCP performed the following 3 experimental runs in sequence:

i. BW-1000K-1 – Altered sintering profile from 1798K for ~5 hrs to 1723K for 1 hr.
ii. BW-1000K-2 – Reduced starting BeO average particle size from 0.5 – 0.6 μm to 0.25 μm and fired with sintering profile determined in Run 1 (1723K for 1 hr).
iii. BW-1000K-3 – Based on results of the first two runs the sintering temperature was reduced to 1698K for 1 hr.

Table 3 provides a summary of the grain size reduction experiments. Further details on the results of the experimental runs are included in Attachment D.

Table 3: Summary of Grain Size Reduction Runs

	BW-1000	Run 1	Run 2	Run 3
Ave. Grain Size	10 μm	9 μm	9 μm	7 μm
Density (%theoretical)	2.89 g/cm^3 (96%)	2.87 g/cm^3 (95%)	2.87 g/cm^3 (95%)	2.86 g/cm^3 (95%)
Ave. BeO Particle Size	0.5 – 0.6 μm	0.5 – 0.6 μm	0.25 μm	0.5 – 0.6 μm
Sintering Time	~5 hrs	1 hr	1 hr	1 hr
Sintering Temperature	1798K	1723K	1723K	1698K

2.4 JOYO Test Matrix for BeO Irradiation Testing

Beryllium oxide has been studied on and off for several decades, however much of the Prometheus design space remains uncharacterized and most of the testing was on different grades and purity of BeO that are no longer commercially available. This is significant since the irradiated material performance of BeO (specifically swelling) has been shown to be sensitive to grain size, compositions and processing techniques. The NRPCT planned to test a modern grade of BeO in the JOYO test reactor.

Details of the proposed JOYO irradiation test are described in References (k) and (l). Materials selected for irradiation testing in JOYO included Ni-based superalloys, refractory metal alloys, silicon carbide (SiC) and BeO. The arrangement consisted of 2 irradiation rigs. One rig was planned to complete a single 60 day cycle and the second would complete two cycles for a 120 day exposure. Each rig was designed to accommodate 30 capsules stacked in tiers with 5 tiers per compartment. The tiers were organized such that Tier 3 was at the core centerline, with Tiers 2 and 1 stacked in order below and Tiers 4 and 5 above. Such an arrangement would allow specimens to be exposed to varying fluences and temperatures by positioning the specimen capsule appropriately.

The planned location for irradiating BeO material in JOYO was a non-instrumented materials irradiation rig inserted in the reflector region. The peak fast neutron flux (E>0.1 MeV) in the core reflector region is approximately 1.9×10^{15} n/cm^2-s with sodium coolant temperatures in the range of 623 – 773K. The typical capsule size for the irradiation rig was 20mm inside diameter by 91mm inside height. Beryllium oxide samples selected for irradiation testing in JOYO consisted of discs and cylinders. Beryllium oxide discs were for thermal diffusivity testing and swelling measurements while cylinders were for compression testing and swelling measurements. References (m) and (n) are the drawings for the BeO disc and cylinder specimens respectively and are included in the Technical Specification for BeO Test Specimen Fabrication (Attachment B).

The capsule layout in both Rigs A and B is shown schematically in Figure 4. Capsules were arranged vertically to indicate tier (elevation) and horizontally to indicate compartment (radial positioning within the tier). An enlarged schematic view of the capsules containing BeO specimens is shown in Figure 5. This schematic does not show sample holders and dividers for all specimens which prevent the BeO specimens from contacting other specimens in the shared capsule. Beryllium oxide specimens (yellow specimens in schematic) are located in Tier 1 and Tier 5 of both Rig A (120 day) and Rig B (60 day).

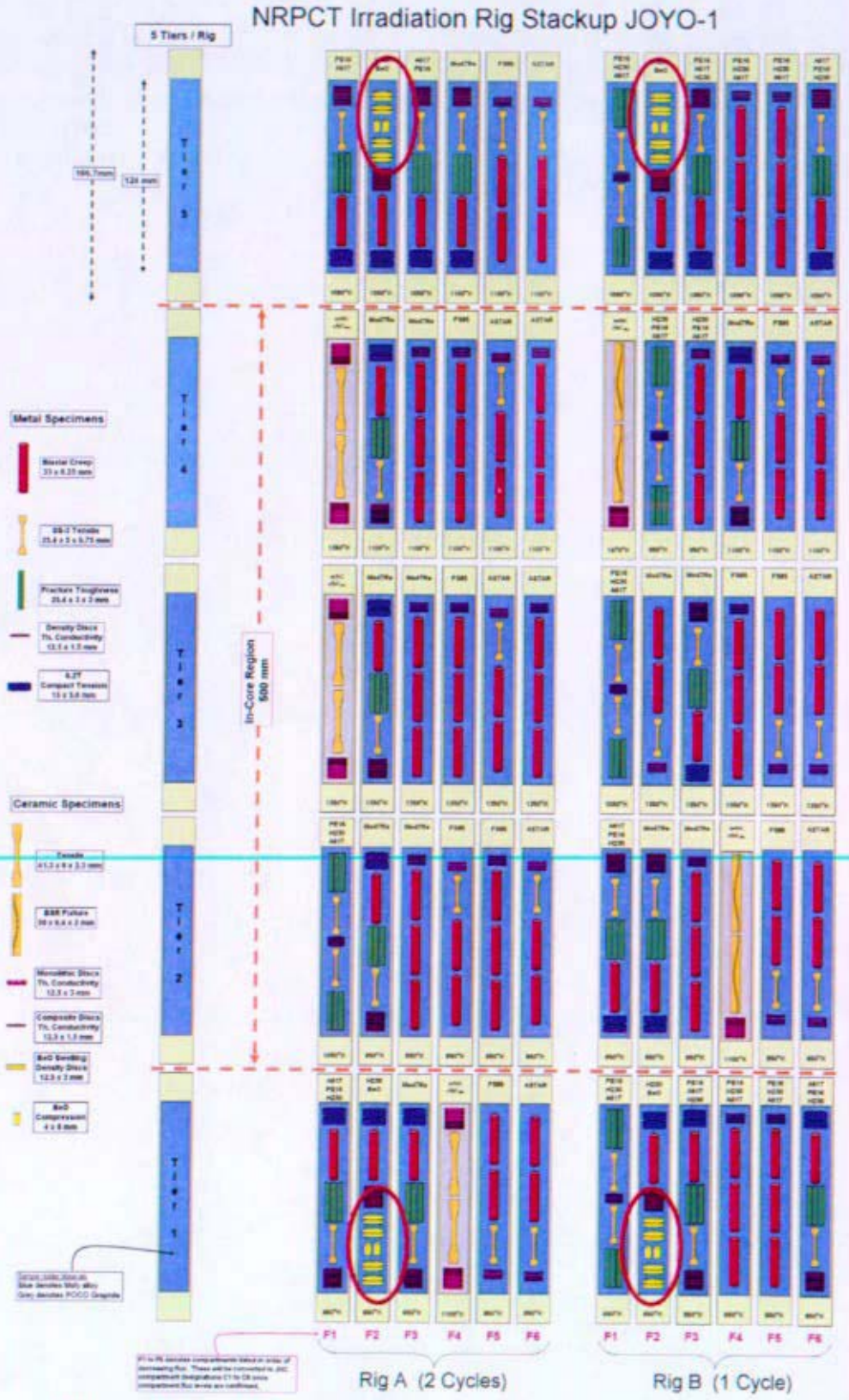

Figure 4: Irradiation Rig Stackup for JOYO (Reference (k))

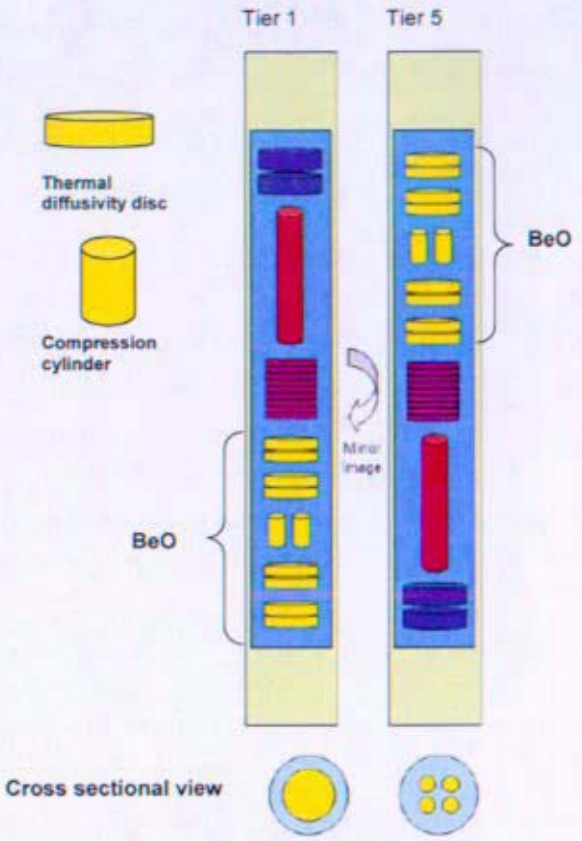

Figure 5: Enlarged View of Irradiation Capsules with BeO Specimens (Reference (k))

The test matrix for the planned irradiation testing of BeO specimens in the JOYO test reactor is given in Table 4. All samples planned for testing had the same grain size (9 – 12 μm), percent theoretical density (96%TD) and fabrication method (isopressed BW-1000K). The Japan Nuclear Cycle Development Institute (JNC) indicated in the March 2005 visit that excessive amounts of materials which could reflect back moderated neutrons (thereby causing local power peaking in adjacent fuel rigs) could generate additional approval requirements. As such, the volume of materials with low atomic number elements (SiC and BeO) were kept as low as possible without sacrificing test objectives.

Table 4: JOYO Test Matrix for BeO Specimens

Location	Cycle	Density and Thermal Diffusivity Disks	Compression Cylinders	Irradiation Temperature	Nominal Testing Fluence (n/cm^2) (E>0.1 MeV)
Tier 1 Rig B	60 days	8	4	850 K	$1.3 - 2.2 \times 10^{21}$
Tier 5 Rig B	60 days	8	4	1050 K	$1.3 - 2.6 \times 10^{21}$
Tier 1 Rig A	120 days	8	4	850 K	$2.6 - 4.5 \times 10^{21}$
Tier 5 Rig A	120 days	8	4	1050 K	$2.7 - 5.1 \times 10^{21}$

Using the correlation for irradiation swelling of BeO provided in (Attachment A), the predicted swelling of the JOYO BeO specimens is shown in Figure 6. The predicted swelling for the Prometheus radial reflector is also shown in this figure. (Note: Prometheus predictions are based on design estimates given in References (o) and (p) which are subject to change based on final design parameters.) These curves were used to predict the swelling at different conditions to allow for proper irradiation capsule design. As noted in Attachment A, no swelling data has been identified in literature greater than 6%. Therefore, the predictions of > 6% swelling in Figure 6 are suspect, but can not be ruled out at this time. Prior testing did not provide sufficient room for BeO samples to swell, resulting in numerous stuck and destroyed specimens (References (g) and (p)). Table 5 highlights some of the differences in the data used for the correlations (References (g) and (r)), JOYO test range and Prometheus reflector operating range. Figure 7 shows the range of existing data, the expected Prometheus reflector operating range and the planned JOYO test range (References (g), (o), (s) and (t)).

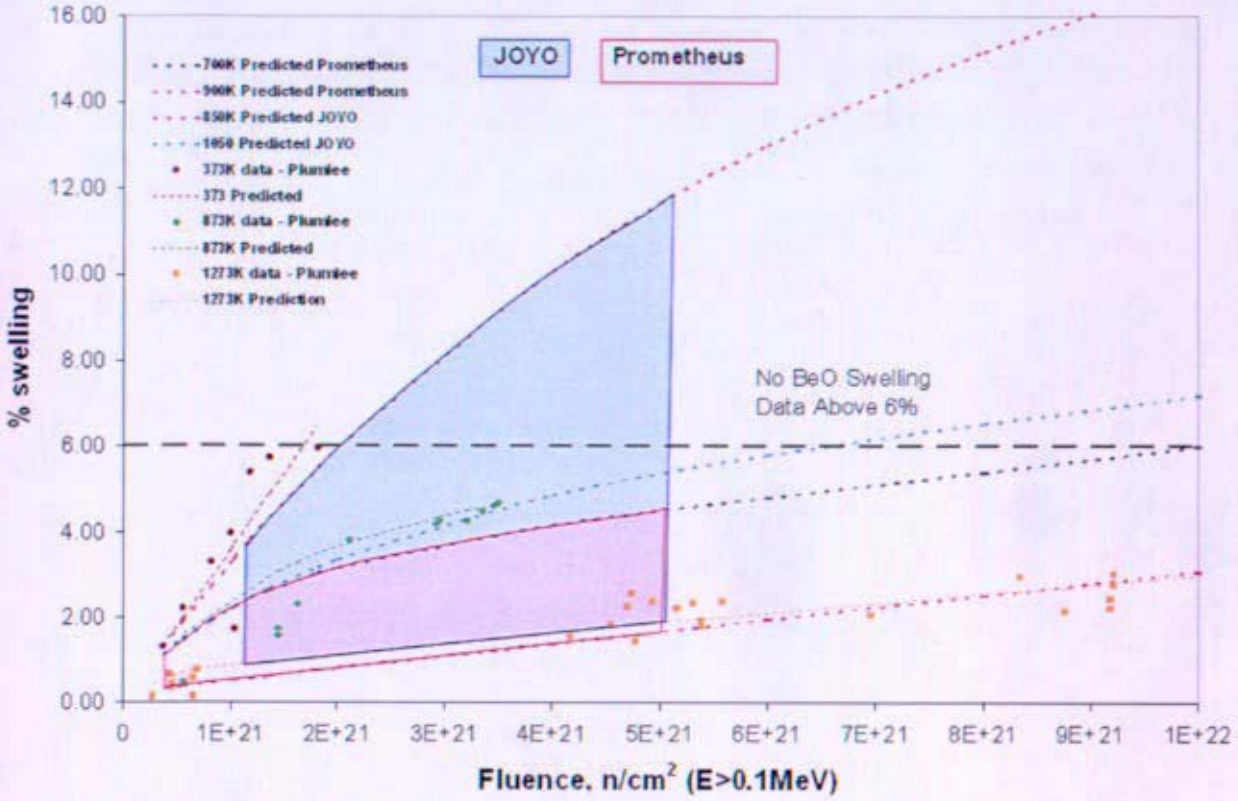

Figure 6: Irradiation Swelling Data of BeO (Reference (g)) and Predicted Swelling of Irradiated BeO in JOYO and Prometheus

Table 5: Existing BeO Irradiation Data, JOYO Test Space and Prometheus Design Space

Test	Flux (n/cm^2-s) (E>0.1MeV)	Fluence (n/cm^2) (E>0.1MeV)	Temperature	Grain Size
Plumlee correlations	2.2 – 2.7 x10^{14}	0.26 – 11 x10^{21}	373K, 873K and 1273K	~ 5 μm
JOYO	5 x10^{14}	1.3 – 5.1 x10^{21}	850K and 1050K	Not yet determined (standard Brush material is 9-12 μm)
Prometheus*	1 x10^{13}	radial: 5 x10^{21} axial: 10x10^{21} (max)	radial: 900K axial: 1250K (max)	Not yet determined (standard Brush material is 9-12 μm)

*Flux, fluence and temperatures predictions for Prometheus are based on design assumptions that are subject to change based on final reactor design (References (o) and (p)).

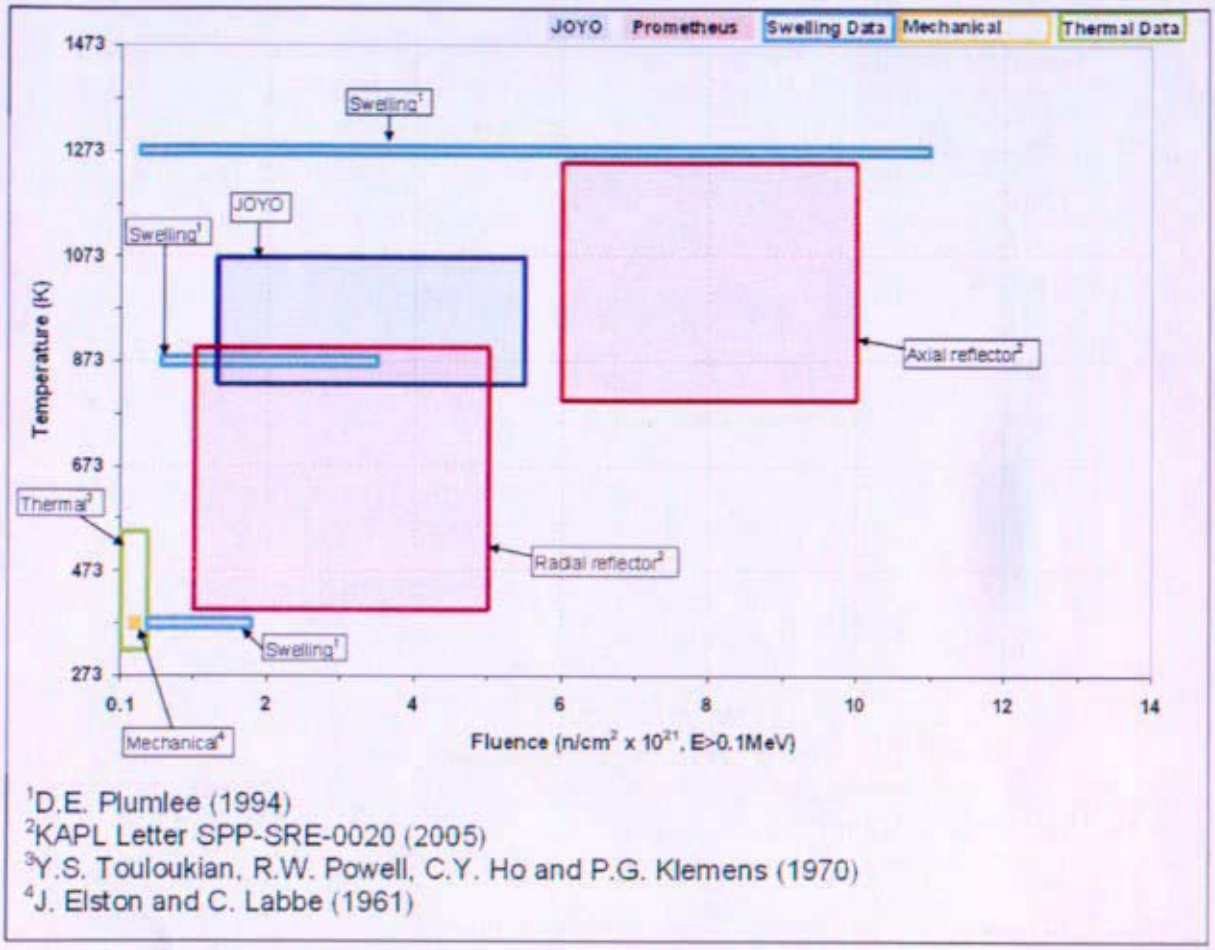

[1]D.E. Plumlee (1994)
[2]KAPL Letter SPP-SRE-0020 (2005)
[3]Y.S. Touloukian, R.W. Powell, C.Y. Ho and P.G. Klemens (1970)
[4]J. Elston and C. Labbe (1961)

Figure 7: Existing Irradiated BeO Thermal, Mechanical and Swelling Data with Prometheus Design Space and JOYO Test Space (References (g), (o), (s) and (t))

2.5 Reflector Material Properties for a Prometheus Reactor

Attachment A provides reflector material property information which supported pre-conceptual Prometheus reactor design efforts. Information provided in Attachment A was formally documented in Reference (i). Beryllium oxide property information replaced the original design basis for preliminary reactor studies (Reference (u)). Reference (u) provided a set of assumptions and information used for early reactor sizing studies enabling various reactor concepts to be evaluated and compared on a common basis.

Attachment A provides data and discussion of data sources where available, for the following BeO properties:

- Composition, density, maximum use temperature, melting temperature
- Thermal conductivity
- Thermal expansion (mean and instantaneous)
- Specific heat
- Modulus of elasticity

- Emissivity
- Yield strength
- Ultimate tensile strength
- Poisson's ratio
- Irradiation swelling

A significant amount of literature review and analysis was performed as part of this effort. To the extent possible, available data, NRPCT-recommended equations and competing equations were provided. However, more work remains to be done, both in terms of literature review to identify further data, and potentially testing to verify the data. Key references are included in the Annotated Bibliography in Enclosure 4.

Since the majority of the data presented in this attachment was obtained from open source literature, the measurement uncertainties in the data are not quantified. For example, it is commonly understood that the measurement uncertainty associated with thermocouples alone can be ± 0.5 to 1.0%. These and other uncertainties are not accounted for specifically in data presented herein. Statistical analysis and review included linear regression and curve-fitting techniques for the raw data, which provides some confidence, but is not a replacement for full understanding of the experiments. Therefore, the robustness of the data is questionable. Since the recommended equations were generated using all available data from the literature, additional data is required to validate these equations and relationships.

This review identified gaps in data, which necessitated testing. As discussed in Section 2.4, BeO specimens were selected for irradiation testing in JOYO. For reflector applications, the most uncertain BeO irradiated properties include thermal conductivity, swelling and compressive strength. These properties were the focus of the planned irradiation testing in JOYO (Section 2.4) and potentially in the High Flux Isotope Reactor (HFIR) at Oak Ridge National Lab (ORNL) (Section 3.1).

2.6 Brush Ceramic Products (BCP) Material Property Report

Unirradiated material property testing of BW-1000 material was performed by BCP (Attachment E). Properties tested included density, specific heat, thermal diffusivity, thermal expansion and compressive strength. With the exception of compressive strength, these properties were tested over the temperature range T_{room} to 1250K. Compression testing was performed at T_{room}, 650K, 850K, 1050K and 1250K. All testing was originally planned to be complimentary to the JOYO irradiation test. Following the restructuring of the project, it was determined that baseline properties for BW-1000 BeO material would be useful to future space nuclear programs. Test specimens were fabricated from isopressed BW-1000 material with a nominal grain size of 10 µm. Specimens were machined out of larger BeO pieces representative of the material expected for use in Prometheus reflector applications.

Material property testing conducted by BCP was compared to the literature review conducted by the NRPCT on BeO (Reference (i)). Density, specific heat and thermal conductivity results were consistent with literature. Thermal conductivity was calculated using thermal diffusivity, density and specific heat data. Thermal expansion measurements were slightly lower than reported for previous grades of BeO in the literature. No meaningful data was obtained from the compression testing due to test complications. More study is required to understand

compression testing and the compressive strength of BeO. Data and summaries of results are presented in Attachment E.

3. Future Work

3.1 HFIR Irradiation Testing of BeO

3.1.1 Historical Data Assessment

Estimated maximum fluence and temperature of the radial reflector is $5x10^{21}$ n/cm^2 (E>0.1 MeV) and 900K (References (o) and (p)). These estimates would be subject to change based upon the reactor and fuel selected for final design, as well as the reflector configuration (e.g., sliders versus drums). Estimated maximum fluence and temperature of the axial fuel pin reflectors is $10x10^{21}$ n/cm^2 (E>0.1 MeV) and 1250K (Reference (o)). Similarly, these estimates would be subject to change based upon the reactor and fuel selected for final design.

3.1.2 HFIR Irradiation Test Plan

Key properties which require irradiation testing to determine the viability of BeO as a reflector material are swelling, thermal conductivity and compressive strength. Some confirmatory testing of other material properties may also be required to fully characterize and qualify modern grades of BeO for use in a nuclear reactor (e.g. thermal expansion, specific heat and elastic modulus). As shown in Figure 7, much of the design space for the Prometheus reflectors is uncharacterized and the planned JOYO testing would only partially fill in the design space. The JOYO test matrix (Table 4) also shows the limited amount of irradiated data to be obtained from the JOYO test (i.e. 4 compression samples per experimental condition). Further testing of BeO was considered in the High Flux Isotope Reactor (HFIR) at Oak Ridge National Laboratory (ORNL). The purpose of this testing was to gain a better understanding of irradiated thermal and mechanical properties over the Prometheus design space. This testing would also compare the effects on BeO of a thermal reactor (HFIR) with a fast reactor (JOYO). (Transmutation effects of Be in a thermal reactor may result in additional helium (^{3}He) and contribute to irradiation swelling of BeO, not accounted for in the correlations presented in Attachment A.)

Swelling was identified as a critical property required in determining the viability of BeO use in reflector applications. Table 6 identifies material properties which require testing, the relative rank of importance (to support design efforts) and the type of data required (irradiated vs. unirradiated and confirmatory vs. full characterization). Swelling (microcracking) influences thermal and mechanical properties. Other properties (specific heat, CTE, elastic modulus and Poisson's ratio) would be required for final design but are not considered critical in selecting BeO as a reflector material. Many of the unirradiated properties of BW-1000 BeO were tested by Brush Ceramics (Attachment E).

Table 6: BeO Material Properties and Required Testing

Property	Status of Data	Data Required	Ranking
Irradiation Swelling	Critical property required to determine viability of BeO use as reflector material	Irradiated	1
Thermal Conductivity	Need full understanding of irradiation effects and confirmatory testing of unirradiated values	Irradiated Un-irradiated	2
Compressive Strength	For canning purposes, irradiated data is required (dependent on amount of swelling)	Irradiated Un-irradiated	2
Specific Heat	Verify no changes due to irradiation and characterize modern grade BeO	Irradiated Un-irradiated	3
CTE	Verify no changes due to irradiation and characterize modern grade BeO	Irradiated Un-irradiated	3
Elastic Modulus	Verify no changes due to irradiation and characterize modern grade BeO	Irradiated Un-irradiated	4
Poisson's Ratio	Verify no changes due to irradiation and characterize modern grade BeO	Irradiated Un-irradiated	4
Tensile Strength	BeO will not be a structural material	X	X
Hardness	BeO will not be a structural material	X	X
Flexural Strength	BeO will not be a structural material	X	X
Fracture Toughness	BeO will not be a structural material	X	X

There are many independent variables which affect irradiated material properties of BeO. Table 7 summarizes these variables and their expected effect on irradiation swelling. The key variables are temperature, fluence and grain size. The effect of flux and neutron spectrum (fast vs. thermal) on BeO swelling is also uncertain. Based on the discussion in Attachment A it would be expected that more swelling (e.g., microcracking) would be expected at higher fluxes. Correlations reported by Plumlee (Reference (g)) predict that swelling will increase as flux increases (recall narrow experimental flux range $1 - 3 \times 10^{14}$ n/cm^2-s). However, Keilholtz (Reference (j)), reported little dependence on flux at temperatures ≤ 1373K (flux range of $0.9 - 2.4 \times 10^{14}$ n/cm^2-s). More investigation is required to determine the effect of flux on swelling. Theoretical density (%TD) of BeO does impact swelling at T≥ 1173K. Reducing the %TD reduces irradiation swelling of BeO by accommodating helium bubble formation at elevated temperatures. However, the neutronic advantages of BeO are diminished with less dense material (i.e. higher fast leakage). Due to the effect of grain size on swelling (Reference (g)), it is expected that the processing method (isopressed, extruded, dry pressed) producing the finest grain size material will be selected, however, other factors will need to be considered, e.g., cost.

Table 7: Variables Affecting Swelling of BeO

Variable	Expected Effect on Swelling of BeO
Temperature	Swelling decreases as temperature increases
Fluence	Swelling increases as fluence increases
Flux	Not yet determined if swelling increases as flux increases or if there is no affect of flux on swelling of BeO
Grain Size	Swelling increases as grain size increases
% Theoretical Density	Swelling decreases as %TD decreases at T≥1173K
Processing	Processing which produces the finest grain size material will be selected
Composition	Sintering aids and impurities may affect irradiation performance of the material

Screening experiments would assist in better defining a final BeO test matrix. The screening experiments would most likely focus on the effect of flux on BeO swelling and the overall variability in the test data (mechanical and thermal). As previously discussed, the effect of flux on irradiation swelling of BeO has not been determined. Additionally, due to limited data over a narrow range of fluxes and conflicting reports in the literature, small scale studies with a limited number of BeO specimens at varying fluxes could be performed at constant temperatures and fluence levels. Results from this screening experiment could eliminate an independent variable in the experimental design. Because of limited data for current grades of BeO, there is little understanding of the variability associated with thermal and mechanical testing. A screening experiment could assess the variability of the proposed testing. Un-irradiated specimens could be thermally aged and tested at temperatures, representative of expected irradiation time at temperature (primarily thermal conductivity and compressive strength). Results from this screening experiment would allow for proper experimental design including the number of test specimens required at each experimental condition for both thermal and mechanical testing. Experimental variability is shown in the property data from BCP in Attachment E.

NRPCT planned irradiation testing of BeO in HFIR is outlined in Table 8. Independent variables include temperature, fluence, flux and grain size. Specimens planned for HFIR irradiation testing were expected to be similar to JOYO specimens (Figure 5). Post irradiation examination (PIE) of the irradiated BeO specimens was planned to include thermal diffusivity testing (ASTM E-1461-01), compression testing (ASTM C-773-88), density measurements (ASTM C-373-88) and dimensional measurements. Thermal diffusivity disks were planned to be used to determine thermal conductivity and swelling. Compression cylinders would be used to determine compressive strength and swelling. The NRPCT planned to fund Oak Ridge National Laboratory (ORNL) to modify an existing laboratory to carry out thermophysical property measurement on irradiated space materials, including BeO (Reference (v)).

Table 8: Proposed Irradiation Testing of BeO in HFIR

Variable	Range
Temperature (K)	350 – 1300K
Fluence (n/cm^2 E>0.1 MeV)	0.5 – 10.5 $x10^{21}$
Grain size (μm)	5-7 (BW-1000K) 9-12 (BW-1000) 15-20 (Thermalox 995)
Flux ($x10^{14}$ n/cm^2-s)	TBD based on screening experiment

Using the correlation for irradiation swelling of BeO summarized in Reference (i) and Attachment A, the predicted swelling of irradiated BeO HFIR specimens is shown in Figure 8. The predicted swelling for the Prometheus radial reflector and JOYO irradiation test is also shown in this figure. As noted in Attachment A, no swelling data has been identified in the literature greater than 6%. Therefore, the predictions of > 6% swelling in Figure 8 are suspect, but can not be ruled out at this time. Table 9 highlights some of the differences in the data used for the correlations (Reference (g) and (r)), HFIR test conditions, JOYO test conditions and Prometheus reflector operating conditions. Figure 9 shows the range of existing data, the expected Prometheus reflector range, the planned JOYO test range and the planned HFIR test range (References (g), (o), (s) and (t)).

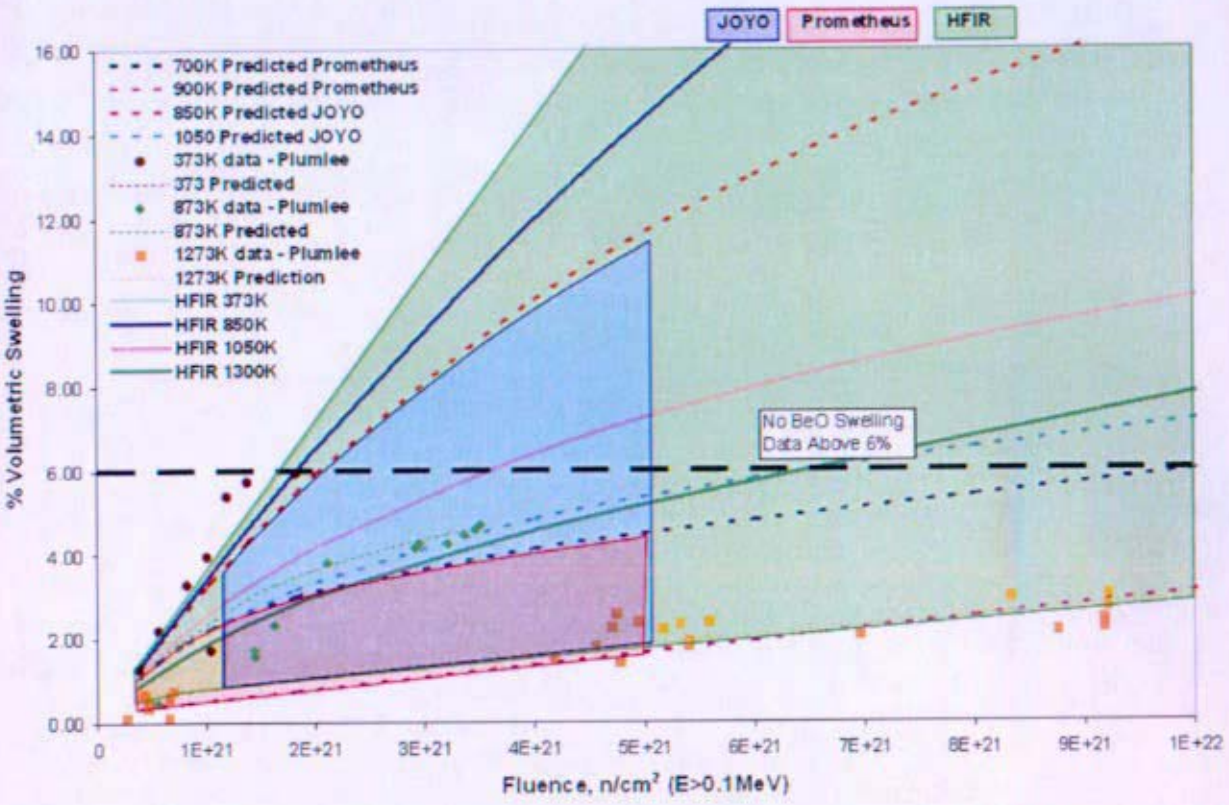

Figure 8: Irradiation Swelling Data of BeO (Reference (g)) and Predicted Swelling of Irradiated BeO in HFIR, JOYO and Prometheus

Table 9: Existing BeO Irradiation Data, HFIR Test Space, JOYO Test Space and Prometheus Design Space

Test	Flux (n/cm²-s) (E>0.1MeV)	Fluence (n/cm²) (E>0.1MeV)	Temperature	Grain Size
Plumlee correlations	$2.2 - 2.7 \times 10^{14}$	$0.26 - 11 \times 10^{21}$	373K, 873K and 1273K	~ 5 μm
JOYO	5×10^{14}	$1.3 - 5.1 \times 10^{21}$	850K and 1050K	Not yet determined (standard Brush material is 9-12 μm)
Prometheus*	1×10^{13}	radial: 5×10^{21} axial: 10×10^{21} (max)	radial: 900K axial: 1250K (max)	Not yet determined (standard Brush material is 9-12 μm)
HFIR	9×10^{14} (max)	$0.1 - 12 \times 10^{21}$	373K, 650K, 850K, 950K, 1050K, 1150K and 1300K	5-7 μm (BW-1000K) 9-12 μm (BW-1000) 15-20 μm (Thermalox 995)

*Flux, fluence and temperatures predictions for Prometheus are based on design assumptions that are subject to change based on final reactor design (Reference (o) and (p)).

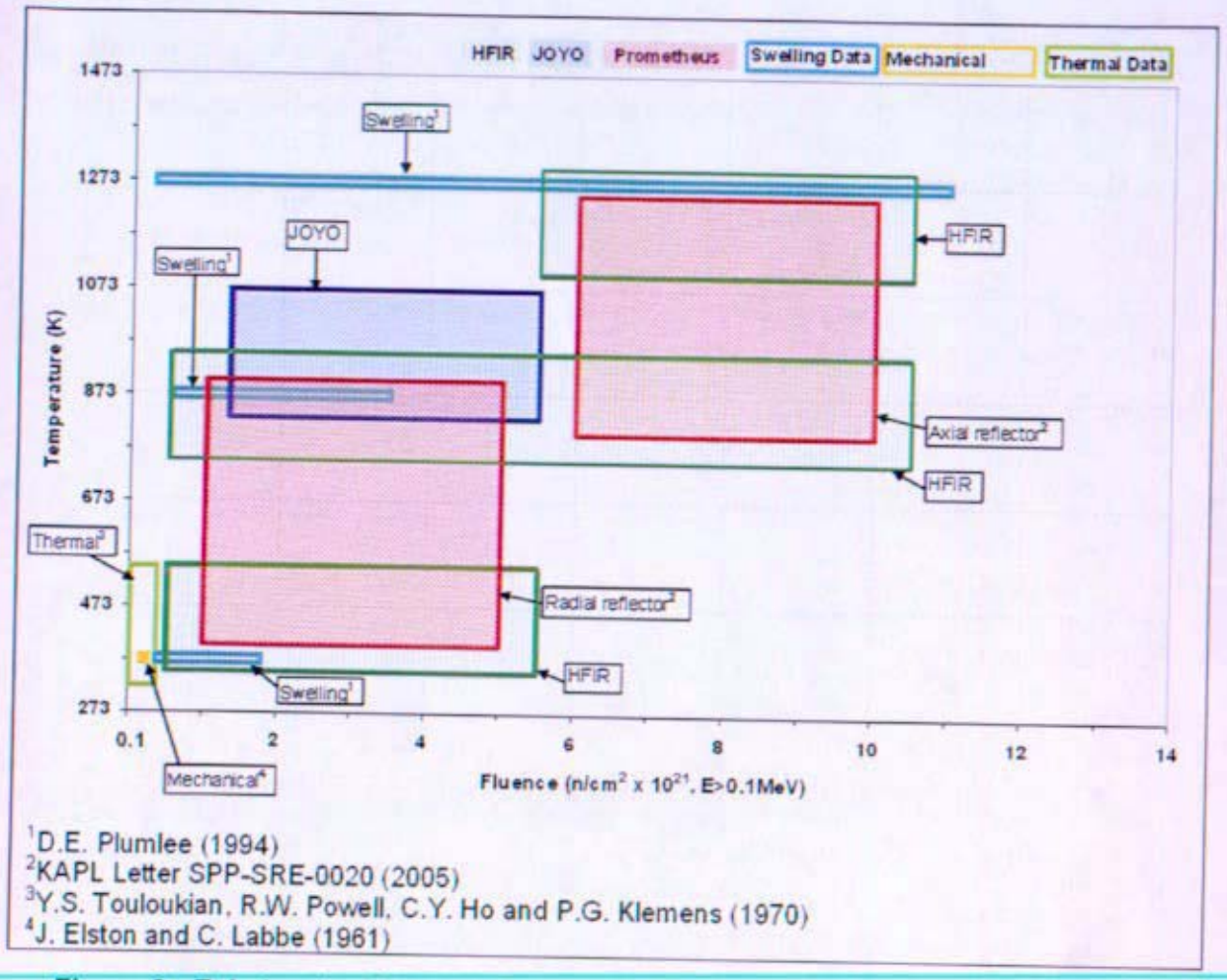

[1]D.E. Plumlee (1994)
[2]KAPL Letter SPP-SRE-0020 (2005)
[3]Y.S. Touloukian, R.W. Powell, C.Y. Ho and P.G. Klemens (1970)
[4]J. Elston and C. Labbe (1961)

Figure 9: Existing Irradiated BeO Thermal, Mechanical and Swelling Data with Prometheus Design Space, JOYO Test Space and HFIR Test Space (References (g), (o), (s) and (t))

4. Conclusions/Key Findings

Beryllium oxide is likely a viable reflector material for a Prometheus application, however some further testing and development is required.

- At the time of program restructuring, fabrication of BeO components larger than 1"x1"x8" with the required grain size requires development.
- Controls are required to handle BeO. However, if dust/loose particle generation processes (i.e. machining and grinding) are avoided, the controls are readily achievable.
- Beryllium oxide grain size is an important factor in the irradiation performance of the material. A very limited experimental effort reduced the grain size of standard BCP BW-1000 BeO material from 10 – 12 μm to 7 μm nominally. The goal of this effort was to reduce the grain size to 5 μm to overlap with prior materials testing, but this was not achieved. The NRPCT judges that with further study the grain size could potentially be reduced to 5 μm.
- Limited data and correlations are given for physical (density, melting temperature, maximum use temperature), elastic (elastic modulus, Poisson's ratio), thermal (thermal

expansion, thermal conductivity, emissivity, specific heat) and mechanical (compressive strength) properties of BeO. From the material property assessment (Attachment A), it was identified that irradiated and unirradiated material property testing is required for BeO. Irradiation swelling was identified as necessary in determining the viability of BeO as a reflector material. Material property testing was conducted at Brush Ceramic Products on un-irradiated BW-1000 BeO material.

- If design conditions (e.g., temperature conditions) allow the use of Be as a reflector material, it would be considered over BeO for the following reasons: potentially lower mass; likely lower cost overall; more simple to design with and fabricate.
- Beryllium oxide would be a leading candidate for high temperature reflector applications (e.g., axial reflectors) due to the neutronic and thermal properties of the material.

5. References

(a) Brush Ceramic Products, Product Guide, Isopressed Ceramics CDI-20, Rev. E (2001).
(b) Brush Ceramic Products, Product Guide, Dry Pressed Ceramics As-Fired or Machined CDDP-10, Rev. F (2001).
(c) World Health Organization, International Agency for Research on Cancer, "Beryllium, Cadmium, Mercury, and Exposures in the Glass Manufacturing Industry", IARC Monographs on the Evaluation of Carcinogenic Risks to Humans V58, August 22, 1997.
(d) OSHA 29 CFR 1910.1000, "Air Contaminants", May 1971.
(e) DOE 10 CFR Part 850, "Chronic Beryllium Disease Prevention Program; Final Rule", December 1999.
(f) KAPL Letter SM-7232-0004, "Discuss Cleaning, Handling and Packaging Procedures at BCP to Ensure Delivery of BeO Specimens with a Surface Contamination Level Below NRPCT Limits", dated September 27, 2005.
(g) Plumlee, D.E., "BeO Performance Lessons Learned" Martin Marietta Report DOE/SF/16006-T1216 (1994).
(h) Winter, M. *Webelements*. 2005. Keyword: Beryllium Oxide Crystal Structure. http://www.webelements.com
(i) KAPL Letter MDO-723-0042, "Reflector and Shield Material Properties for Project Prometheus", dated November 2, 2005.
(j) Keilholtz, G.W., J.E. Lee Jr. And R.E. Moore, "Irradiation Damage to Sintered Beryllium Oxide as a Function of Fast-Neutron Dose and Flux at 110, 650 and 1100°C", *Nuclear Science and Engineering*, **26** (1966) 329-338.
(k) NRPCT Letter MDO-723-0021/B-MT(SRME)-21, "Request for Technical and Funding Approval of the Test Matrix and Associated Changes for the JOYO-1 Irradiation Test of Structural Materials in the JOYO Experimental Fast Reactor to Support Space Reactor Development", dated April 18, 2005.
(l) NRPCT Letter MDO-723-0044/B-MT(SRME)-52, "JOYO-1 Irradiation Test Campaign, For NR Information", dated January 31, 2006.
(m) KAPL Drawing SK216C9453, "Sample, Thermal Diffusivity Disc, JOYO", dated October 26, 2005.
(n) KAPL Drawing SK216C9454, "Sample, Compression Cylinder, JOYO", dated October 26, 2005.
(o) KAPL Letter SPP-SRE-0020, "Documentation of Fluence Values Given to Space Mechanical Reactor Engineering and Space Materials", dated October 18, 2005.
(p) NRPCT Letter SPP-67410-0013/B-SE(RE)-0003, "Project Prometheus Space Reactor Pre-conceptual Design Report," January 27, 2006.

(q) Paxton, D.M., "Irradiation and Examination of Beryllium Oxide Pellets from the SP-100 Special Purpose Materials Test", WHC-SP-1007 (1993).

(r) Collins, C.G., "Radiation Effects in BeO", *J. Nucl. Mat.*, **14** (1964) 69-86.

(s) Elston, J. and C. Labbe, "Effect of the Thermal Treatments and the Irradiation by neutrons on the Physical and Mechanical Properties of Beryllium Oxide Under Load", *J. Nucl. Mat.*, **4** (1961) 143-164.

(t) Touloukian, Y.S., R.W. Powell, C.Y. Ho and P.G. Klemens, Thermophysical Properties of Matter Vol. 2 (1970) 123.

(u) KAPL Letter SPP-67410-0004, "Space Power Program, Preliminary Reactor Design Basis, Revision 1, for NR Information", dated December 22, 2004.

(v) KAPL Letter MDO-723-0048, "The Evaluation of Lithium Hydride for Use in a Space Nuclear Reactor Shield, Including a Historical Perspective, for NR Information", dated December 9, 2005.

Attachment A to Enclosure 2 to MDO-723-0046/B-MT(SPME)-23:

Reflector Material Properties for Project Prometheus

Author:
James Nash

Reviewed by:
Barri Gurau

1. Introduction

Selection of potential reflector materials for a space reactor includes consideration of factors such as mass, neutronics, thermal, mechanical and radiation stability. Historically, beryllium (Be) and beryllium oxide (BeO) have been considered for space reactor designs as reflector materials due to low mass and excellent neutronic properties. The NRPCT did not plan to use either Be or BeO without supporting structural materials (e.g., canning).

1.1 Beryllium (Be)

Beryllium has been considered for use in nuclear applications since the beginning of the nuclear era. There is a vast experience base with use of Be in core, e.g., the Advanced Test Reactor (ATR) and the High Flux Isotope Reactor (HFIR) have used Be as reflectors for years. Beryllium possesses many attractive features for use in a space reactor:

- High neutron scattering cross section
- Low thermal neutron absorption cross section
- High (n, 2n) neutron multiplication cross section
- Low atomic weight
- High melting point (T_{melt} = 1558K)

Additionally, Be has been evaluated for nuclear fusion applications such as first wall protective armor and solid breeding blankets. Research for use in these applications involved testing of modern grades of Be representative of the material likely to be used in space reactor applications (S-65 grade Be from Brush Wellman). These efforts have largely characterized the unirradiated and irradiated properties of Be.

1.2 Beryllium Oxide (BeO)

Most space reactor studies since the 1950's have assumed that BeO would be used in situations where reflection was necessary. In addition to the attributes listed above for Be, BeO has a higher Be number density, is better at moderating fast flux (both due to the higher Be number density and the inelastic scattering by oxygen), and has high temperature capability (T_{melt} = 2840K). However, BeO is denser than Be (~3.01 vs. 1.85 g/cm^3 (theoretical)). For space applications, a design trade off of reflecting performance versus mass is required.

Despite having more attractive nuclear properties for reflection than Be metal, BeO technology and material property database remains at about the same level of maturity achieved during the early 1970's. Effort is required to understand both unirradiated and irradiated properties for modern grades of BeO (Thermalox 995 and BW-1000 material available from Brush Ceramic Products Attachment C).

1.3 Explanation of Attachment

This attachment provides reflector material property information to support pre-conceptual Project Prometheus reactor design efforts (Reference (a)). The information provided herein supersedes the applicable portions of Revision 1 to the Space Power Program Preliminary Reactor Design Basis (Reference (b)). Reference (b) provided a set of assumptions and information used for early reactor sizing studies enabling various reactor concepts to be

evaluated and compared on a common basis. These sizing studies and comparisons were used to support the recommendation of a gas cooled reactor.

This attachment provides the available information together with a discussion of data sources. The following properties are examined:

- Composition, density, maximum use temperature, melting temperature
- Thermal conductivity
- Thermal expansion (mean and instantaneous)
- Specific heat
- Modulus of elasticity
- Emissivity
- Yield strength
- Ultimate tensile strength
- Poisson's ratio
- Irradiation swelling

A significant amount of literature review and analysis was performed as part of this effort. To the extent possible, the underlying phenomenon was explained, as well as providing available data, a recommended equation, and competing equations. However, more work remains to be done, both in terms of literature review and data analysis to identify further data.

Since the majority of the data presented in this attachment was obtained from open source literature, the measurement uncertainties in the data are not quantified. For example, it is commonly understood that the measurement uncertainty associated with thermocouples alone can be ± 0.5 to 1.0%. These and other uncertainties are not accounted for specifically in the data presented. Statistical analysis and review included linear regression and curve-fitting techniques for the raw data, which provides some confidence, but is not a replacement for full understanding of the experiments. Therefore, the robustness of the data is unknown. Since the recommended equations were generated using all available data from the literature, future data is required to validate these equations and relationships.

All data was plotted with Microsoft Excel and/or JMP, statistical analysis software (SAS Institute). JMP was used to fit data using the least squares method. Residual plots were examined to determine the quality of the regression data fit. In some analyses Cook's D statistics were used to examine the influence of individual data points on the least squares model (Reference (c)). Where applicable, 95% prediction intervals were determined which specify the confidence on a single future value. However, these confidence intervals do not account for uncertainty associated with the individual measurements.

2. Beryllium (Be)

Many different industrial grades of Be are available (Brush Wellman, Elmore, OH). Data for the structural grades of Be (S-65, S-65H, S-200F and S-200FH) are most commonly reported in the literature. The main differences between the various grades are impurity levels (particularly the BeO content) and processing/fabrication method. S-65 and S-200F grade Be are vacuum hot pressed (VHP) materials while S-65H and S-200FH grade Be are hot isostatically pressed (HIP) materials. The S-65 and S-65H material has a maximum BeO content of 1% while the S-200

and S-200FH material has a maximum BeO content of 1.5%. Further information on the effect of processing and impurities in Be can be found in Reference (d) and (e). Generally, Be is not recommended as a structural material for radiation environments due to loss of ductility at relatively low fluences (References (f) and (g)). Ductility and elongation are not presented herein, but could be studied based on design requirements.

2.1 Beryllium (Be) Properties

2.2 Composition

Table 1 gives the composition of S-65 structural grade beryllium from Reference (h) (Brush Wellman).

Table 1: S-65 Beryllium Composition (Brush Wellman)

Element (max unless otherwise stated)	wt%
Be (min %)	99
BeO	1.0
Al	0.06
C	0.10
Fe	0.08
Mg	0.06
Si	0.06
Other metallic impurities	0.04

2.3 Melting Temperature and Maximum Use Temperature

The melting temperature of beryllium is (Reference (i)):

$$T_{melt} = 1558 \pm 10\ K$$

For structural application in a radiation environment, the maximum use temperature is 823K. Above 873K embrittlement and reduction in strength are limiting factors (Section 2.9 and 2.11).

2.4 Density

From Scaffidi-Argentina (Reference (d)) for all grades of Be, the room temperature (293K) theoretical density is 1.85 g/cm^3. The following curve is recommended for the temperature range 293K ≤ T ≤ 1500K.

$$\rho = 1.823 - 6.933x10^{-5} \cdot (T - 273) - 1.514x10^{-8} \cdot (T - 273)^2$$

where

ρ = density, g/cm^3
T = temperature, K

Dombroski (Reference (e)) includes a data table of the variation in density of S-65 grade beryllium (Brush Wellman) with temperature (Table 2). Figure 1 shows some slight variation (+/- 0.02) is observed at higher temperatures because the equation was fit to data from industrially available Be grades and the tabular data is only for S-65 grade Be, shown in Figure 1.

For the density of Be, the equation given by Scaffidi-Argentina (Reference (d)) is recommended.

Table 2: Density Data for Be

	Scaffidi-Argentina (2000)	S-65 Dombrowski (1995)
T (K)	Density (g/cc)	Density (g/cc)
324	1.819	1.82
412	1.813	1.814
456	1.810	1.811
515	1.805	1.806
564	1.802	1.801
609	1.798	1.797
673	1.793	1.791
737	1.788	1.785
816	1.781	1.777
892	1.774	1.769
973	1.767	1.76
1127	1.753	1.742
1269	1.739	1.725

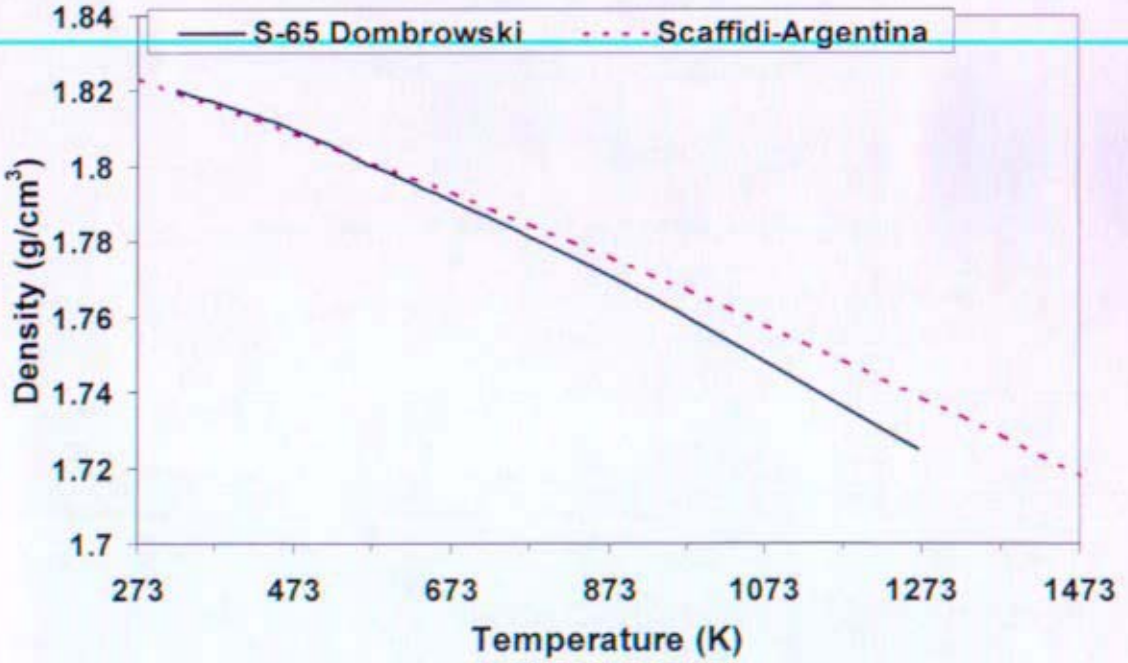

Figure 1: Density of Be

2.5 Thermal Conductivity

2.5.1 Unirradiated

From Scaffidi-Argentina (Reference (d)) the unirradiated, thermal conductivity of Be is given by the following curve for the temperature range 293K ≤ T ≤ 1500K.

$$k = 189.8 - 0.2694 \cdot (T - 273) + 2.543x10^{-4} \cdot (T - 273)^2 - 1.010x10^{-7} \cdot (T - 273)^3$$

where
k = thermal conductivity, W/m-K
T = temperature, K

Billone (Reference(j)) also proposed an equation for the thermal conductivity of Be based on data from various grades of Be up to 973K. This equation accounts for the fact that thermal conductivity is dependent upon the porosity of the material. This equation for the effective thermal conductivity is for hot pressed Be in the 0-50% porosity range.

$$k = \left(\frac{1-p}{1+3.7p^2}\right) \cdot \left(291 - 0.48015 \cdot T + 4.2602x10^{-4} \cdot T^2 - 1.4914x10^{-7} \cdot T^3\right)$$

where
k = thermal conductivity, W/m-K
p = fraction porosity
T = temperature, K

Dombroski (Reference (e)) includes a data table of the variation in thermal conductivity of S-65 grade Be with temperature. Again, some variation is observed at higher temperatures (T>1073K) because the equation was fit to data from industrially available Be grades and the tabular data is only for S-65 grade Be.

The tabulated data (
Table 3) for S-65 grade Be from Reference (e) and the predicted values from the equations given in Reference (d) and Reference (i) assuming zero porosity are plotted in Figure 2. At temperatures between 400 – 973K, little variation is observed between the three sources.

For the thermal conductivity of Be, the equation given by Billone (Reference (j)) is recommended. This curve is recommended because it accounts for the porosity of the material (0-50% range). This curve is given for T ≤ 973K.

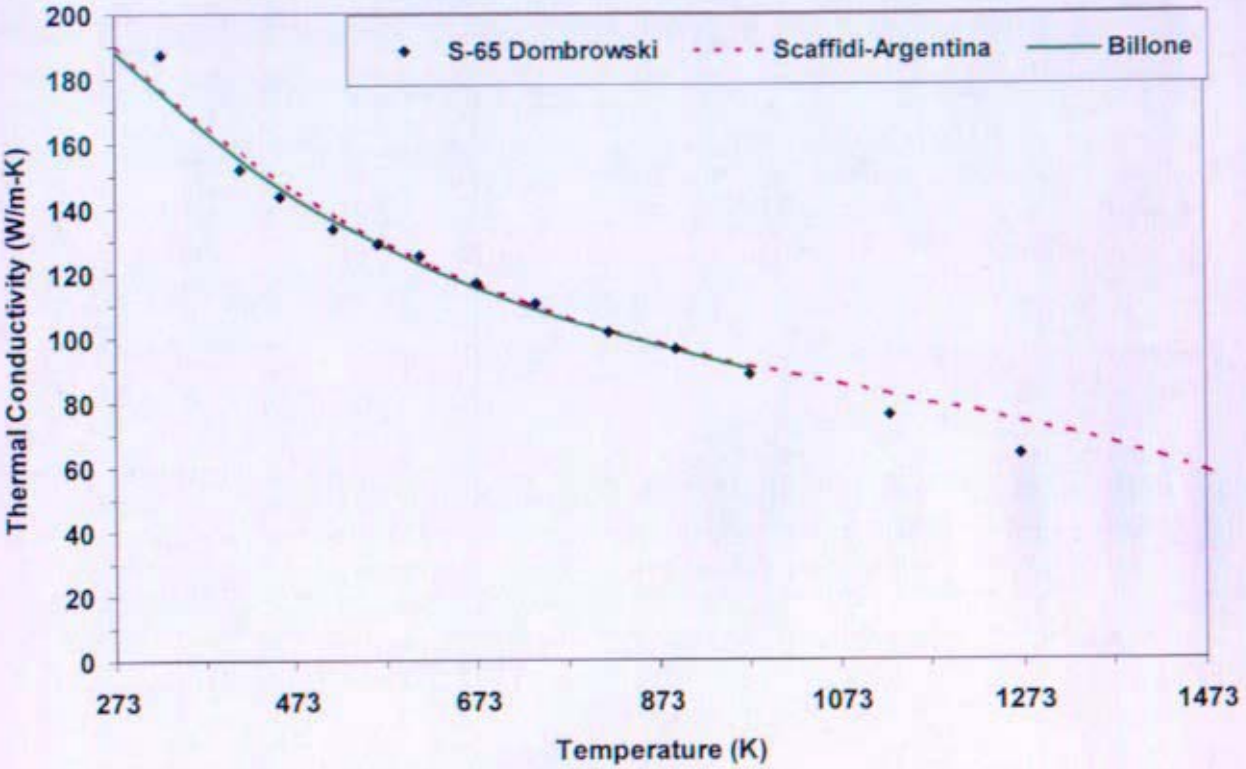

Figure 2: Thermal Conductivity of Be

Table 3: Thermal Conductivity Data for Be

S-65	Dombrowski (1995)
T (K)	Thermal Conductivity (W/m-K)
324	187.3
412	152.3
456	143.8
515	133.8
564	128.8
609	125.2
673	116.6
737	110.4
816	101.8
892	96.1
973	88.4
1127	75.8
1269	63.8

	Scaffidi-Argentina (2000)	Billone (1995)
T(K)	W/m-K	W/m-K
273	189.8	188.6
373	165.3	163.4
473	145.3	143.4
573	129.1	127.7
673	116.3	115.4
773	106.0	105.5
873	97.88	97.28
973	91.17	89.76
1073	85.29	
1173	79.66	
1273	73.65	
1373	66.67	
1473	58.10	
1573	47.35	

2.5.2 Irradiated

The irradiated thermal properties, including thermal conductivity, have been studied for beryllium. Snead and Barabash (References (k) and (l)) summarize the neutron irradiation data

for S-65 and S-200F Brush Wellman beryllium grades. Snead (Reference (k)) reported that significant reductions in thermal conductivity of Be are not expected until He bubbles and swelling become more prominent (He bubbles form at grain boundaries from 598 – 873K and form at dislocations within the grain at temperatures around 723 – 823K). This is because for irradiations above 573 K the He is no longer in solid solution and therefore He diffusion and bubble formation begin to occur. Snead (Reference (k)) showed that the effect of radiation on the thermal conductivity of S-65 Be at ~$1x10^{21}$ n/cm^2 (E>0.1 MeV) and approximately 573K was within the ~4% experimental error of the unirradiated value. For S-200F Be irradiated to fluences of $4.5x10^{20}$ n/cm^2 (E>1MeV) at 473K, the thermal conductivity decreased approximately 5% (Reference (l)). At this time there is no recommended equation for irradiated thermal conductivity of Be.

2.6 Thermal Expansion

It should be noted that due to the anisotropic nature of the hexagonal lattice, some amount of anisotropy is expected in thermal expansion. However, as described by Scaffidi-Argentina (Reference (d)), there is little difference (less than a few percent) observed for polycrystalline, isotropic sintered Be parts (S-65 Brush Wellman grade Be). Extruded grades of Be may exhibit 15-20% differences in the longitudinal and transverse thermal expansion, while HIP Be (S-65H and S-200FH) are more isotropic.

2.6.1 Unirradiated Linear Expansion

Billone (Reference (j)) reports the following equation, plotted in Figure 3, developed for the percent change in length ($\Delta L/L_0$) of Be based on data up to 1558K. The unirradiated percent change in length ($\Delta L/L_0$) is given by:

$$\frac{\Delta L}{L_0} = 8.43x10^{-4} \cdot (1 + 1.36x10^{-3} \cdot T - 3.53x10^{-7} \cdot T^2) \cdot (T - 298)$$

where
$\Delta L/L_0$ = change in length from 298K, percent
T = temperature, K

T (K)	% Linear Expansion
298	0
373	0.092
473	0.231
573	0.386
673	0.555
773	0.737
873	0.930
973	1.13

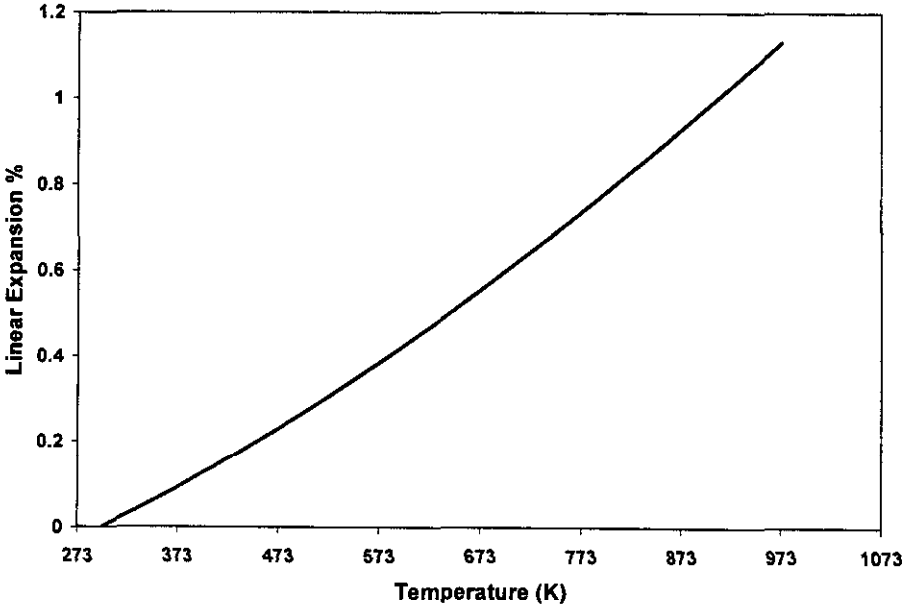

Figure 3: Linear Expansion of Be with Data Table Included

2.6.2 Unirradiated Instantaneous Coefficient of Thermal Expansion

From Scaffidi-Argentina (Reference (d)), for the temperature range 293K ≤ T ≤ 1473K the unirradiated instantaneous coefficient of thermal expansion (α_i) is given by the following equation.

$$\alpha_i = 10.8 + 0.022 \cdot (T - 273) - 1.35x10^{-5} \cdot (T - 273)^2 + 3.45x10^{-9} \cdot (T - 273)^3$$

where
α_i = instantaneous coefficient of thermal expansion, 10^{-6} K^{-1}
T = temperature, K and the reference temperature is 293K

2.6.3 Unirradiated Mean Coefficient of Thermal Expansion

From Scaffidi-Argentina (Reference (d)), for the temperature range 293K < T < 1473K the unirradiated mean coefficient of thermal expansion (α_m) is given by:

$$\alpha_m = 11.04 + 0.0109 \cdot (T - 273) - 4.474x10^{-6} \cdot (T - 273)^2 + 8.631x10^{-10} \cdot (T - 273)^3$$

where
α_m = mean coefficient of thermal expansion, 10^{-6} K^{-1}
T = temperature, K and the reference temperature is 293K

Figure 4 includes the instantaneous coefficient of thermal expansion (α_i) and the mean coefficient of thermal expansion (α_m) as determined by Scaffidi-Argentina (Reference (d)) for all grades of Be, and the mean thermal expansion coefficient as determined by Dombrowski (Reference (e)) for S-65 Be containing 0.9% BeO. The values are tabulated in Table 4.

For the mean coefficient of thermal expansion of Be, the equation given by Scaffidi-Argentina (Reference (d)) is recommended.

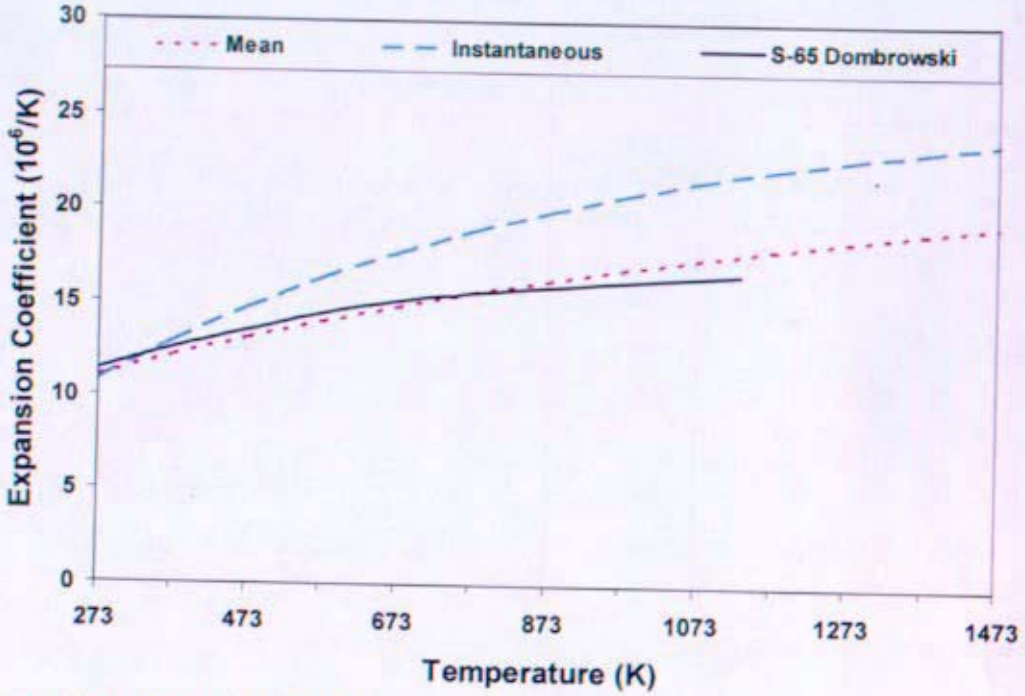

Figure 4: Mean and Instantaneous Thermal Expansion Coefficient of Be

Table 4: Mean and Instantaneous Thermal Expansion Data for Be

S-65	Dombrowski (1995)
T (K)	CTE (10^{-6})/K
270	11.32
381	12.58
524	14.00
607	14.66
688	15.14
758	15.44
952	16.10
1130	16.61

	Scaffidi-Argentina (2000)	
	instantaneous	mean
T(K)	CTE (10^{-6})/K	CTE (10^{-6})/K
273	10.80	11.04
373	12.87	12.10
473	14.69	13.07
573	16.28	13.96
673	17.66	14.78
773	18.86	15.53
873	19.89	16.22
973	20.77	16.85
1073	21.53	17.42
1173	22.18	17.95
1273	22.75	18.43
1373	23.26	18.88
1473	23.72	19.29
1573	24.16	19.68

2.6.4 Irradiated

From Reference (d) it is expected that the coefficient of thermal expansion in isotropic Be grades is not affected by neutron irradiation.

2.7 Specific Heat

2.7.1 Unirradiated

From Scaffidi-Argentina (Reference (d)), the unirradiated specific heat of Be is given by the following equation. This equation is based on experimental data from Be grades with ≤ 1% BeO content (S-65 Brush Wellman Be). The equation is valid for 293 ≤ T ≤ 1558K.

$$C_p = 1741.8 + 3.3358 \cdot (T - 273) - 3.1125x10^{-3} \cdot (T - 273)^2 + 1.2748x10^{-6} \cdot (T - 273)^3$$

where
C_p = specific heat, J/kg-K
T = temperature, K

Billone (Reference (j)) proposed an equation for the specific heat based on data from various grades of Be up to 973K.

$$C_p = 2432 + 0.6428 \cdot (T - 273) - 0.7111 \cdot (T - 273)^{-2}$$

where
C_p = specific heat, J/kg-K
T = temperature, K

Dombrowski (Reference (e)) includes a data table of the variation in specific heat of S-65 grade Be with temperature. Figure 5 is of the tabular data, given in
Table 5, for S-65 Be from Reference (e) and the predicted values from the equations given in Reference (d) and Reference (j) for the unirradiated specific heat of Be. Some variation is observed between Reference (d) and (j) at lower temperatures (T<573K).

For the specific heat of Be, the equation given by Scaffidi-Argentina (Reference (d)) is recommended.

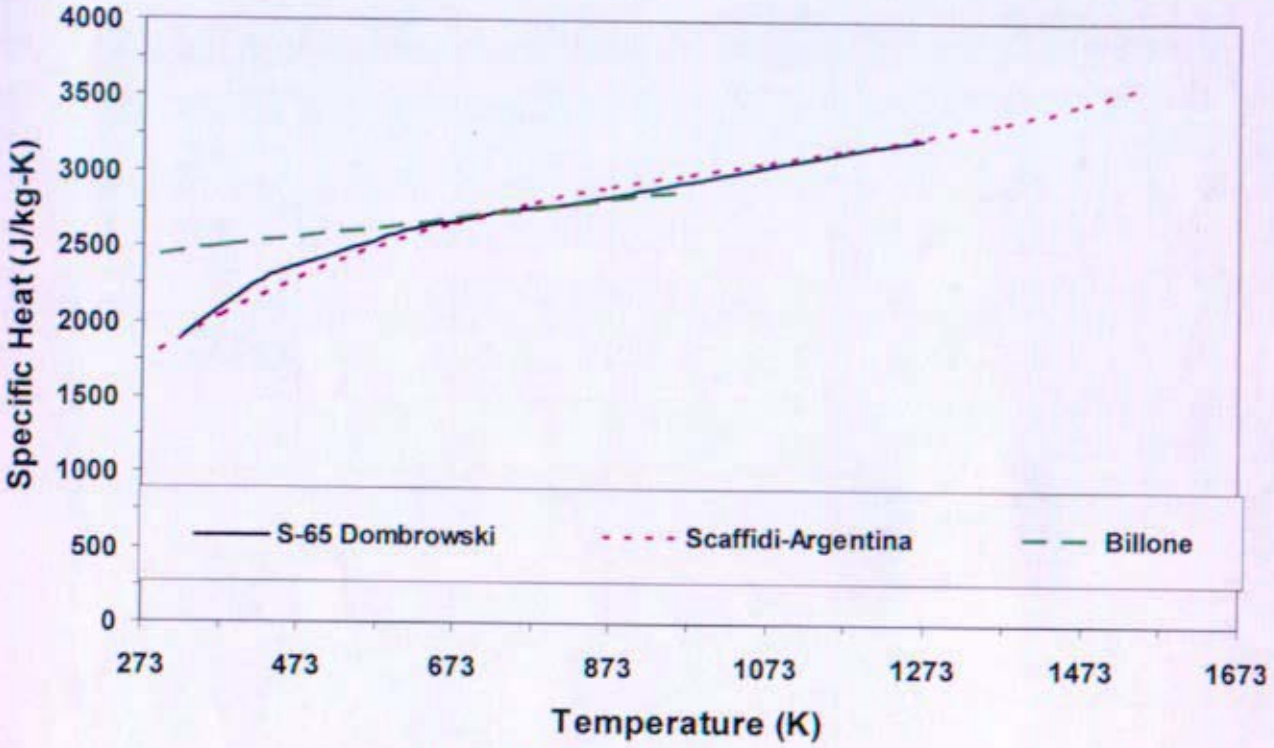

Figure 5: Specific Heat of Be

Table 5: Specific Heat Data for Be

S-65	Dombrowski (1995)
T (K)	Cp (J/kg-K)
324	1905
412	2240
456	2344
515	2441
564	2529
609	2613
673	2667
737	2734
816	2780
892	2860
973	2939
1127	3086
1269	3220

	Scaffidi-Argentina (2000)	Billone (1995)
T(K)	Cp (J/kg-K)	Cp (J/kg-K)
293	1807	2445
373	2046	2496
473	2295	2561
573	2497	2625
673	2660	2689
773	2791	2753
873	2898	2818
973	2989	2882
1073	3071	
1173	3152	
1273	3240	
1373	3342	
1473	3466	
1550	3581	

2.7.2 Irradiated

Scaffidi-Argentina (Reference (d)) reports minimal effects on the specific heat of irradiated Be. It was also reported that the specific heat remains fairly independent of the Be grade. At this time it is assumed that the specific heat of Be will remain independent of irradiation.

2.8 Modulus of Elasticity

2.8.1 Unirradiated

Variation in the elastic modulus of S-65 Be with temperature is given by Dombrowski (Reference (e)) over the temperature range 273K ≤ T ≤ 1273K, shown in Figure 6. Based on the limited data points reported, no equation is given at this time.

T (K)	Young's Modulus (GPa)
273	310
473	300
673	290
873	230
1073	97
1273	48

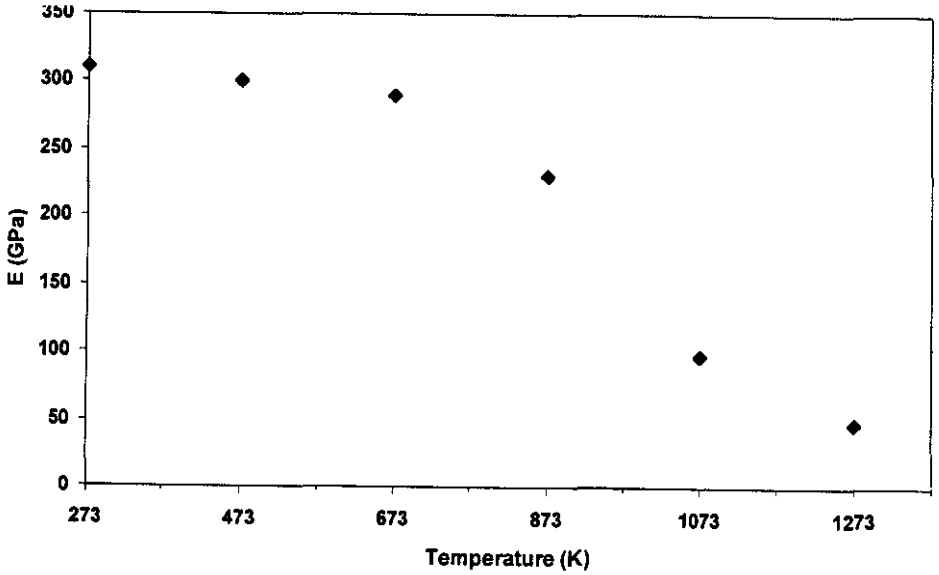

Figure 6: Elastic Modulus of Be with Data Table Included.

2.8.2 Irradiated

Hickman (Reference (g)) reports that radiation effects in Be are expected to be negligible because of the lack of significant displacement type damage above 373K (no fluence limit was reported by Hickman). Some variation in the elastic modulus of Be may occur due to helium bubble formation and swelling. Generally, variations in the elastic modulus are related to temperature as shown above.

2.9 Tensile Yield Strength

2.9.1 Unirradiated

Multiple references have reported on the unirradiated tensile yield strength of Be (References (f), (m), (n) and (o)). The below equations are based on data from unirradiated VHP (S-65 and S-200F Brush Wellman) and HIP (S-65H and S-200FH Brush Wellman) Be grades. In general, HIP grade Be exhibits a higher tensile yield strength than VHP grade Be. These equations are linear regressions of the data in the temperature range 293K ≤ T ≤ 1228K (See Figure 7 and Figure 8 in Section 2.9.2).

$$VHP\ YS = -0.2574 \cdot T + 350.1$$

$$HIP\ YS = -0.3289 \cdot T + 449.3$$

where
VHP YS = tensile yield strength of VHP Be, MPa
HIP YS = tensile yield strength of HIP Be, MPa
T = temperature, K

2.9.2 Irradiated

Irradiation effects on the tensile yield strength of multiple grades of Be (S-65, S-65H, S-200F and S-200FH) have been studied by many references (References (f), (m), (n) and (o)). Irradiated Be exhibits a higher yield strength than in the unirradiated state. Below is a linear regression fit to the irradiated VHP Be and HIP Be data over a temperature range of 293K ≤ T ≤ 823K and fluence range of 0.75 – 2.45x10^{21} n/cm^2 (E>1 MeV). The plot of irradiated and unirradiated tensile yield strength data for multiple grades of Be is also shown below (Figure 7 and Figure 8). Neutron irradiation studies have observed that above 823K the strength of irradiated Be dramatically decreases due to He bubble formation. In beryllium He bubbles begin to form at grain boundaries at T>673K and at dislocations within the grains at T>823K. Additionally, Be has a high fast neutron cross-section for (n,α) reactions and therefore at higher temperatures He embrittlement becomes a concern (corresponding to 0.5 T_{melt}). All high temperature irradiated data (T ≥823K) was excluded from the regression analysis. Additionally, Moons (Reference (f)) performed thermal ageing studies to isolate thermal effects from radiation effects. The thermal results are not included in this linear regression analysis. Data reported from Reference (f), (m), (n) and (o) were from samples tested at the irradiation temperature. The equations exhibit a good fit for 293 – 823K.

$$VHP\ YS_{irr} = -0.6270 \cdot T + 692.5$$

$$HIP\ YS_{irr} = -0.6985 \cdot T + 791.7$$

where
VHP YS_{irr} = irradiated tensile yield strength of VHP Be, MPa
HIP YS_{irr} = irradiated tensile yield strength of HIP Be, MPa
T = temperature, K

The unirradiated and irradiated tensile yield strength of Be is plotted in Figure 7 for VHP and HIP grades are plotted in Figure 8. The 95% confidence intervals for the least square fits to the data are shown on the graphs. Further study is required to define the effects on yield strength for fluences below 0.75x10^{21} n/cm^2 (E>1MeV).

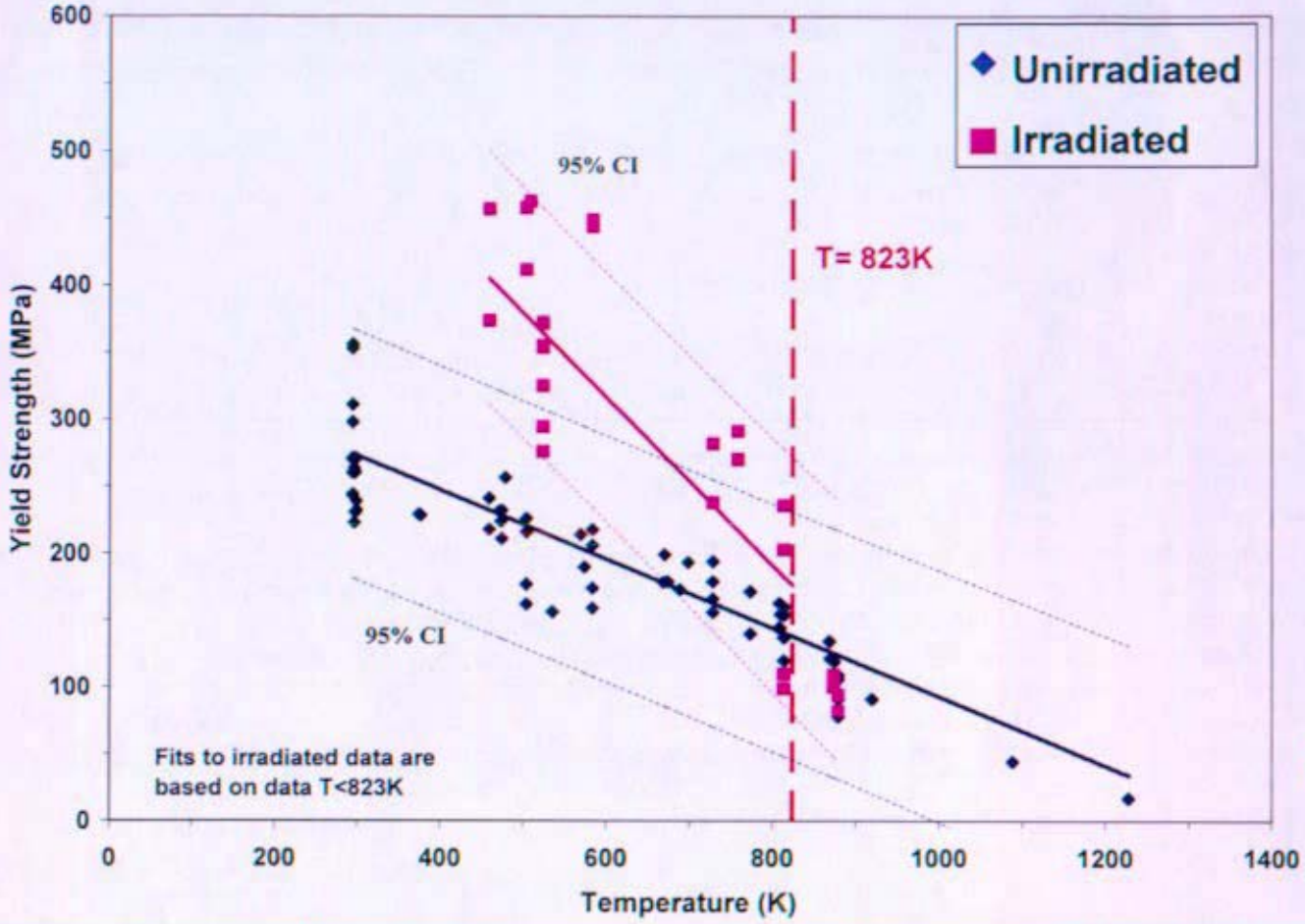

Fluences 0.75 – 2.45x10^{21} n/cm^2 (E>1 MeV)

Figure 7: Irradiated and Unirradiated Tensile Yield Strength of VHP Be

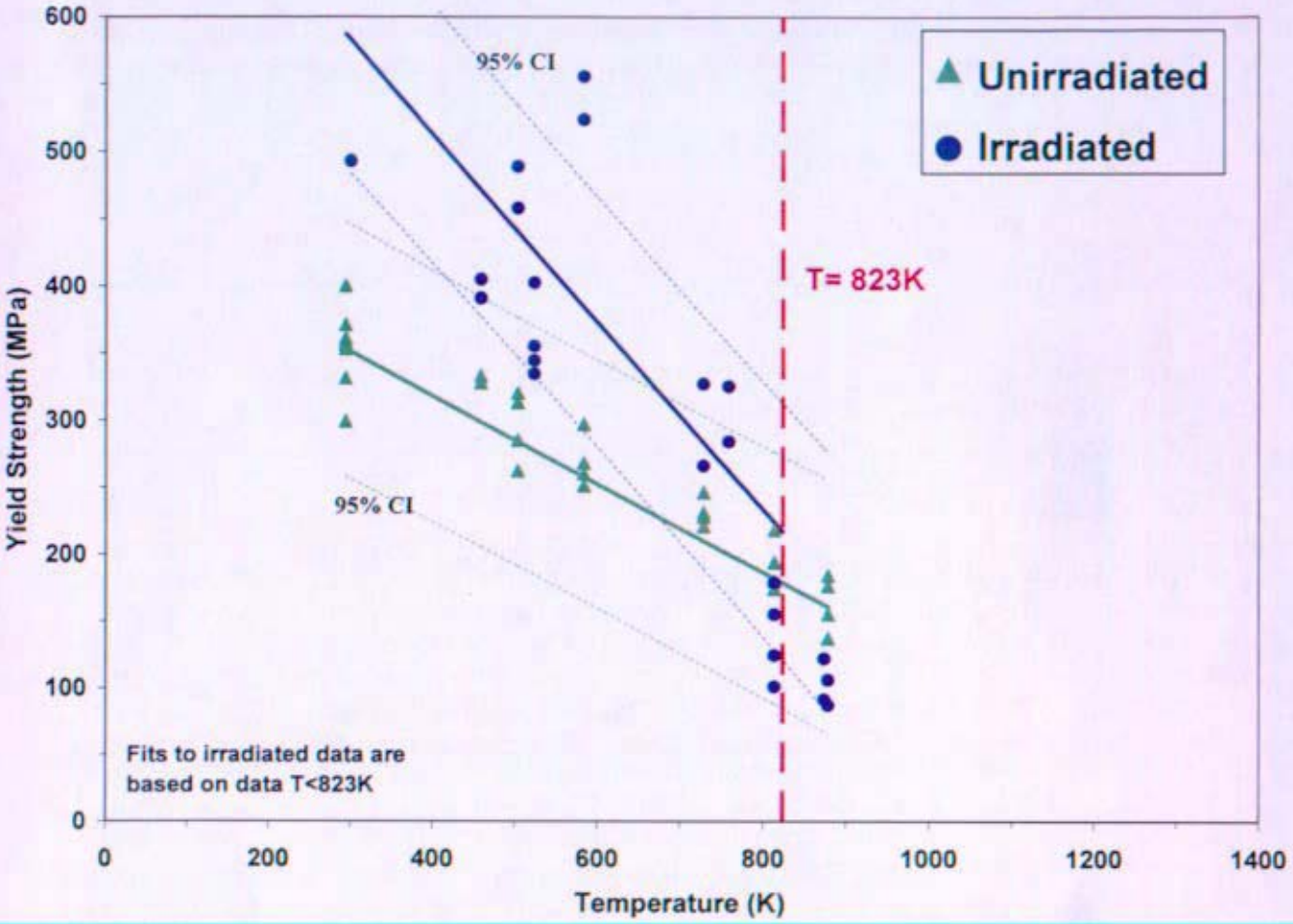

Fluences 0.75 – 2.45x10^{21} n/cm^2 (E>1 MeV)

Figure 8: Irradiated and Unirradiated Tensile Yield Strength of HIP Be

2.10 Emissivity

Reference (i) reports the emissivity of Be for $T < T_m$:

$$\varepsilon = 0.61$$

The emissivity of Be is not expected to vary with irradiation, however the emissivity may vary with material processing (i.e. surface finish).

2.11 Ultimate Tensile Strength

2.11.1 Unirradiated

Multiple references have reported on the unirradiated ultimate tensile strength of Be (References (f), (m), (n) and (o)). The below equations are based on data from unirradiated VHP (S-65 and S-200F Brush Wellman) and HIP (S-65H and S-200FH Brush Wellman) Be grades. In general, HIP grade Be exhibits a higher ultimate tensile strength than VHP grade Be. These equations are based on data in the temperature range 293K ≤ T ≤ 923K (See Figure 9 and Figure 10 in Section 2.11.2).

$$VHP\ \ UTS = -0.4139 \cdot T + 515.3$$

$$HIP\ \ UTS = -0.4897 \cdot T + 609.9$$

where
VHP UTS = ultimate tensile strength of VHP Be, MPa
HIP UTS = ultimate tensile strength of HIP Be, MPa
T = temperature, K

2.11.2 Irradiated

Irradiation effects on the ultimate tensile strength of multiple grades of Be (S-65, S-65H, S-200F and S-200FH) have been studied by many references (References (f), (m), (n) and (o)). Irradiated Be exhibits a slightly higher ultimate tensile strength than in the unirradiated state. Below is a fit to the VHP Be and HIP Be data over a temperature range of 293K ≤ T ≤ 823K and fluence range of 0.75 – 2.45x10^{21} n/cm^2 (E>1 MeV). The plot of irradiated and unirradiated ultimate tensile strength data for multiple grades of Be are shown in Figure 9 and Figure 10. Neutron irradiation studies have observed that above 823K the strength of irradiated Be dramatically decreases due to He bubble formation. In beryllium He bubbles begin to form at grain boundaries at T>673K and at dislocations within the grains at T>823K. Additionally, Be has a high fast neutron cross-section for (n,α) reactions and therefore at higher temperatures He embrittlement becomes a concern (corresponding to 0.5 T_{melt}). All high temperature irradiated data (T ≥823K) was excluded from the regression analysis. Additionally, Moons (Reference (f)) performed thermal ageing studies to isolate thermal effects from radiation effects. The thermal results are not included in this linear regression analysis. Data reported from Reference (f), (m), (n) and (o) were from samples tested at the irradiation temperature. The equations exhibit a good fit for 293 – 823K.

$$VHP\ \ UTS_{irr} = -0.7980 \cdot T + 849.0$$

$$HIP\ \ UTS_{irr} = -0.8738 \cdot T + 943.6$$

where
VHP UTS_{irr} = irradiated ultimate tensile strength of VHP Be, MPa
HIP UTS_{irr} = irradiated ultimate tensile strength of HIP Be, MPa
T = temperature, K

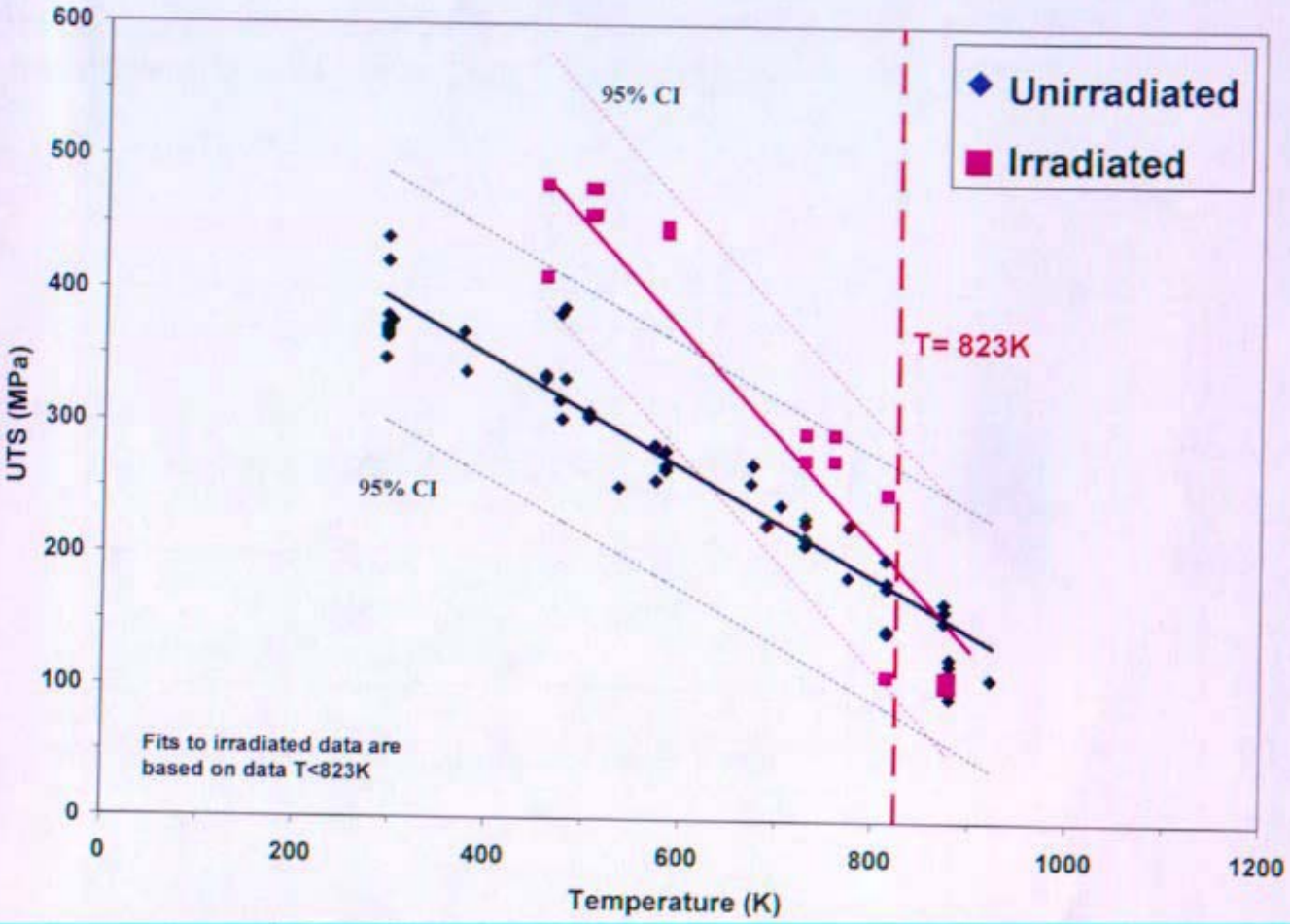

Fluences 0.75 – 2.45x10^{21} n/cm^2 (E>1 MeV)

Figure 9: Irradiated and Unirradiated Ultimate Tensile Strength of VHP Be

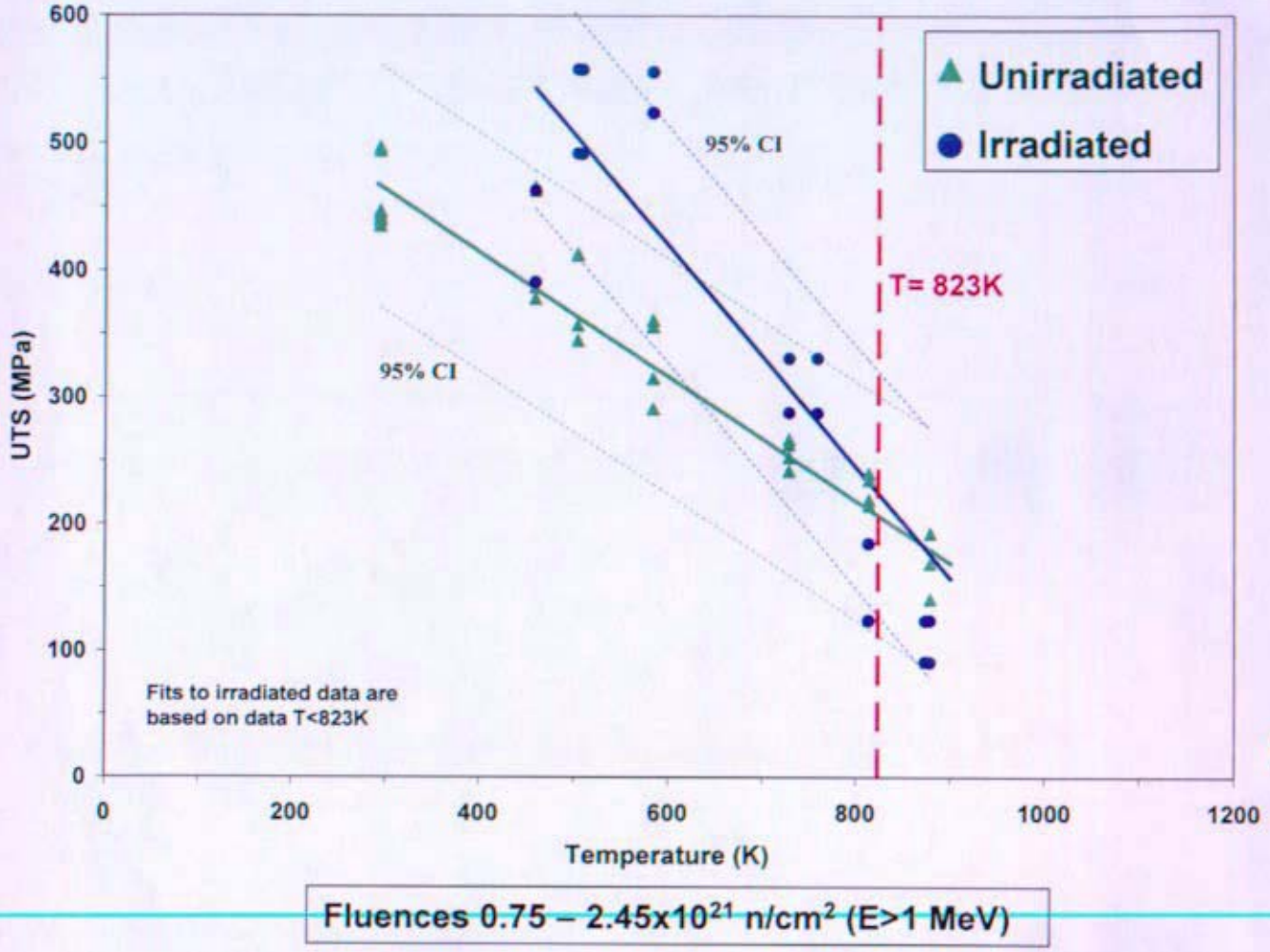

Figure 10: Irradiated and Unirradiated Ultimate Tensile Strength of HIP Be

2.12 Poisson's Ratio

Dombrowski (Reference (e)) gives a table (Table 6) of room temperature data for Poisson's ratio of Brush Wellman Be grade S-200F. Note, scatter in the data is possibly attributed to the low value of the measurements. Because Be grades S-200F and S-65 are similarly processed, these results should be similar for S-65 grade Be.

Table 6: Poisson Ratio Data for S-200F Be

Orientation	Stress Axis	Direction of Orthogonal Strain	Poisson's Ratio
LC	Longitudinal	Circumferential	0.102 0.064 0.072
LR	Longitudinal	Radial	0.102 0.080 0.105
TL	Transverse	Longitudinal	0.069 0.071 0.108
TR	Transverse	Radial	0.102 0.058 0.066

Scaffidi-Argentina (Reference (d)) reported that Poisson's ratio ranges between 0.01 – 0.13 (0.07 +/- 0.06) while Billone (Reference (j)) reported Poisson's ratio at room temperature to be 0.08 +/- 0.02. Reference (d) also reported that Poisson's ratio is generally independent of temperature, grain size, porosity and radiation damage. Additional data on S-65 grade Be may be required to validate these assumptions.

2.13 Irradiation Swelling

As described by Scaffidi-Argentina and Gelles (References (d) and (p)), damage due to irradiation in Be occurs primarily from fast neutron transmutation reactions resulting in the formation of helium (He) and tritium (^{3}H) via the following reactions (Reference (q)):

$$^9Be + n \rightarrow {}^8Be + 2n \text{ (threshold energy 2.7 MeV)}$$

$$^8Be \rightarrow 2\ {}^4He$$

$$^9Be + n \rightarrow {}^6He + {}^4He \text{ (threshold energy 1.4MeV)}$$

$$^6He \rightarrow {}^6Li$$

$$^6Li + n \rightarrow {}^4He + {}^3H \text{ (primarily thermal neutrons)}$$

Swelling is considered an important irradiation effect. He formed by the transmutation reactions is responsible for swelling at high fluences and high temperatures. Gelles (Reference (p)) determined that minimum swelling at high temperatures occurred in Be grades with the smallest grain size and highest BeO content. Helium migration and the formation of large helium bubbles are limited by the large quantity of small BeO particles. The swelling of Be was also examined by Dalle Donne (Reference (r)) in an attempt to characterize the behavior of the material in solid breeder blanket applications. It was established by Scaffidi-Argentina (Reference (d)) that swelling generated from a given gas concentration was dependent on the He bubble size and therefore dependent upon the bubble density. Dalle Donne (Reference (r)), using this and other constitutive relationships for Be (surface tension, grain boundary energy, self-diffusion, He

diffusion, vapor pressure etc.) created the computer code ANFIBE (Analysis of Fusion Irradiated Beryllium). The ANFIBE code accounts for the important mechanistic processes that affect the gas generation and swelling behavior in Be.

Reference (r) illustrates how the ANFIBE code has shown agreement with a variety of experimental data. Experimental data ranges from 2.1-50 x 10^{21} n/cm^2 (E>1MeV) from 300-973K. Experimental data was obtained from S-65 and S-200F beryllium irradiated in the EBR-II (fast reactor), BR2 (fast reactor) and the ATR (PWR reactor). Swelling predictions from the ANFIBE model were reported by Dalle Donne to fluences of 25x10^{21} n/cm^2 (E>1MeV) and temperatures of 973K. Dalle Donne (Reference (r)) presented a comparison of the ANFIBE calculated swelling versus experimental swelling shown for a range of data (Figure 11). Additionally, the ANFIBE predictions for swelling at 0.5-10 x 10^{21} n/cm^2 (E>1MeV) over the temperature range of 273-973K are shown in Figure 12.

Efforts continue to develop the ANFIBE code, providing greater capability and confidence in the model (References (d) and (s)). While much of the data used in validating the code is for higher fluences at lower temperatures or lower fluences at higher temperatures, the model is expected to yield reasonable predictions at higher temperatures and higher fluences.

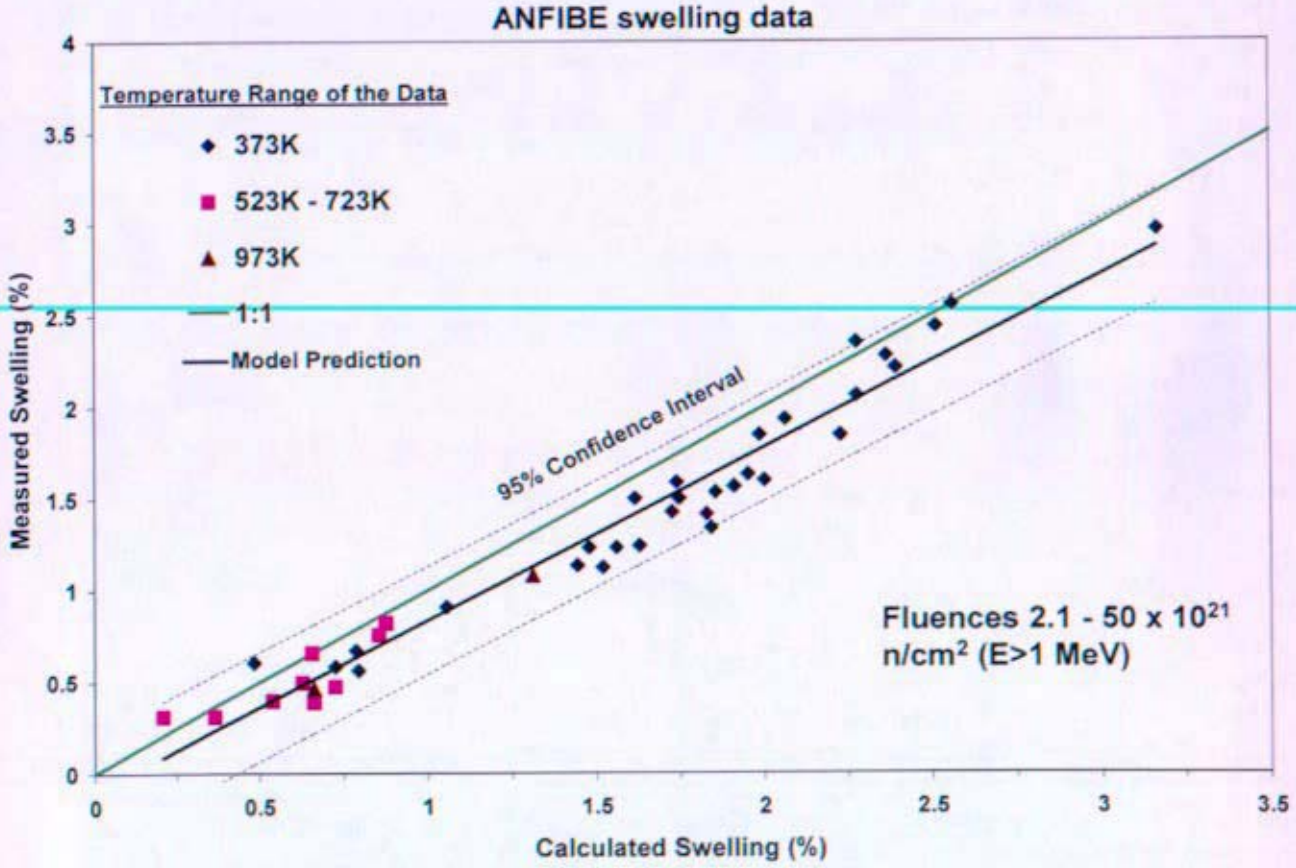

Figure 11: Measured Be Swelling Data Versus the ANFIBE Calculated Swelling

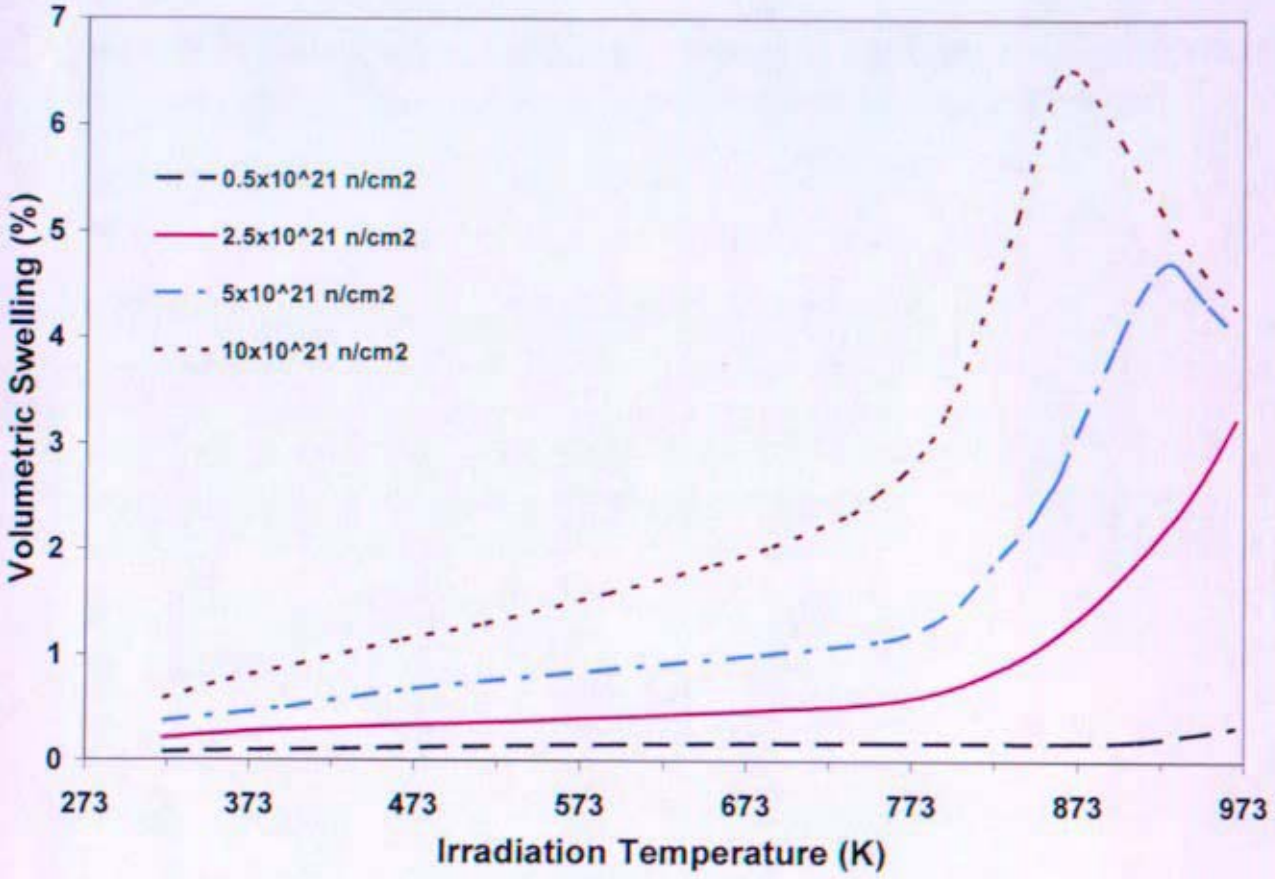

Figure 12: Predicted Be Swelling Based on ANFIBE Code

3. Beryllium Oxide (BeO)

3.1 Composition

Table 7 gives a typical composition of Thermalox 995 BeO (Brush Ceramic Products Reference (t)).

Table 7: Composition of Thermalox 995 BeO

Thermalox 995 BeO	
Element (max unless otherwise stated)	**wt%**
BeO (min %)	99.5
Al	0.035
Cr	0.0015
Ca	0.015
Fe	0.015
Mg*	0.13
Ni	0.0015
Si*	0.25
Na	0.015
Zn	0.002

*Si and Mg are added to the Thermalox 995 as sintering aids.

3.2 Melting Temperature and Maximum Use Temperature

The melting temperature of beryllium oxide is (Reference (u)):

$$T_{melt} = 2843 \pm 30K$$

A practical maximum use temperature (unirradiated) is approximately 2300K (Reference (u)). Irradiation may affect other properties (thermal conductivity and compressive strength) and lower this maximum use temperature.

3.3 Density

Busboom (Reference (u)) reported the room temperature (298K), theoretical density of BeO is 3.010 g/cm^3. The actual BeO density is calculated by:

$$\rho_{actual} = TD \cdot (1 - P)$$

where
TD = theoretical density
P = volume fraction porosity

3.4 Thermal Conductivity

3.4.1 Unirradiated

Data given from Reference (v) for the temperature range 273K ≤ T ≤ 2300K is shown in Figure 13. The following equation is for the unirradiated thermal conductivity of BeO. This equation is based on data from various grades of BeO with densities varying from 2.60 – 2.97 g/cm^3 (86 – 99% TD). From Figure 13 it is observed that there is some slight dependence of thermal conductivity on porosity. Generally in ceramics, increasing the porosity decreases the thermal conductivity (Reference (w)). The effect of porosity is not accounted for in the following equation.

$$k = 8.31 x 10^5 \cdot T^{-1.42}$$

where
k = thermal conductivity, W/m-K
T = temperature, K

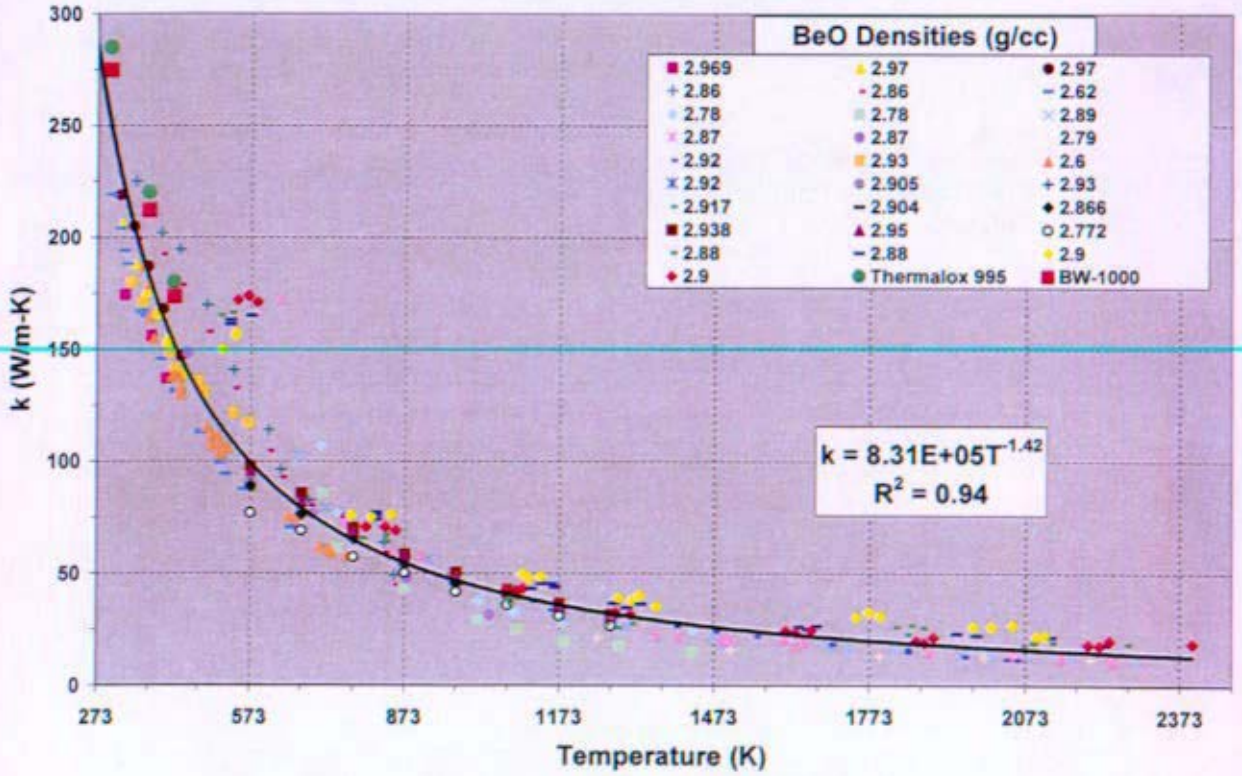

Figure 13: Thermal Conductivity of BeO

3.4.2 Irradiated

Low temperature (350 – 373K) thermal conductivity studies by Pryor (Reference (x)) reported a reduction in BeO thermal conductivity at doses as low as $2x10^{18}$ n/cm^2 (E>1MeV). Pryor (Reference (x)) found large reductions in thermal conductivity as dose increased. The thermal conductivity decreased as the dose increased up to the highest dose evaluated, $0.2x10^{21}$ n/cm^2 (E>1MeV). Measurements at higher doses were not performed due to microcracking in the material, which is expected to affect thermal conductivity (see swelling discussion). Hickman (Reference (y)) estimated values of thermal conductivity at elevated temperatures based on the low temperature data. Predictions indicated that as irradiation temperature increased the degradation in thermal conductivity may be minimal in the vicinity of 1073K. More data is required to validate the predictions from Reference (y) on currently available grades of BeO at higher temperatures and fluences.

Snead (Reference (z)) reported effects of neutron irradiation at 333K on the thermal conductivity of currently available Brush Wellman Thermalox 995 grade BeO. Minimal changes in thermal conductivity were observed at fluences of $1x10^{18}$ n/cm^2 (E>0.1MeV).

Touloukian (Reference (v)) provided limited irradiation data for BeO irradiated at $8.6x10^{18}$, $2x10^{20}$ and $3.7x10^{20}$ n/cm^2 (E>1MeV) over the narrow temperature range of 330 – 560K. Figure 14 illustrates the degradation in the thermal conductivity of BeO, similar to the trends in Reference (y).

Due to limited thermal conductivity data for currently available grades of BeO irradiated at high temperatures and high fluence, irradiation testing of BeO was planned in the JOYO fast reactor to characterize the material.

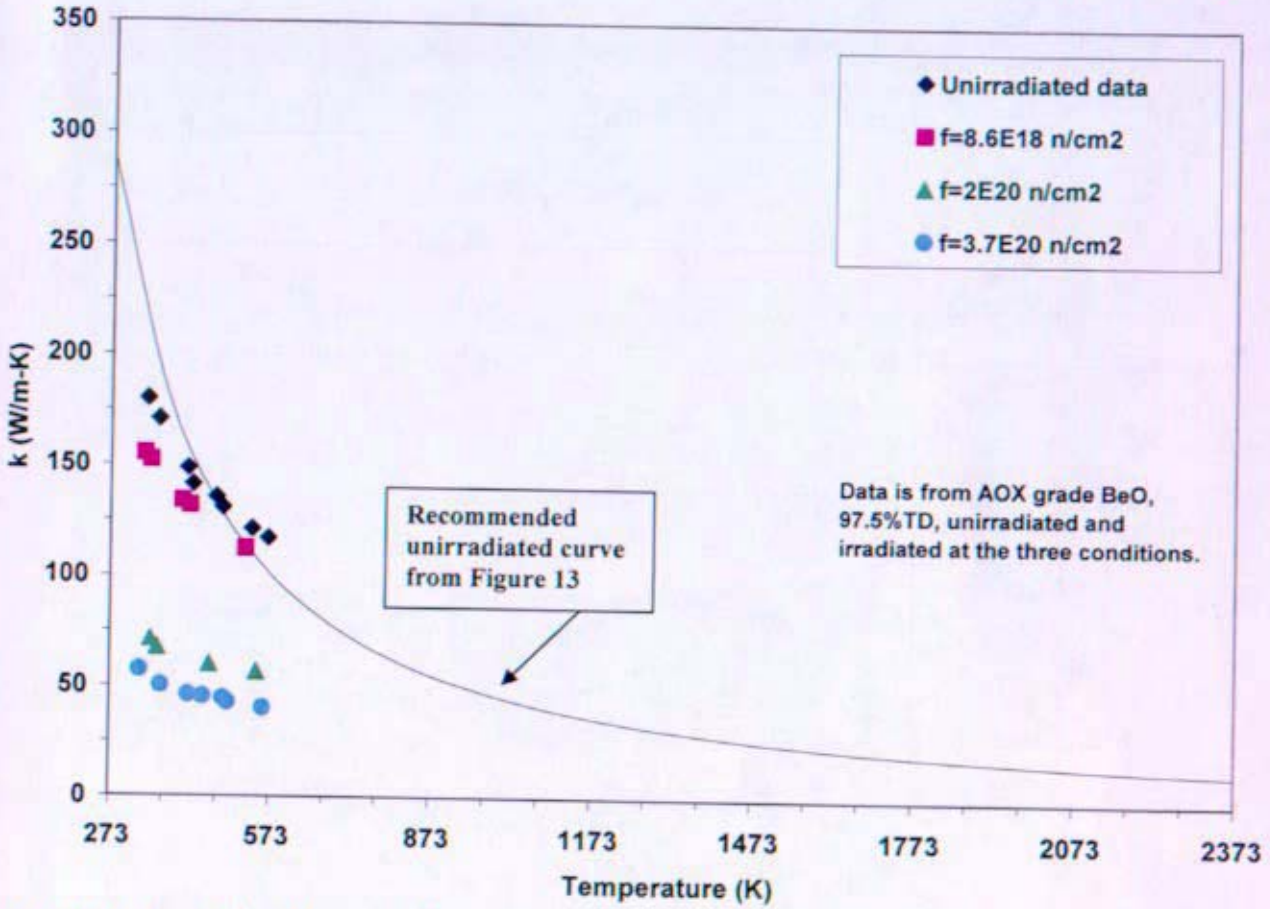

Figure 14: Irradiated Thermal Conductivity of BeO Compared to Curve Fit in Figure 13

3.5 Thermal Expansion

3.5.1 Unirradiated Linear Expansion

Data compiled by Touloukian (Reference (aa)) over the temperature range 293K ≤ T ≤ 2300K is shown in Figure 15. From the data it is observed that there is no correlation between changes in the density of BeO and linear expansion (Figure 15). The unirradiated percent change in length ($\Delta L/L_0$) is given by the following equation. This equation is based on data from various grades of BeO with densities varying from 2.68 – 2.99 g/cm^3.

$$\frac{\Delta L}{L_0} = 1.69x10^{-7} \cdot T^2 + 6.65x10^{-4} \cdot T - 0.229$$

where
$\Delta L/L_0$ = change in length from 293K, percent
T = temperature, K

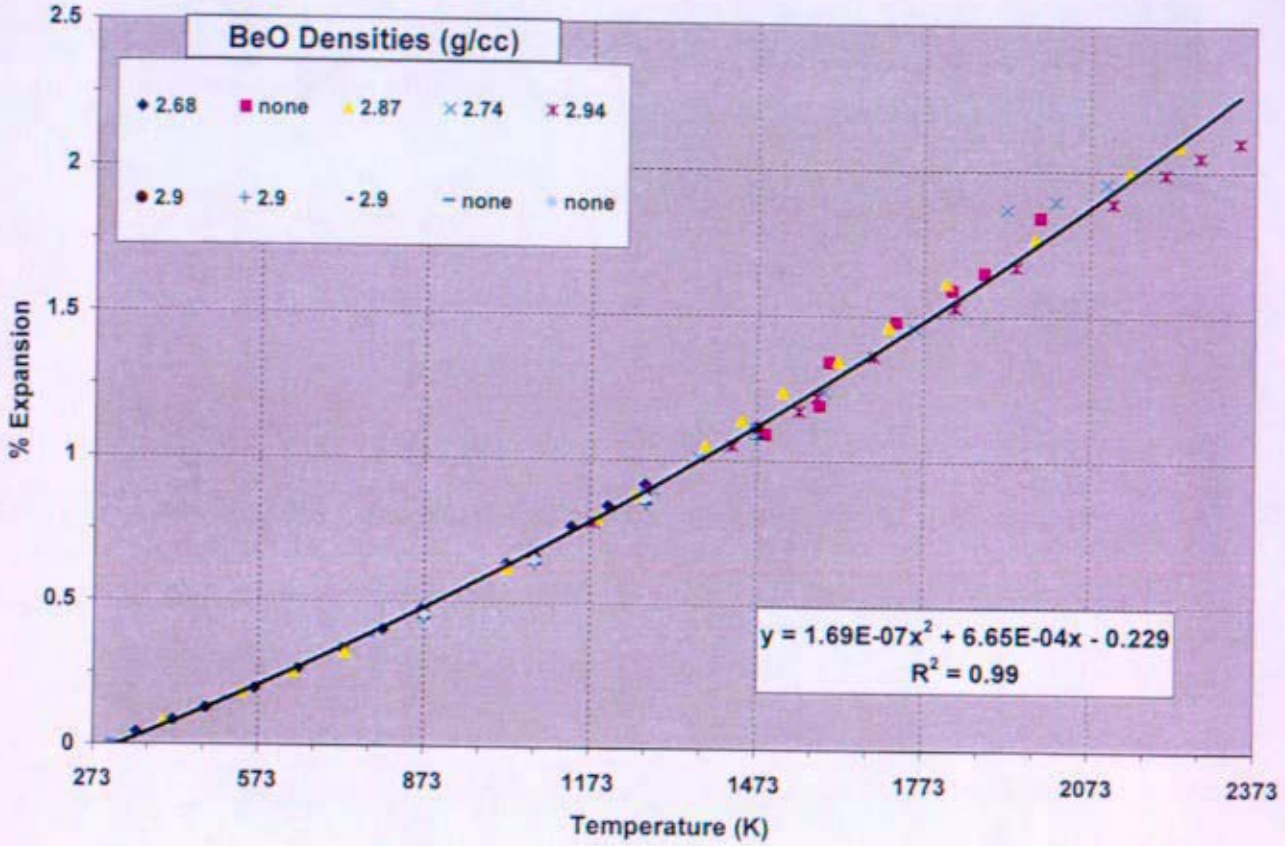

Figure 15: Linear Expansion of BeO

3.5.2 Unirradiated Instantaneous Coefficient of Thermal Expansion (CTE)

From Reference (u) for the temperature range 293K ≤ T ≤ 2300K the unirradiated instantaneous coefficient of thermal expansion (α_i) is given by:

$$\alpha_i = 4.433x10^{-6} + 6.552x10^{-9} \cdot T - 8.262x10^{-13} \cdot T^2$$

where
α_i = instantaneous linear coefficient of thermal expansion, K^{-1}
T = temperature, K

3.5.3 Unirradiated Mean Coefficient of Thermal Expansion (CTE)

The definition of mean coefficient of thermal expansion (α_m) is given by:

$$\alpha_m = \frac{\left(\frac{\Delta L}{L_0}\right)}{100 \cdot (T - T_{ref})}$$

where
α_m = mean linear coefficient of thermal expansion, K^{-1}
$\Delta L/L_0$ = change in length, percent (Section 3.5.1)
T = temperature, K
T_{ref} = average reference temperature

Data from Touloukian (Reference (aa)) for the linear expansion ($\Delta L/L_0$) of BeO was used to determine the mean coefficient of thermal expansion over the temperature range 353K ≤ T ≤ 2300K. Because the reference temperature (T_{ref}) varied for different data sets, an average value was used for the reference temperature (299 K). The change in slope of the mean CTE curve, shown in Figure 16, around 473K appears reasonable based on the single data point at 299 K [curve 53, Reference (aa)]. The reference temperature used to calculate the mean CTE of the curve 53 point is 79 K.

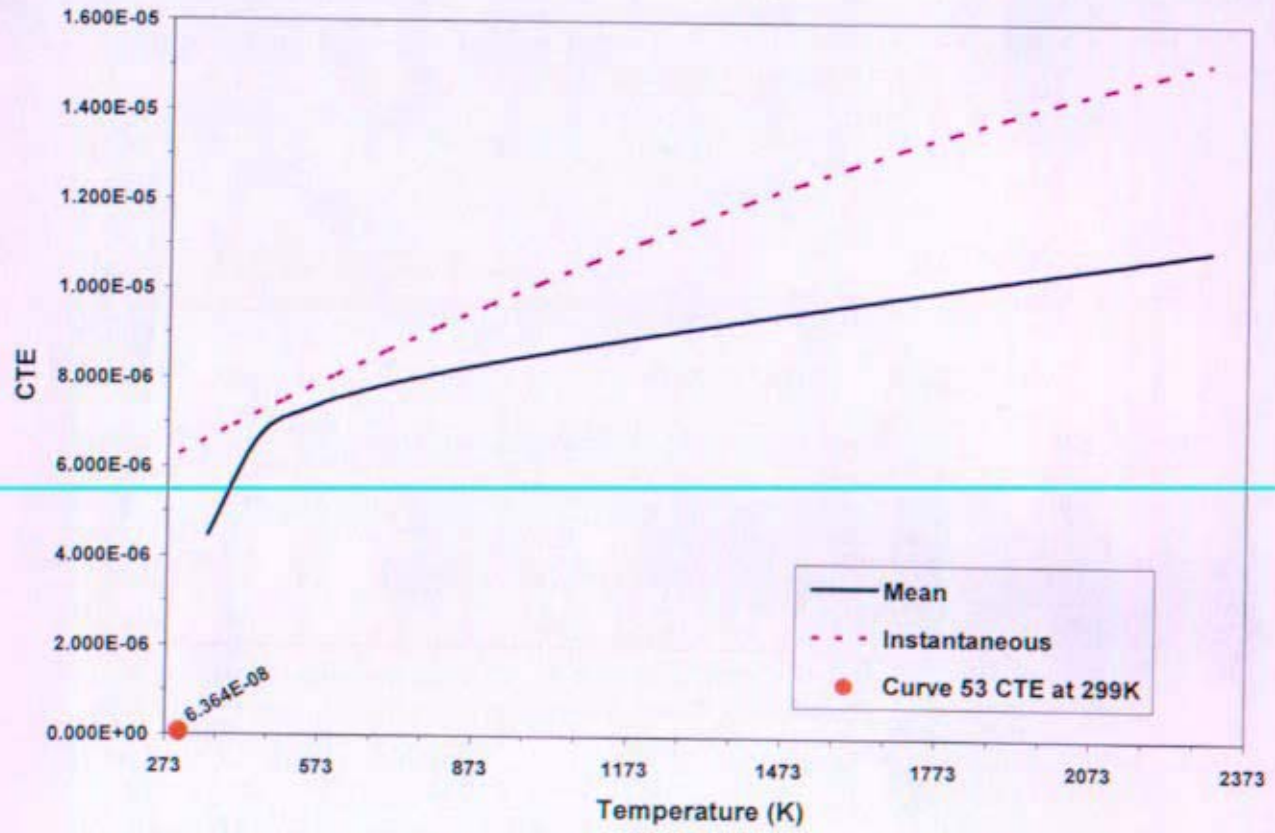

Figure 16: Mean and Instantaneous Coefficient of Thermal Expansion of BeO

The recommended equation over the range 353K ≤ T ≤ 2300K for the mean CTE of BeO is given by:

$$\alpha_{mean} = \frac{\left(1.69x10^{-7} \cdot T^2 + 6.65x10^{-4} \cdot T - 0.229\right)}{100 \cdot (T - 299)}$$

where
α_{mean} = mean coefficient of thermal expansion
T = temperature, K

3.5.4 Irradiated

It is expected that the coefficient of thermal expansion is not affected by irradiation. Collins (Reference (bb)) reported no change (+/-5%) in the coefficient of thermal expansion for BeO irradiated at 373K. Additionally, Walker (Reference (cc)) reported no change (+/- 0.02%) in the coefficient of thermal expansion of BeO irradiated to $0.65x10^{21}$ n/cm^2 (E>1MeV) at 923 – 963K.

3.6 Specific Heat

3.6.1 Unirradiated

From Reference (dd) (Table 8 and Figure 17) for the temperature range 298K ≤ T ≤ 2820K the unirradiated specific heat of BeO is given by the following equation:

$$C_p = 3.61x10^{-7} \cdot T^3 - 1.69x10^{-3} \cdot T^2 + 2.87 \cdot T + 418$$

where
C_p = specific heat, J/kg-K
T = temperature, K

Table 8: Data Reported in Figure 17 for Specific Heat of BeO

Curve Number	Specifications and Remarks
2	99.9 BeO, with impurities of Al, Ni, Cu, Zn, Ag, Fe and Ti; pressed and sintered at 1673 – 2073K.
3	No description of sample given.
4	99.96 BeO, 0.01 Si, 0.007 Al, 0.002 Na, 0.001 Cs, 0.001 Fe, <0.001 Ca, <0.001 Cu, <0.00005 Li, <0.00005 Mg; supplied by Norton Co.; pressed, fired at 2073K and sintered.
5	99.5 BeO, 0.0090 si, 0.0050 Al, 0.0020 Mo, 0.0010 Ca, 0.0010 Cr, 0.0010 Fe, 0.0010 Na, 0.0010 Ni, 0.0003 Mn, <0.0001 B, Cd, Li, <0.0001 Co, Cu; supplied by Brush Beryllium Co.; cold pressed; density 2.87 g/cm^3.
6	Sample supplied by Zirconium Corp. of America; crushed in hardened steel mortar to pass 100-mesh screen; pressed and sintered; density at 298K before exposure: apparent density (ASTM method B311-58) 2.93 g/cm^3, true density (by immersion in xylene) 3.00 g/cm^3.

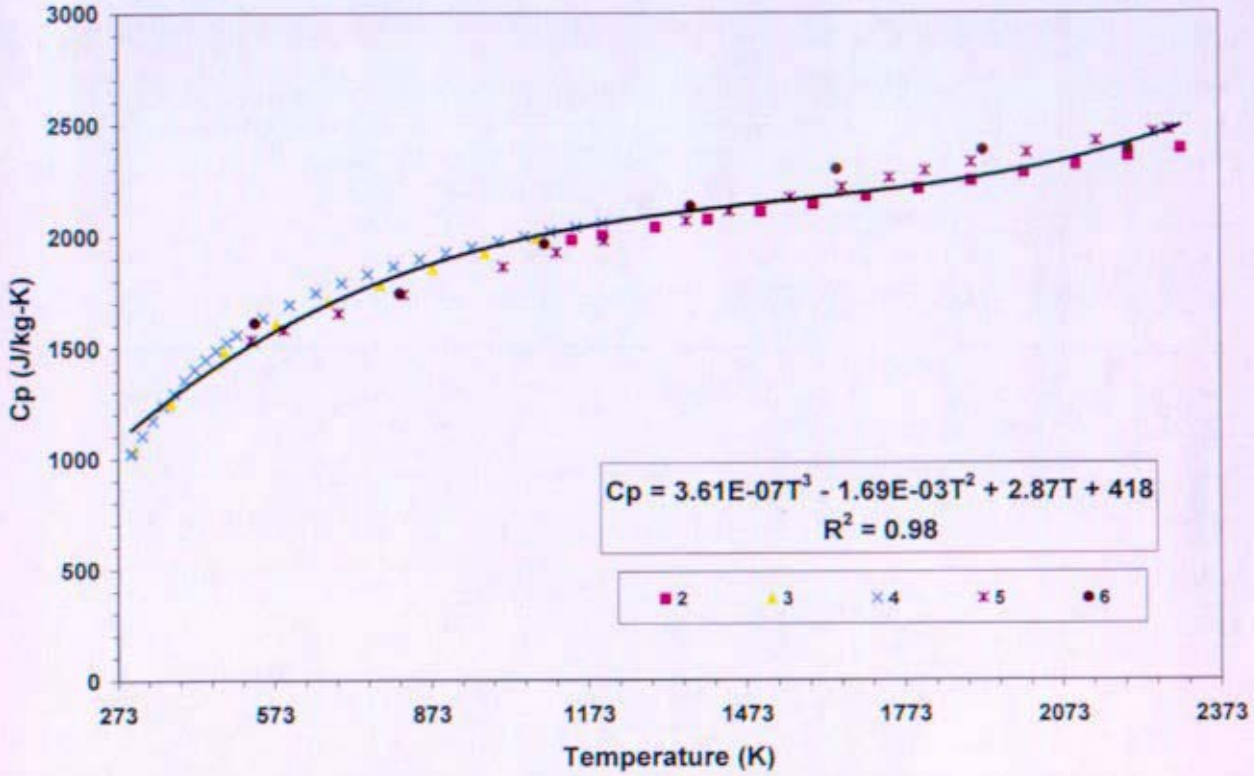

Figure 17: Specific Heat of BeO

3.6.2 Irradiated

Hickman (Reference (ee)) reported no measurable change in enthalpy of irradiated BeO at 573K, 873K and 1173K after removing the effects due to stored energy. Measurements of stored energy in irradiated BeO samples indicate a significant amount of energy is stored at high fluences. However, the stored energy has minimal effects on the specific heat of irradiated BeO at or below the irradiation temperature.

3.7 Modulus of Elasticity

3.7.1 Unirradiated

From Reference (u) the elastic modulus (Figure 18) is given over two temperature ranges with porosity ranging from 0 – 30% for BeO by the following:

For 298K < T < 800K

$$E = 344.7 - 805.7 \cdot P$$

For 800K < T < 1500K

$$E = (344.7 - 805.7 \cdot P) \cdot (1.31 - 1.75x10^{-3} \cdot T + 2.82x10^{-6} \cdot T^2 - 1.39x10^{-9} \cdot T^3)$$

where
E = modulus of elasticity, GPa
P = volume fraction porosity, 0 < P < 0.3
T = temperature, K

T (K)	E (GPa)
300	304.4
400	304.4
500	304.4
600	304.4
700	304.4
800	304.4
801	304.4
805	304.5
850	305.2
900	305.0
1000	299.8
1100	286.4
1200	262.2
1300	224.7
1400	171.3
1500	99.43

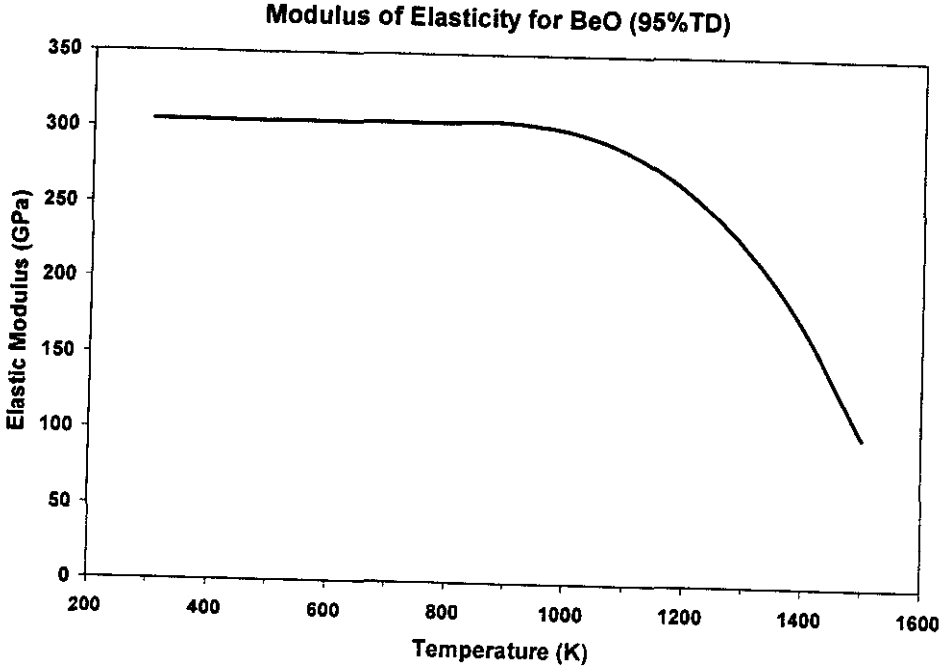

Figure 18: Elastic Modulus of 95% Theoretical Density BeO with Data Table Included

3.7.2 Irradiated

The modulus of elasticity remains independent of irradiation effects. Using resonance frequency methods, Collins (Reference (bb)) reported a small decrease in the elastic modulus of BeO as a function of irradiation dose, which is consistent with the decrease in density to the point at which microcracking occurred. The elastic modulus of samples that experienced microcracking could not be determined. Generally, variations in the elastic modulus are related to temperature as shown in Section 3.7.1.

3.8 Compressive Strength

3.8.1 Unirradiated

From Reference (u) (Figure 19) the compressive strength for BeO over the temperature range 293K ≤ T ≤ 1500K and porosity range of 0 – 30% is given by the following:

$$C = (1585 - 3273 \cdot P) \cdot (1.232 - 8.284x10^{-4} \cdot T + 1.142x10^{-7} \cdot T^2)$$

where
C = compressive strength, MPa
P = volume fraction porosity, $0 < P < 0.3$
T = temperature, K

T (K)	CS (MPa)
293	1420
400	1306
500	1203
600	1103
700	1006
800	913
900	823
1000	736
1100	652
1200	572
1300	495
1400	421
1500	350

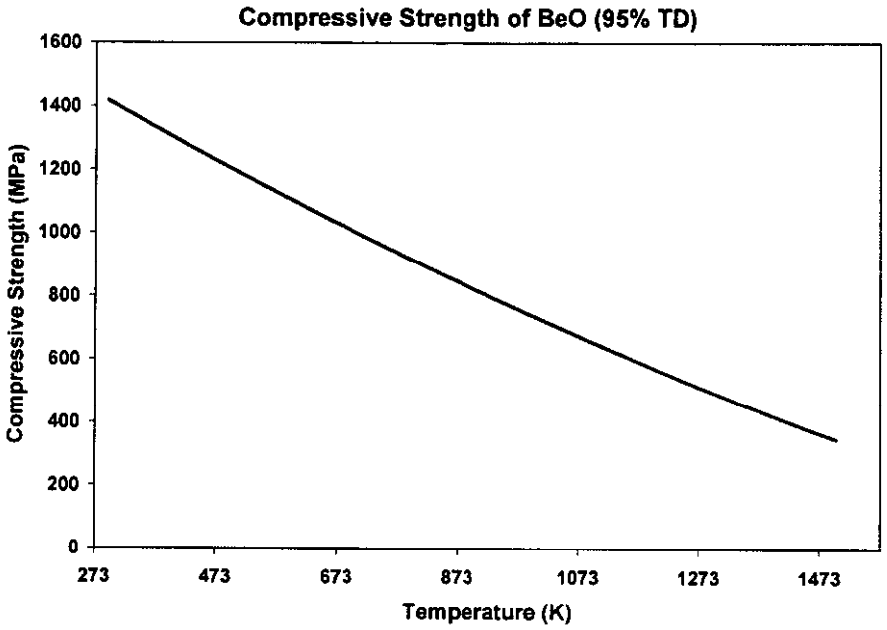

Figure 19: Compressive Strength of 95% Theoretical Density BeO with Data Table

3.8.2 Irradiated

There is limited data on irradiated compressive strength of BeO. Elston and Labbe (Reference (ff)) reported the compressive strength of BeO irradiated at 373K. Measurements were performed at T< 373K and T< 673K. This reference shows that the strength dramatically decreases at doses above $6x10^{19}$ n/cm^2 (E>1 MeV). Note that the material tested had an average grain size of 50 – 100 microns; therefore significant microcracking from irradiation likely occurred (see Section 3.13).

Due to limited compressive strength data for currently available grades of BeO irradiated at high temperatures and high fluence, irradiation testing of BeO was planned in the JOYO fast reactor to characterize the material.

3.9 Tensile Yield Strength

The compressive strength of BeO is given above in Section 3.8. There is limited data on the tensile properties of BeO due to the brittle nature of ceramics.

3.10 Emissivity

From Reference (u) the emissivity is given over three temperature ranges for BeO by the following equations. These equations fit the data presented by Touloukian (Reference (gg)) as shown in Figure 20.

For 300K < T < 800K
$\varepsilon = 0.2$

For 800K < T < 2200K
$\varepsilon = -0.235 + 6.65x10^{-4} \cdot T - 1.51x10^{-7} \cdot T^2$

For 2200 < T
$\varepsilon = 0.5$

where
ε = emissivity
T = temperature, K

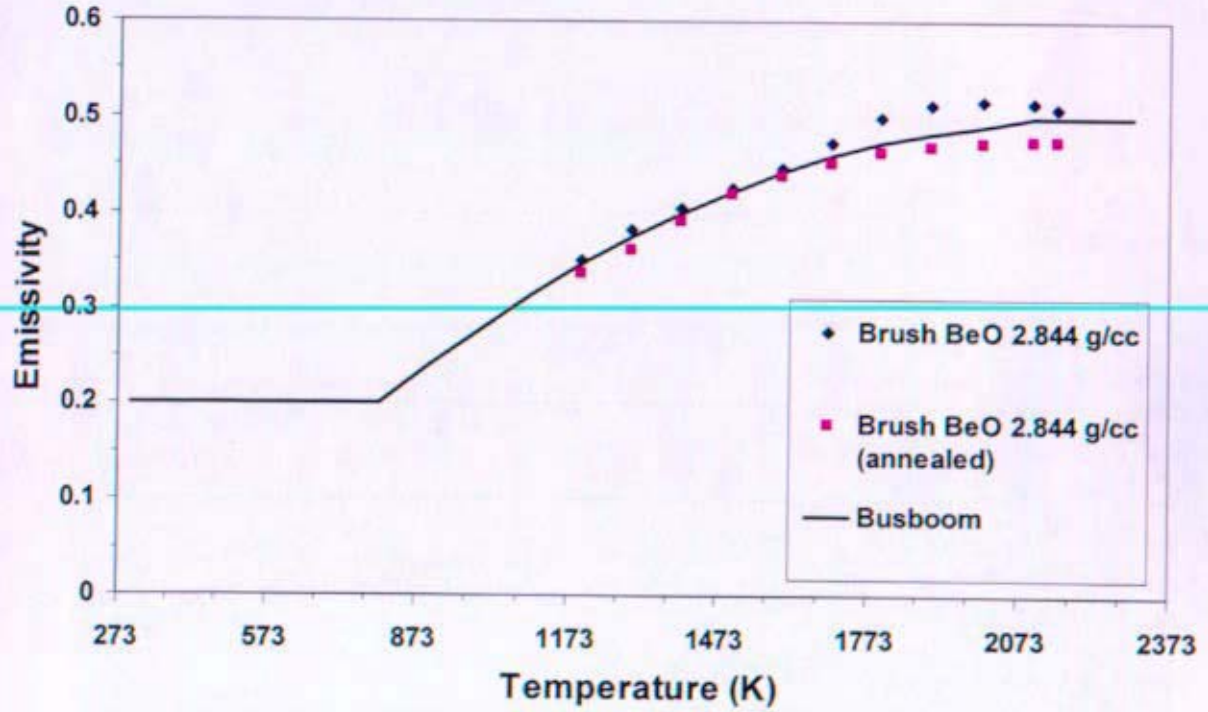

Figure 20: Emissivity of BeO

3.11 Ultimate Tensile Strength

The compressive strength of BeO is given above in Section 3.8. There is limited data on the tensile properties of BeO due to the brittle nature of ceramics.

3.12 Poisson's Ratio

From Reference (u) the best estimate for Poisson's ratio is 0.3 for 298K to 1400K. It is expected that Poisson's ratio for BeO will remain independent of irradiation effects, similar to the elastic modulus.

3.13 Irradiation Swelling

Several factors are believed to influence the swelling behavior of BeO exposed to neutron irradiation, primarily grain size, temperature, fluence, flux and density. Plumlee (Reference (hh)) reported expressions based on lattice defects ($\Delta V/V_D$), microcracking ($\Delta V/V_{MC}$) and helium bubble formation ($\Delta V/V_{He}$) to predict the swelling of BeO. The grain size, temperature, fluence, flux and density affect these swelling mechanisms and are summarized in Table 9. It should be noted that these equations have been developed with relatively limited data, flux range (0.65 – 3.2×10^{14} n/cm^2-s) (E>1MeV) and fine grain size (5 – 20 microns) BeO.

$$\frac{\Delta V}{V_{total}} = \frac{\Delta V}{V_D} + \frac{\Delta V}{V_{MC}} + \frac{\Delta V}{V_{He}}$$

where
$\Delta V/V$ = total volume expansion fraction
$\Delta V/V_D$ = volume expansion fraction due to lattice defect mechanisms
$\Delta V/V_{MC}$ = volume expansion fraction due to microcracking
$\Delta V/V_{He}$ = volume expansion fraction due to helium bubble formation

Collins (Reference (bb)) formulated an expression for the volume expansion due to lattice defects ($\Delta V/V_D$). Collins assumed high temperature damage is due to competing processes of annealing and production. Collins accounts for the rate of atomic displacements, K, and annealing effects, A_m and A_i. These annealing constants are proportional to the diffusion rate of defects (interstitials and vacancies). Assuming first order kinetics the following expression describes the volume expansion due to lattice defect mechanisms ($\Delta V/V_D$). At temperature above 1073K, this equation underestimates the volume change $\Delta V/V_D$.

$$\frac{\Delta V}{V_D} = \frac{K}{A_m}(1 - e^{-A_m t}) + \frac{K}{A_i}(1 - e^{-A_i t})$$

where
$K = 3.3 \times 10^{-23} \cdot F$
F = neutron flux, n/cm^2-s (E>1MeV)
$A_m = 6.1 \times 10^{-5}\ e^{-10300/RT}$
$A_i = 0.113 e^{-22100/RT}$
R = gas constant = 1.987 cal/mol-K
T = temperature, K
t = time, sec

Based on Reference (u) and (hh), the predicted volume expansion due to microcracking, $\Delta V/V_{MC}$ (grain boundary separation), is described by the following equation when $\Delta V/V_D \geq$

$\Delta V/V_{threshold}$. This equation accounts for the fact that microcracking does not initiate until $\Delta V/V_D \geq \Delta V/V_{threshold}$.

$$if \ \frac{\Delta V}{V_D} < \frac{\Delta V}{V_{threshold}} \qquad then \ \frac{\Delta V}{V_{MC}} = 0$$

$$if \ \frac{\Delta V}{V_D} \geq \frac{\Delta V}{V_{threshold}} \qquad then \ \frac{\Delta V}{V_{MC}} = 5.7x10^{-24}(Ft - f)$$

where
$\Delta V/V_{MC}$ = volume expansion due to microcracking
$\Delta V/V_D$ = volume expansion due to lattice defects
$\Delta V/V_{threshold}$ = microcracking threshold
F = neutron flux, n/cm^2-s (E>1MeV)
t = time, sec
f = microcracking fluence threshold where $\Delta V/V_D = \Delta V/V_{threshold}$

For BeO there is a microcracking threshold ($\Delta V/V_{threshold}$) at which microcracking initiates for a given temperature. When the swelling due to lattice defects ($\Delta V/V_D$) is greater than the microcracking threshold ($\Delta V/V_{threshold}$), microcracking initiates and contributes to the total swelling. The following equation for the microcracking threshold illustrates that microcracking is a function of irradiation temperature.

$$\frac{\Delta V}{V_{threshold}} = 2.16x10^{-3} + 6.27x10^{-6} \cdot T$$

where
$\Delta V/V_{threshold}$ = microcracking threshold
T = temperature, K

Plumlee (Reference (hh)) states that for the temperature range 373K < T <873K, the volume expansion of BeO should be attributed only to defect growth and microcracking. At T>873K helium bubbles begin to form and become a significant mechanism contributing to swelling in BeO above 1173K. Helium bubbles first form at grain boundaries and later with increasing fluence, bubbles begin to form within the grains. Reference (hh) states that He bubble size and density increase with increasing grain size. Helium release from BeO and volume expansion due to He bubbles are difficult to correlate. It was reported in Reference (hh) that substantial experimental data will be required for adequate correlation of the volume expansion due to He bubble formation. For the volume expansion due to helium bubble formation ($\Delta V/V_{He}$) the following equation was proposed, accounting for the theoretical density of the BeO. This equation is based on limited data and more effort is required to verify the theory. This equation assumes that the volume expansion due to He bubble formation varies linearly between 86% and 96% theoretical density (Reference (hh)).

$$\frac{\Delta V}{V_{He}} = 4.40x10^{-24}(0.036D - 2.456)Ft$$

where
F = neutron flux, n/cm^2-s (E>1MeV)
t = time, sec
D = percent of theoretical density

3.13.1 Grain Size Effect on Swelling

Previous irradiation testing results (Reference (hh)) have shown that grain size is a key factor influencing swelling; however the functionality is not known. Testing in Reference (y) has focused on BeO with fine grain sizes (~5 microns) and limited testing of materials with grain size up to 100 microns. Plumlee (Reference (hh)) demonstrated that larger grain sizes decreased the threshold fluence at which microcracking of BeO occurred near room temperature irradiation. Figure 21 shows the neutron dose required to produce microcracking during irradiation at 323 – 373K as a function of grain size. Increased microcracking results in increased swelling. It should be noted that this figure is valid only at lower temperatures (~373K).

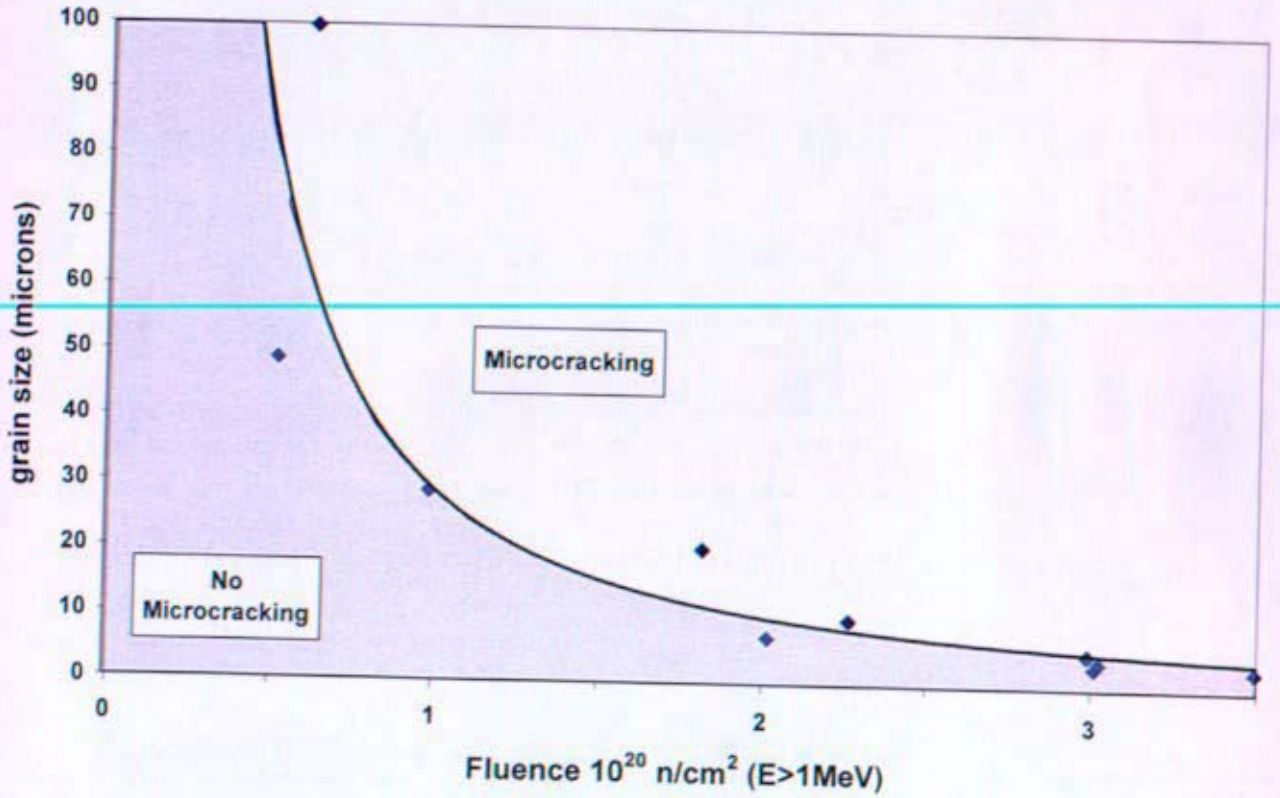

Figure 21: Neutron Dose Required to Produce Microcracking in BeO

3.13.2 Temperature Effect on Swelling

Figure 22 from Plumlee (Reference (hh)) presents data from fine grain size (nominally 5μm, 96%TD) BeO at 373K, 873K and 1273K and the model described in Section 3.13. It is observed that as the irradiation temperature increases the swelling begins to anneal out of the BeO and the swelling rate decreases. Recall that over the temperature range 373 < T < 873 the volume expansion of BeO should be attributed to defect growth and microcracking only. At T>873K helium bubbles begin to form and become a significant mechanism contributing to swelling in BeO above 1173K.

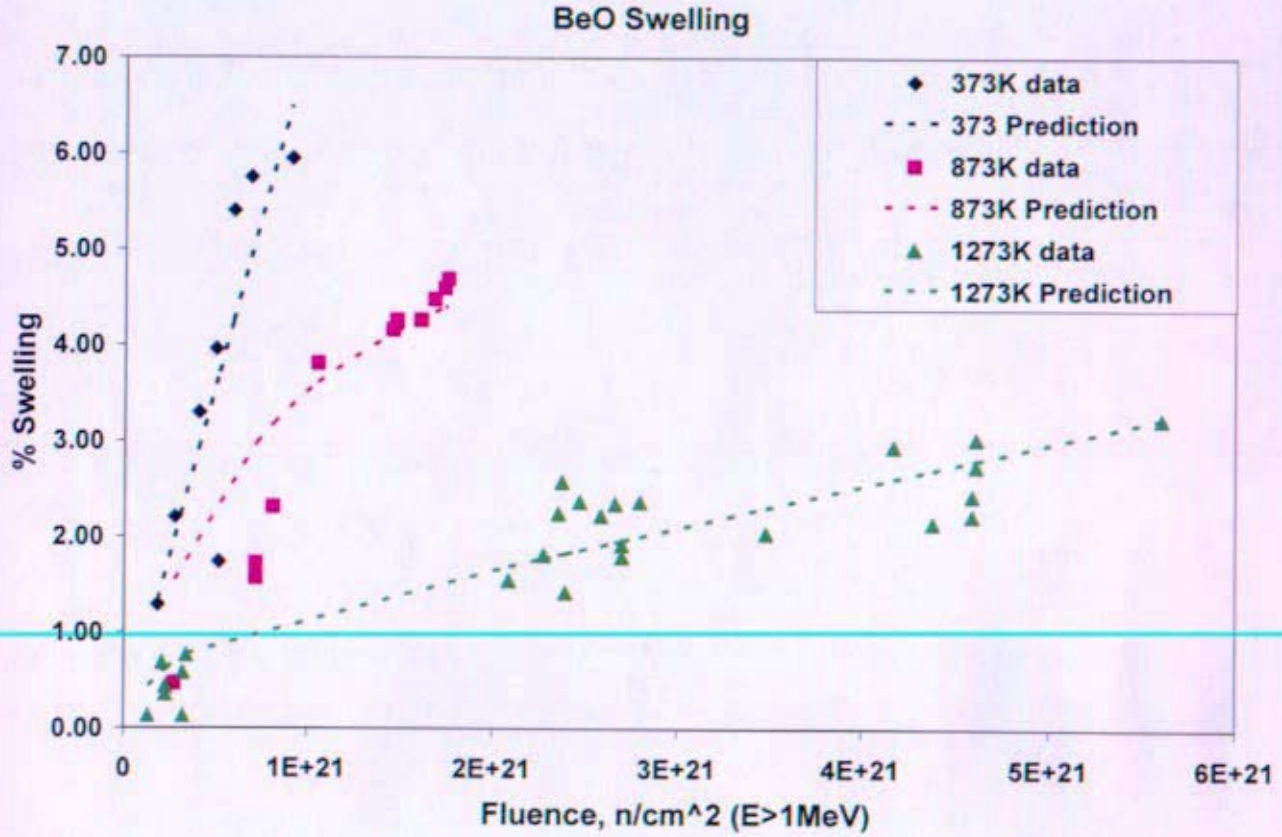

Figure 22: Irradiation Swelling of BeO with Predicted Curves from Plumlee (Reference (hh))

3.13.3 Fluence Effect on Swelling

From Figure 22 (Section 3.13.2), Plumlee (Reference (hh)) reports that as the fluence increases, the swelling in BeO also increases. At lower temperatures (T<873K) increased fluence leads to increased anisotropic swelling and microcracking. At higher temperatures (T>873K) the increasing fluence levels, increase the formation of helium. Irradiation testing was proposed to help identify irradiation behavior and performance such as maximum swelling boundaries at each temperature.

3.13.4 Flux Effect on Swelling

In the definition of volume expansion due to lattice defects ($\Delta V/V_D$), Collins (Reference (bb)) defines the rate of atomic displacements, K, based on lattice expansion data, which increases with flux over a range of ~0.55 – 3.2 x10^{14} n/cm^2-sec (E>1MeV). Therefore, the correlation given for volume expansion due to lattice defects ($\Delta V/V_D$) (Section 3.13), predicts an increase in swelling with increasing flux at constant fluence. It should be noted that for these correlations the rate of atomic displacements, K, only covers a small experimental range of fluxes. It is not clear if the correlation is valid over a broader range than initially defined. Keilholtz, however, reported little dependence on flux at temperatures ≤1373K (flux range of 0.9-2.4x10^{14} n/cm^2-s) (Reference (ii)).

The extent to which flux affects swelling at constant fluence, needs to be confirmed with experimental data. Data from future BeO irradiation testing is required to refine the correlation and better predict swelling over a larger flux range.

3.13.5 *Theoretical Density Effect on Swelling*

There is some evidence to suggest that density plays a role in determining swelling behavior – perhaps due to increased ability to accommodate helium bubble formation, or an increased ability to release helium outside the BeO volume. Plumlee (Reference (hh)) shows that in particular, sub-dense (86% TD) BeO appears to swell less than full dense (95% TD) BeO at higher temperatures (T>1173) and the model by Plumlee overpredicts the swelling. Recall that at T>873K helium bubbles begin to form and become a significant mechanism contributing to swelling in BeO above 1173K. It is expected that for lower temperature applications (T<873K), there may be little advantage to using sub-dense BeO.

3.13.6 Swelling Predictions for BeO

Based on the above correlations for the swelling of BeO, swelling values were extrapolated above the known range of temperatures (373K, 873K and 1273K) and fluences (0.37 – 12x10^{21} n/cm^2). Predictions assumed the same flux level used in Reference (hh), 2.3x10^{14} n/cm^2-s (E>1MeV). Results of these extrapolations yielded results which do not appear to be reasonable based on the limited amount of data. It should be noted that in the literature reviewed, no swelling above ~6% has been observed, however some irradiated samples have disintegrated to powder (Reference (ii)). Future testing is required to validate these predictions over a range of fluxes, fluences, temperatures and BeO grain sizes.

Table 9 summarizes how the various parameters (grain size, temperature, fluence, flux and density) influence the swelling of BeO. References for each parameter are also given.

Table 9: Key Parameters that Effect Irradiation Swelling of BeO

Parameter	Result	Reference
Increasing Grain Size	Increased Swelling	(y) (bb) (hh)
Increasing Temperature (at fixed fluence)	Decreased Swelling	(y) (bb) (hh)
Increasing Fluence (at fixed temperature)	Increased Swelling	(y) (bb) (hh)
Increasing Flux	Increased Swelling (based on correlation)	(y) (bb) (ii)
Increasing % Theoretical density	Increased Swelling (due to He bubble retention) T>1173K	(hh)

4. References

(a) KAPL Letter, MDO-723-0042, "Reflector and Shield Material Properties for Project Prometheus", dated November 2, 2005.
(b) KAPL Letter, SPP-67410-0004 dated December 22, 2004.
(c) Neter, J., M.H. Kutner, C.J. Nachtsheim and W. Wasserman, *Applied Linear Statistical Models* 4th ed., McGraw-Hill (1996).
(d) Scaffidi-Argentina, F., G.R. Longhurst, V. Shestakov and H. Kawamura, "Beryllium R&D for fusion applications", *Fusion Eng. and Design*, **51-52** (2000) 23-41.
(e) Dombrowski, D.E., E. Deksnis and M.A. Pick, "Thermomechanical Properties of Beryllium", Brush Wellman Report TR-1182, February 20, 1995.
(f) SCK CEN Progress report FT/Mol/96-03 ITER Task 23 "Beryllium Characterization: Tensile Tests on Neutron Irradiated and Reference Beryllium", F. Moons, February 1996.
(g) Hickman, B.S., "Radiation Effects in Beryllium and Beryllium Oxide", *Studies in Radiation Effects, Series A Physical and Chemical Vol. 1*, 1966.
(h) Brush Wellman specification, S-65 Structural Grade Beryllium Block, Rev C, July 1, 1987.
(i) Beeston, J.M., "Beryllium Metal as a Neutron Moderator and Reflector Material", *Nuclear Eng. and Design*, **14** (1970) 445-474.
(j) Billone, M.C., "Recommended Design Correlations for S-65 Beryllium", Proceedings 2nd IEA International Workshop on Beryllium Technology for Fusion, September 6-8, 1995 348 – 363.
(k) Snead, L.L., "Low-Temperature Low-Dose Irradiation Effects on Beryllium", *J. Nucl. Mat.*, **326** (2004) 114-124.
(l) Barabash, V., G. Federici, M. Rödig, L.L. Snead and C.H. Wu, "Neutron Irradiation Effects on Plasma Facing Materials", *J. Nucl. Mat.*, **283-287** (2000) 138-146.
(m) Smith, M.F., R.D. Watson, J.B. Whitley and J.M. McDonald, "Thermomechanical Testing of Beryllium for Limiters in ISX-B and JET", *Fusion Technology*, **8** (1985) 1174-1183.

(n) Goods, S.H. and D.E. Dombrowski. 1997. "Mechanical Properties of S-65C Grade Beryllium at Elevated Temperatures", Proceedings of the 3rd IEA International Workshop on Beryllium Technology for Fusion, Mito City, Japan, 22-24 October.

(o) Chaouadi, R., F. Moons and J.L. Puzzolante. 1997. "Tensile and Fracture Toughness Test Results of Neutron Irradiated Beryllium", Proceedings of the 3rd IEA International Workshop on Beryllium Technology for Fusion, Mito City, Japan, 22-24 October.

(p) Gelles, D.S., G.A. Sernyaev, M. Dalle Donne and H. Kawamura, "Radiation Effects in Beryllium used for Plasma Protection", *J. Nucl. Mat.*, **212-215** (1994) 29-38.

(q) Baum, E.M., H.D. Knox, and T.R. Miller. 2002. Nuclides and Isotopes: Chart of the Nuclides, 16th ed. New York: Lockheed Martin.

(r) Dalle Donne, M., F. Scaffidi-Argentina, C. Ferrero and C. Ronchi, "Modeling of Swelling and Tritium Release in Irradiated Beryllium", *J. Nucl. Mat.*, **212-215** (1994) 954-960.

(s) Rabaglino, E., C. Ferrero, J. Reimann, C. Ronchi and T. Schulenberg, "Study of the Microstructure of Neutron Irradiated Beryllium for the Validation of the ANFIBE Code", *Fusion Eng. and Design*, **61-62** (2002) 769-773.

(t) Harrison, K., 2005. Brush Ceramic Products, personal communication, 15 April.

(u) Busboom, H., "Material Properties for Beryllium Oxide (BeO)", GE specification 23A3186, (1989).

(v) Touloukian, Y.S., R.W. Powell, C.Y. Ho and P.G. Klemens, Thermophysical Properties of Matter Vol. 2 (1970) 123.

(w) Francl, J. and W.D. Kingery, "Thermal Conductivity: IX, Experimental Investigation of Effect of Porosity on Thermal Conductivity", *J. Am. Ceram. Soc.*, **37** [2] (1954) 99-107.

(x) Pryor, A.W., R.J. Tainsh and G.K. White, "Thermal Conductivity at Low Temperature of Neutron Irradiated BeO", *J. Nucl. Mat.*, **14** (1964) 208-219.

(y) Hickman, B.S. and A.W. Pryor, "The Effect of Neutron Irradiation on Beryllium Oxide", *J. Nucl. Mat.*, **14** (1964) 96-110.

(z) Snead, L.L. and S.J. Zinkle, "Use of Beryllium and Beryllium Oxide in Space Reactors", ORNL report.

(aa) Touloukian, Y.S., R.W. Powell, C.Y. Ho and P.G. Klemens, Thermophysical Properties of Matter Vol. 13 (1970) 195.

(bb) Collins, C.G., "Radiation Effects in BeO", *J. Nucl. Mat.*, **14** (1964) 69-86.

(cc) Walker, D.G., R.M. Mayer and B.S. Hickman, "X-ray Diffraction Studies of Irradiated Beryllium Oxide", *J. Nucl. Mat.*, **14** (1964) 147-158.

(dd) Touloukian, Y.S., R.W. Powell, C.Y. Ho and P.G. Klemens, Thermophysical Properties of Matter Vol. 5 (1970) 45.

(ee) Hickman, B.S., "Radiation Effects in Beryllium and Beryllium Oxide", *Studies in Radiation Effects, Series A Physical and Chemical Vol. 1*, 1966.

(ff) Elston, J. and C. Labbe, *J. Nucl. Mat.*, **4** (1961) 143-164.

(gg) Touloukian, Y.S., R.W. Powell, C.Y. Ho and P.G. Klemens, Thermophysical Properties of Matter Vol. 8 (1970) 201.

(hh) Plumlee, D.E., "BeO Performance Lessons Learned", SP-100 Program, Martin Marietta, March 2, 1994.

(ii) Keilholtz, G.W., J.E. Lee, Jr. and R.E. Moore, "Irradiation Damage to Sintered Beryllium Oxide as a Function of Fast-Neutron Dose and Flux at 110, 650 and 1100°C", *Nuclear Science and Engineering*, **26** (1966) 329-338.

Attachment B to Enclosure 2 to MDO-723-0046/B-MT(SPME)-23:

Technical Specification for BeO Test Specimen Fabrication
Rev. 12 dated 9/2/05

Author:
James Nash

Reviewed by:
Brian Campbell

TECHNICAL SPECIFICATION FOR BeO TEST SPECIMEN FABRICATION
REV. 12

DATED 9/2/05

1. PURPOSE & SCOPE

The purpose of this specification is to produce BeO test specimen disks and cylinders for irradiation testing.

2. GOVERNMENT FURNISHED MATERIAL

The Buyer shall provide no equipment, tools, parts, raw material, or other material for the fabrication of the deliverables on the project.

3. APPLICABLE SKETCHES

   a. KAPL Sketches: BeO-K-1 (Figure 1), BeO-K-2 (Figure 2), BeO-K-3 (Figure 3), BeO Post Machining Process (Figure 4)

4. MATERIAL SPECIMENS

   a. Fabricate 130 BeO test specimen disks per KAPL Sketch BeO-K-1 and 100 test specimen cylinders per Sketch BeO-K-2. The starting material shall be standard grade BeO BW-1000, fabricated using isostatic processes that produce a nominal 9 micron grain sized finished product. The quality control level shall be standard Brush Ceramic Products (BCP) Visual Defect Criteria Level 1 (Rev. E: August 2001), and Machine Dimensional Tolerances Class 2 (Rev. E: August 2001). BCP shall utilize existing block material (roughly, 20mm x 20mm x 200mm), and then machine the required disks and cylinders from it. Note the 0.25 mm (+/- 0.13mm) 45° chamfers on sketch BeO-K-1 and BeO-K-2 to reduce the risk of cracking and damage during testing. Laser mark 120 of the 130 disk specimens in accordance with Sketches BeO-K-1 and all 100 cylinder specimens in accordance with BeO-K-2 using the identification system discussed below. Note each character is preceded by a dot symbol (•) to orient all as-built measurements per Figures 1 and 2. BCP shall be responsible for all scrap and waste material disposal.

      1) First Piece Inspection

      - As a standard "good engineering practice", in order to reduce the risks of schedular delays, BCP shall perform a quality control inspection of the first specimen produced in any production run to ensure it meets specifications, prior to performing the entire production run.

      2) Specimen Identification

      - Test that all specimens fabricated in step 4a meet the BCP Level 1 and Class 2 Quality Control requirements (Rev. E: August 2001) prior to laser marking.
      - 120 disk specimens and 100 cylinder specimens shall be identified using laser markings as shown in sketches BeO-K-1 and BeO-K-2.
      - Specimens shall be labeled sequentially using the identification scheme indicated in Table 1.
      - 10 disk specimens shall remain unmarked for a comparative study on the effect of laser scribing on thermal diffusivity.

3) Special Machining Instructions

- Compliance with KAPL Specification on detrimental materials is required during all aspects of this fabrication and testing (Attachment 1).
- All specimens shall be identified by a bag and tag method with the ID's and description as noted in Table 1.
  - The ID method for disk samples will be sequenced as follows: B-AAA, B-AAB, B-AAC ... B-ABA, B-ABB...excluding U and Q.
  - The ID method for cylinder samples will be sequenced as follows: AA, AB, AC... BA, BB, BC... excluding U and Q.
- Lot and billet ID shall be identified for each sample (note: it is the buyers preference for all samples to be from the same billet and/or lot, however it is not a requirement).

Table 1: Specimen Identification Sheet

Powder Lot #	Block # (Billet ID)	SPECIMEN TYPE	SPECIMEN ID	Sketch No.
XXXX	XXXX	Disk	•B-AAA to •B-AEZ	BeO-K-1
XXXX	XXXX	Cylinder	•AA to •ED	BeO-K-2

4) Low Temperature Annealing

- All specimens shall receive a low temperature anneal (approximately 1350°C) for approximately 1 hour in dry, flowing air following machining and laser marking to remove machining micro-cracks. This will minimize the chance that the samples fracture during follow-on testing, which could skew the results.
- Per Figure 4 (Sketch BeO Post Machining Process), specimens shall not remain in air at T<100°C for more than 2 hours while mass measurements are performed. If necessary specimens shall be stored in an inert atmosphere, vacuum or desicant.

b. Test and certify that all delivered specimens fabricated in step 4a meet the BCP Level 1 and Class 2 Quality Control requirements (Rev. E: August 2001). All accepted specimens shall be measured for mass (+/- 0.0005 g) and final dimensions (+/- 0.003 mm) (as built values) after laser marking as noted in Table 2.

Table 2: As Built Measurements for Each Sample

Disks

Specimen ID	Mass (g)	D1 (mm)	D2 (mm)	T1 (mm)	T2 (mm)	T3 (mm)	T4 (mm)
•B-AAA to •B-AEZ (excluding U and Q)							

Cylinders

Specimen ID	Mass (g)	D1 (mm)	D2 (mm)	D3 (mm)	D4 (mm)	T1 (mm)	T2 (mm)	T3 (mm)	T4 (mm)
•AA to •ED (excluding U and Q)									

c. In addition to the requirements in step 4b, verify specimen properties as follows:

- Randomly select 5% of the disks and cylinders (total 16) to determine their average grain size per ASTM E-112. These selected specimens shall be disk and cylinder samples with 0.8mm chamfers specified in Technical Specification for BeO Test Specimen Fabrication Rev. 11 dated 7/21/05. Grain size in areas adjacent to laser marking, as well as bulk average shall be determined. BCP shall photograph each measured microstructure, and forward photographs and analysis results to KAPL. Grain size shall be measured at three different locations for each specimen depth as follows: (1) 3 at the surface; (1) 3 at 25% through the thickness; (1) 3 at 50% through thickness (total of 144 micrographs).

d. If already completed, forward the elemental certification for the BeO used to make the specimens. If that analysis has not previously been performed, perform the standard BeO elemental analyses typically reported for BW-1000.
e. Take digital photographs of the specimens from all sides (top, bottom and side) at 5X nominal magnification with a reference unit for measurement (e.g. ruler) included in the photograph. Photographs shall be taken after specimens are verified to be free of surface contamination (cleaned) as described in paragraph 6. All photos shall be at least 3 megapixels in size and TIFF format.

5. GRAIN SIZE REDUCTION RUNS

a. Perform 3 grain size reduction runs in a small-scale research program fashion. The starting material shall be standard grade BeO powder used to produce BW-1000. BCP shall target a reduction in the grain size to 5 +/- 2 micron average grain size in a final processed block as shown in sketch BeO-K-3. Should this be successful, the material will hereafter be referred to as BW-1000K. The research process shall proceed generally as follows:
    1. Make minor adjustments to the starting material and process as part of the research as needed.
    2. Complete processing of the block(s).
    3. Measure the grain size in accordance with step 4.c. (surface, 25% through thickness and 50% through thickness in 3 different locations totaling 9 measurements each run), except the block (per Sketch BeO-K-3) can be used rather than cylinders or disks, and laser marking is not required.
    4. Discuss the results with KAPL prior to runs 2 and 3.
    5. Perform all 3 runs regardless of success or failure.
    6. Repeat step 4d for the product from the run that produced the grain size closest to 5 microns and identify and quantify any non-standard additives not normally tested.

6. CLEANING

a. All samples shall be cleaned and a subset shall be tested for surface contamination per Figure 4 (BeO Post Machining Process).
    1. Immersion in HNO_3
    2. Neutralizing agent soak
    3. Immersion in H_3PO_4
    4. DI water rinse
b. Wet swipe testing will be performed on 19 specimens to verify acceptable levels of loose contamination on the surface of cleaned parts.
    - Specimens used for swipe testing shall be cylinders and discs with 0.8mm chamfers specified in Technical Specification for BeO Test Specimen Fabrication Rev. 11 dated 7/21/05.
    - Surface contamination must be $\leq 0.25\ \mu g/100cm^2$
    - Samples with surface contamination $> 0.25\ \mu g/100cm^2$ shall be re-cleaned and tested until levels are below the specified limit.

c. BCP is responsible for disposal of all 19 surface contamination test specimens each time cleaning is repeated per Figure 4 (Sketch BeO Post Machining Process) and all waste associated with cleaning and swipe testing.

7. BAKE OUT

a. Only after specimens are cleaned and certified to be free of loose surface contamination (6.a and 6.b), can the specimens be baked out.
b. Specimens shall be baked out in a nitrogen (≥ 99.999%) atmosphere furnace at 400°C. This equipment shall remain dedicated to fabrication of KAPL Inc specimens until released by KAPL Inc, or 2 years after termination of work contracted by KAPL Inc., whichever comes first.
   - Ramp at 10°C/minute
   - Hold at 400 ± 20°C for 3 hours ± 30 minutes.
   - Cool at 10°C/minute or slower.
c. Specimens shall be placed on BeO furnace furniture which has been cleaned using step 6.a above.
d. Per Figure 4 (Sketch BeO Post Machining Process), specimens shall not remain in air at T<100°C for more than 2 hours prior to packaging in an inert atmosphere. If necessary specimens shall be stored in an inert atmosphere, vacuum or desiccant.

8. SHIPPING

a. All samples shall be individually packaged in an inert environment, and ensuring they will not be lost or damaged in shipment. Packaging shall be transparent to allow specimen numbers to be readable through the packaging. The specimen ID shall also be written on the outside of each package.
b. Seller shall ensure there is no loose BeO contamination on the outside of any packaging, and seal groups of individual packages within larger overall bags.
c. BCP shall select 40 disks and 20 cylinders of BW-1000 specimens and obtain KAPL concurrence prior to shipment. BCP shall ship samples in five boxes (each with 8 disks and 4 cylinders) to Bettis.
d. BCP shall ship the remaining specimens in two boxes (one with disks and one with cylinders) to KAPL unless otherwise directed.

9. REPORTING

10. DATA SUBMITTALS

a. Data required for submittal (Table 3):

Table 3: Data Required for Submittal

Description (Reference Paragraph)	No. of Copies	Date Due	Type
Specimen Identification Sheet (Table 1, Par. 4.a.3)	2	Prior to shipment	Information
Final As Built Measurements (Table 2, Par. 4.b)	2	Prior to shipment	Information
Grain Size Measurements (including micrographs), (Par. 4.c)	2	As soon as available	Information
Elemental Certification (Par. 4.d)	2	As soon as available	Information
Digital photographs of specimens after cleaning (Par. 4.e)	2	As soon as available	Information
BW-1000 Technical Report (Par. 11 and Par. 13)	2	Prior to shipment	Information
BW-1000K Technical Report (Par. 11 and Par. 13)	2	Prior to shipment	Information
BW-1000K Grain Size Reduction Runs (Par. 5 and Par. 11)	2	Prior to Run 2	Information
Thermal diffusivity and specific heat of 10 unmarked disks and 10 laser marked disks (Par. 13)	2	Prior to shipment	Information
Results from wet swipe testing done on 19 specimens ($\mu g/cm^2$) (Par. 6.b)	2	Prior to shipment	Information
Manufacturing Process Documentation (Par. 11)	2	Prior to shipment	Information
Certification of Compliance with KAPL specification on detrimental materials (Par. 13)	2	Prior to shipment	Information
Option 1 – BW-1000K documentation of samples (Par. 4 and Par. 13)	2	Prior to shipment	Information
Option 2 – Materials Property Testing Report for BW-1000 (Par. 13)	2	At conclusion of testing	Information
Option 3 – Materials Property Testing Report for BW-1000K (Par. 13)	2	At conclusion of testing	Information

11. MANUFACTURING PROCESS DOCUMENTATION

The Seller shall provide to the Buyer a detailed description of the fabrication process used to manufacture the BW-1000 and BW-1000K specimens, noting proprietary information as appropriate. This document shall include where available:

- Raw material chemical analysis;
- Binder, grain growth inhibitors, sintering agents, etc... used (if any);
- BeO feedstock grain size;
- Compacting protocol, including press pressure, hold time, and other process parameters;
- Drawings or sketches for the compaction tooling (punch and die);
- Punch lubricant, chemical composition, identification numbers and vendor;
- Sintering protocol, including hold time and temperature, and time vs. temperature plots;
- Cutting tool identification numbers and vendor;
- Cutting fluid identification numbers and vendor;

- General machining feeds, speeds, and depths of cut; and
- Final-pass feeds, speeds, and depths of cut for each specimen.
- Provide sketches of the orientation of the specimens relative to the original billet.

12. OPTIONS

KAPL retains the right to exercise the following optional tasks.

OPTION 1: Using the optimum material processing steps determined during step 5.a in terms of being most likely to produce BeO specimens with 5 +/- 2 micron grain size (BW-1000K), fabricate 130 disks and 200 cylinders in accordance with step 4. Identify disk specimens with id's starting at B-AKA and cylinders with id's starting at FA.

OPTION 2: MATERIALS PROPERTY TESTING using BW-1000 Samples: Using either the samples used in step 4.c, or other spare samples or representative product from step 4a, perform a minimum of 5 runs (except where noted below) of each of the following materials characterization tests using the nominal temperature range: 300 to 1250K except as noted below. The seller shall dispose of the samples following testing.

1. Coefficient of thermal expansion per ASTM E-228-95
2. Thermal diffusivity using laser flash method per ASTM E-1461-01
   - Measure thermal diffusivity and specific heat of 10 unmarked disks and 10 laser marked disks.
3. Specific heat per ASTM C-351-92b
4. Density per ASTM C-373-88
5. Compressive strength per ASTM C-773-88 (10 samples at each of the 5 temperatures – Room Temperature, 650K, 850K, 1050K and 1250K.

OPTION 3: MATERIALS PROPERTY TESTING using BW-1000K Samples: Using either the samples used in step 4.c, or other spare samples or representative product from step 4a, perform a minimum of 5 runs (except where noted below) of each of the following materials characterization tests using the nominal temperature range: 300 to 1250K except as noted below. The seller shall dispose of the samples following testing.

1. Coefficient of thermal expansion per ASTM E-228-95
2. Thermal diffusivity using laser flash method per ASTM E-1461-01
   - Measure thermal diffusivity and specific heat of 10 unmarked disks and 10 laser marked disks.
3. Specific heat per ASTM C-351-92b
4. Density per ASTM C-373-88
5. Compressive strength per ASTM C-773-88 (10 samples at each of the 5 temperatures – Room Temperature, 650K, 850K, 1050K and 1250K.

13. DELIVERABLES

- 230 BeO specimens using standard BW-1000 BeO starting powder fabricated in accordance with step 4.
  - 130 BeO disks per sketch BeO-K-1
  - 100 BeO cylinders per sketch BeO-K-2
- Samples shipped in accordance with step 8 (130 disks and 100 cylinders) to Bettis (Par. 8.c) and KAPL (Par. 8.d).
- Certifications of Compliance with KAPL specification on detrimental materials.
- Elemental certifications for BeO material.
- Final dimensions and mass measurements for each specimen.

- Test data, delivered in hard copy (figure and tabular) and on CD including electronic micrographs of the samples and tabular data in Microsoft Excel format.
- Manufacturing process documentation as described in step 11.
- Final report (PDF format) documenting all technical aspects of BW-1000 and efforts related to BW-1000K development including but not limited to material processing and grain size reduction efforts, shall be provided.

OPTION 1 Deliverables:

- 330 BeO specimens using BW-1000K BeO fabricated in accordance with step 4.
  - 130 BeO disks per sketch BeO-K-1
  - 200 BeO cylinders per sketch BeO-K-2
- Samples shipped in accordance with step 8 (130 disks and 200 cylinders) to KAPL or as otherwise directed.
- Certifications of Compliance with KAPL specification on detrimental materials.
- Elemental certifications for BeO material.
- Final dimensions and mass measurements for each specimen.
- Data, delivered in hard copy (figure and tabular) and on CD including electronic micrographs of the samples and tabular data in Microsoft Excel format.
- Final report (PDF format) documenting all technical efforts related to BW-1000K development including but not limited to material processing and grain size reduction efforts, shall be provided.

OPTION 2 Deliverables:

- Material property report on BW-1000 material.
- Data, delivered in hard copy (figure and tabular) and on CD including electronic micrographs of the samples and tabular data in Microsoft Excel format.

OPTION 3 Deliverables:

- Material property report on BW-1000K material.
- Data, delivered in hard copy (figure and tabular) and on CD including electronic micrographs of the samples and tabular data in Microsoft Excel format.

14. DELIVERY

The Seller shall be responsible for all shipping documentation, packaging, shipping costs, and compliance with all hazardous material requirements (if required).

15. DELIVERY DATE

The delivery date shall be specified on the purchase order.

16. KAPL TECHNICAL CONTACT

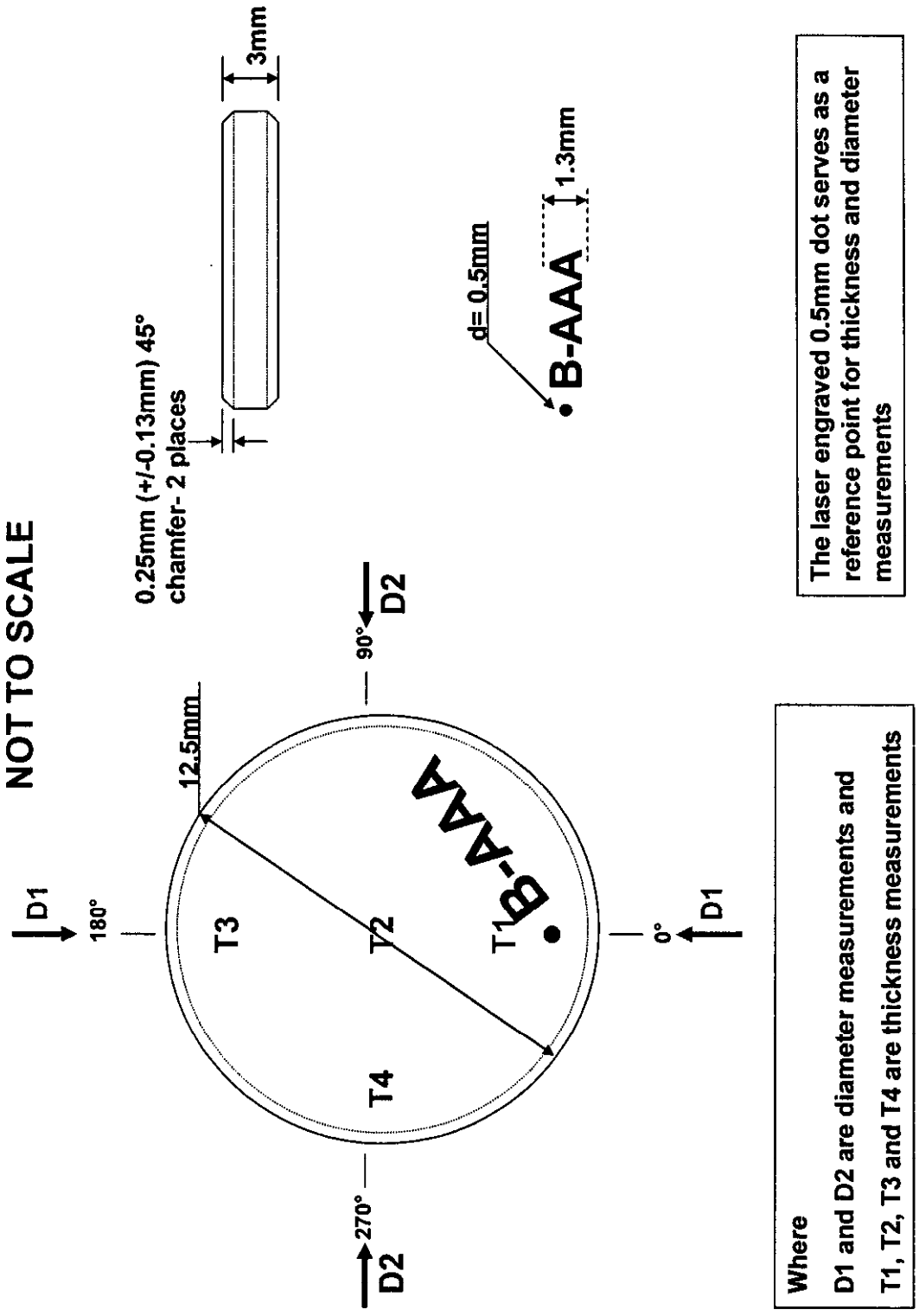

Figure 1: Sketch BeO-K-1: BeO Disks. [BCP Visual Defect Criteria Level 1 (Rev. E: August 2001), and Machine Dimensional Tolerances Class 2 (Rev. E: August 2001)]

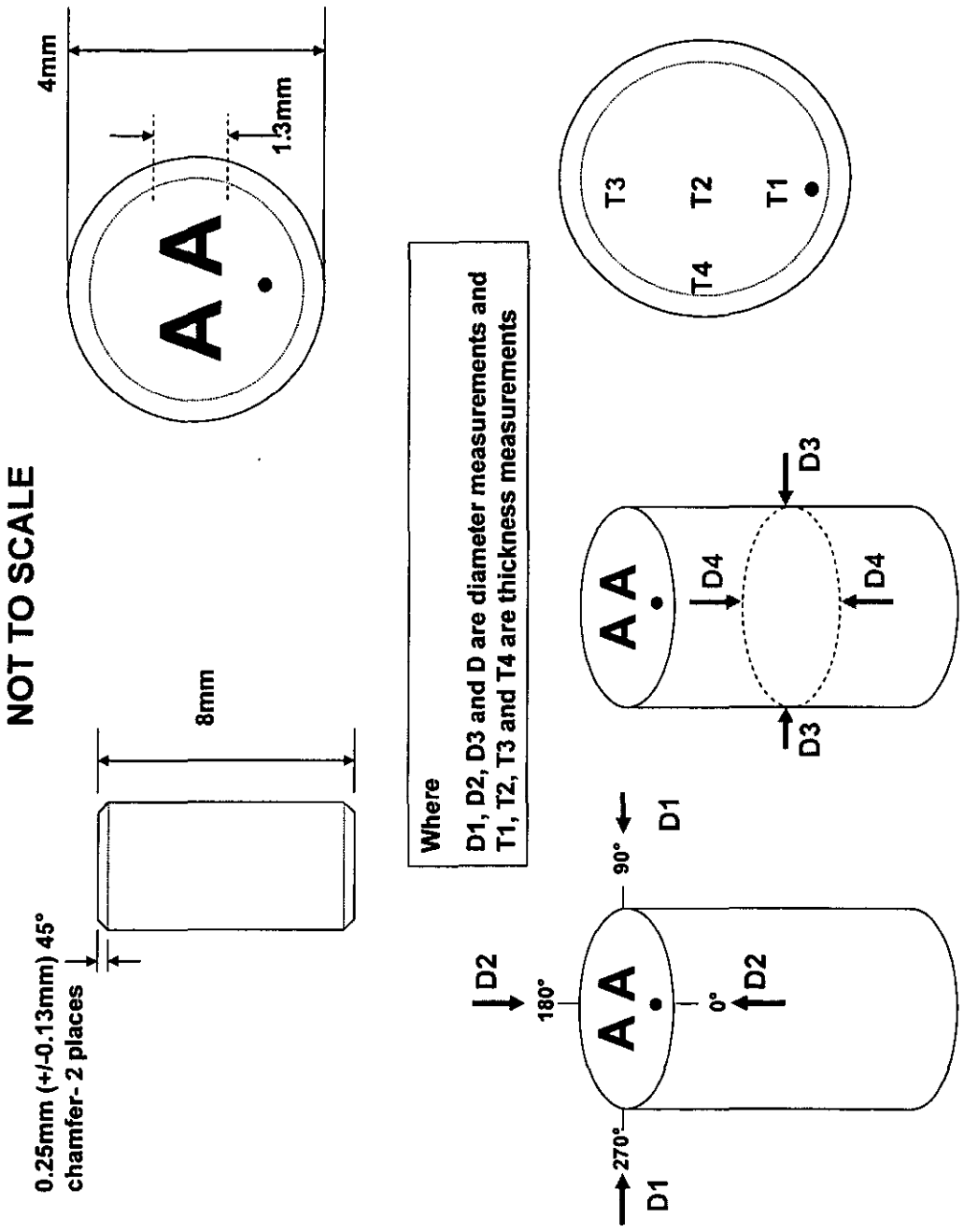

Figure 2: Sketch BeO-K-2:BeO Cylinders. [BCP Visual Defect Criteria Level 1 (Rev. E: August 2001), and Machine Dimensional Tolerances Class 2 (Rev. E: August 2001)]

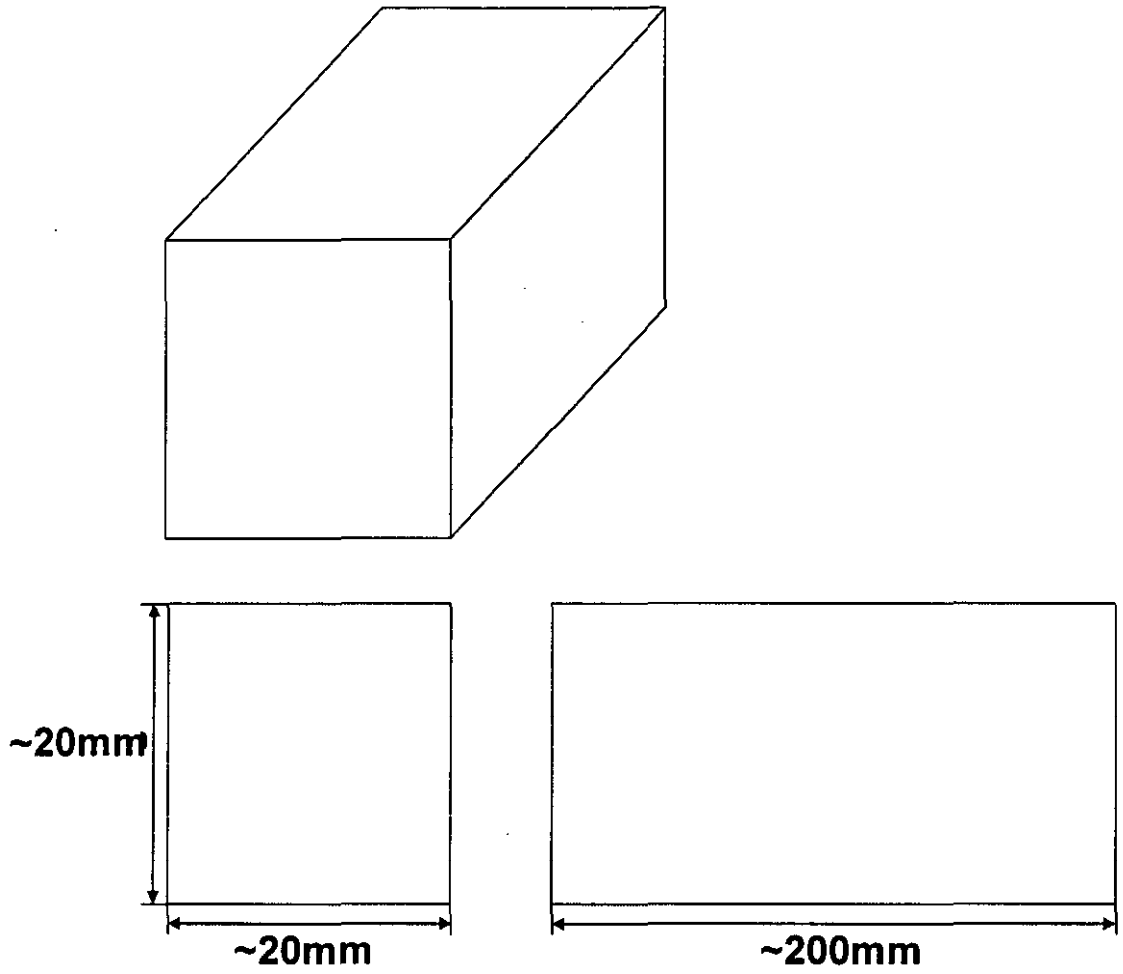

Figure 3: Sketch BeO-K-3: BeO Full Size Part. (Not to scale).

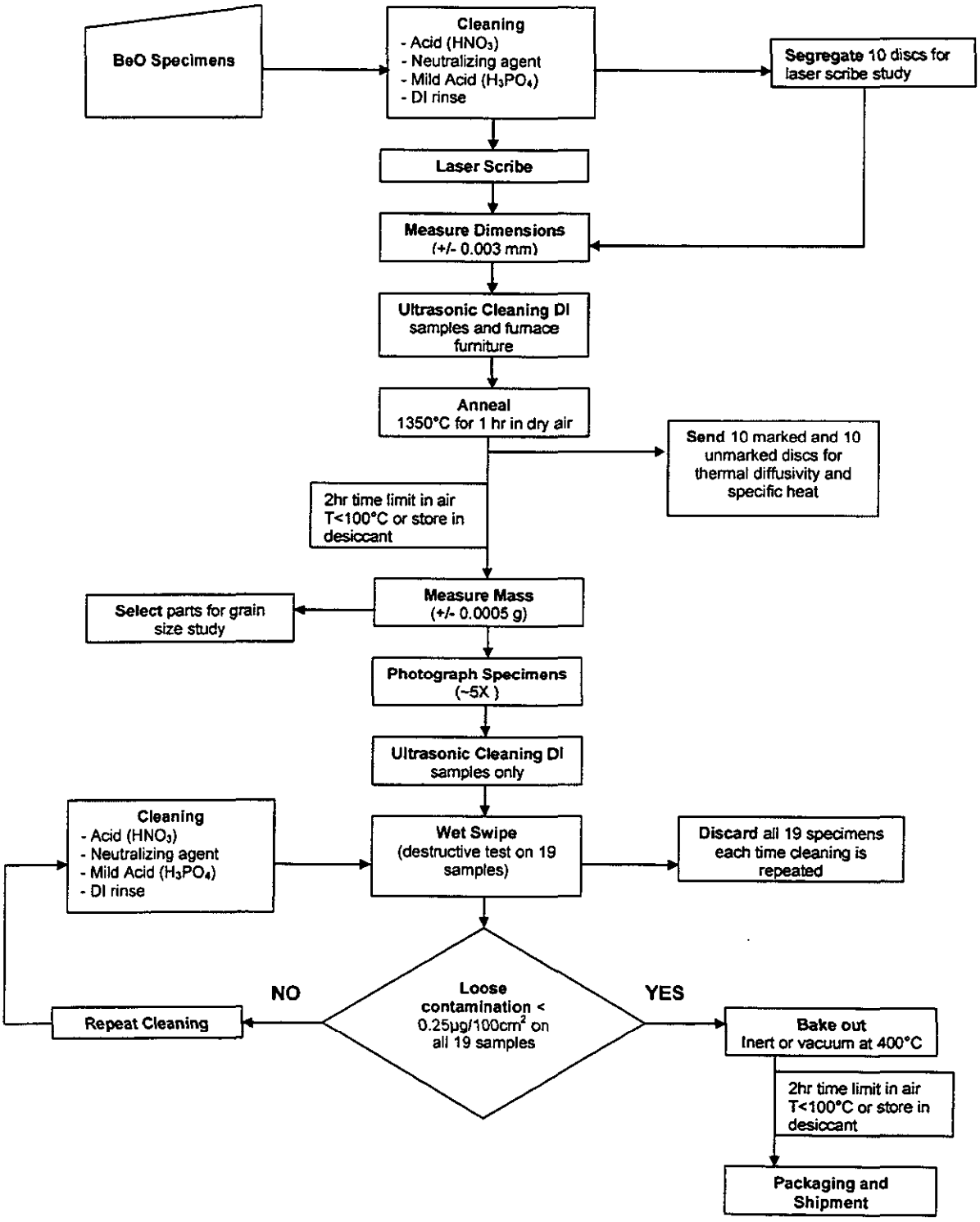

Figure 4: Sketch BeO, Post Machining Process

Attachment 1 to Technical Specification for BeO Test Specimen Fabrication, dated 5/24/05

Detrimental Materials Prohibitions and Restrictions for BeO Materials

Certain chemical elements in contact with a test specimen may cause premature failure of the specimen under test. Those chemical elements known as detrimental materials must not be allowed to contaminate the specimens at any time before or during the test. Therefore, the specimens must be guarded against contamination from detrimental materials during such activities as manufacturing, packaging, shipping, inspection, or testing.

1.0 During the machining, handling, storage, or shipping of specimens, the specimens shall not come in direct contact with:

1.1 Mercury, compounds containing mercury in excess of 10 ppm, or any mercury-containing device employing a single boundary of containment.

1.2 Lead or compounds containing lead in excess of 250 ppm.

1.3 Cadmium, particularly cadmium plated tools or hardware, or alloys containing more than one percent cadmium, or compounds containing more than 250 ppm cadmium.

1.4 Compounds containing halogens in excess of 250 ppm (total where fluorine is restricted to 25 ppm) except lubricants used in machining.

1.5 Salt, or saline solutions, or any solid surface that may introduce alkali metals (e.g., sodium, potassium, lithium).

1.6 Compounds with molybdenum disulfide in excess of 250 ppm.

2.0 Compounds with compositions listed below shall not directly contact specimen surfaces after final machining.

2.1 Compounds containing more than 250 ppm of any of the following antimony, bismuth, copper, phosphorus, sulfur, tin, zinc, total halogens (except that total fluorine shall be restricted to a maximum of 25 ppm).

2.2 Nuclear poisons (e.g., boron) in excess of 100 ppm.

2.3 Liquids which are not water-soluble except as allowed in Paragraphs 5.1 and 5.2.

3.0 Thread sealants, such as teflon tape, teflon jam nuts, or epoxy resins shall not be used to affix or secure specimens to fixtures.

4.0 Aluminum, copper, nickel, and alloys of these materials containing more than 50 percent aluminum, copper, or nickel shall not be used as soft pads, hammers, or tools which contact the specimens during or subsequent to final machining.

5.0 Solvent and Cleaning Solution Requirements:

5.1 Solutions having a pH of less than 6 at the temperature at which they are to be used shall not be used to clean parts with inaccessible areas.

5.2 All halogenated cleaning solutions (250 ppm or more halogens, with fluorine restricted to 25 ppm) are prohibited from use.

6.0 Temperature indicating crayons, marking materials (including white-out) lubricants and low melting alloys shall not contact the final machined surfaces of the specimens if they contain:

6.1 More than 250 ppm of any of the following antimony, arsenic, bismuth, copper, phosphorus, sulfur, tin, zinc, and total halogens (except that fluorine shall be restricted to a maximum of 25 ppm).

6.2 Metals or alloys which melt at 1000 degrees F or less (e.g., Cerrolow, Kirksite, Cerrobend, and cadmium).

7.0 Test and machining fixtures and other components, which directly contact the final machined surfaces of the specimens shall not come in direct contact with items specified in Paragraph 1.0. If fixtures have previously contacted the items specified in Paragraph 1.0, then rigorous cleaning (such as by acid pickling) is required prior to use on the specimens.

8.0 Bench tops and work surfaces upon which the final machined specimens will be placed shall be covered by KimPak creped wadding paper (Kimberly-Clark Co.) or a similar product prior to use.

9.0 Seller shall provide a statement of conformance with the requirements of this specification.

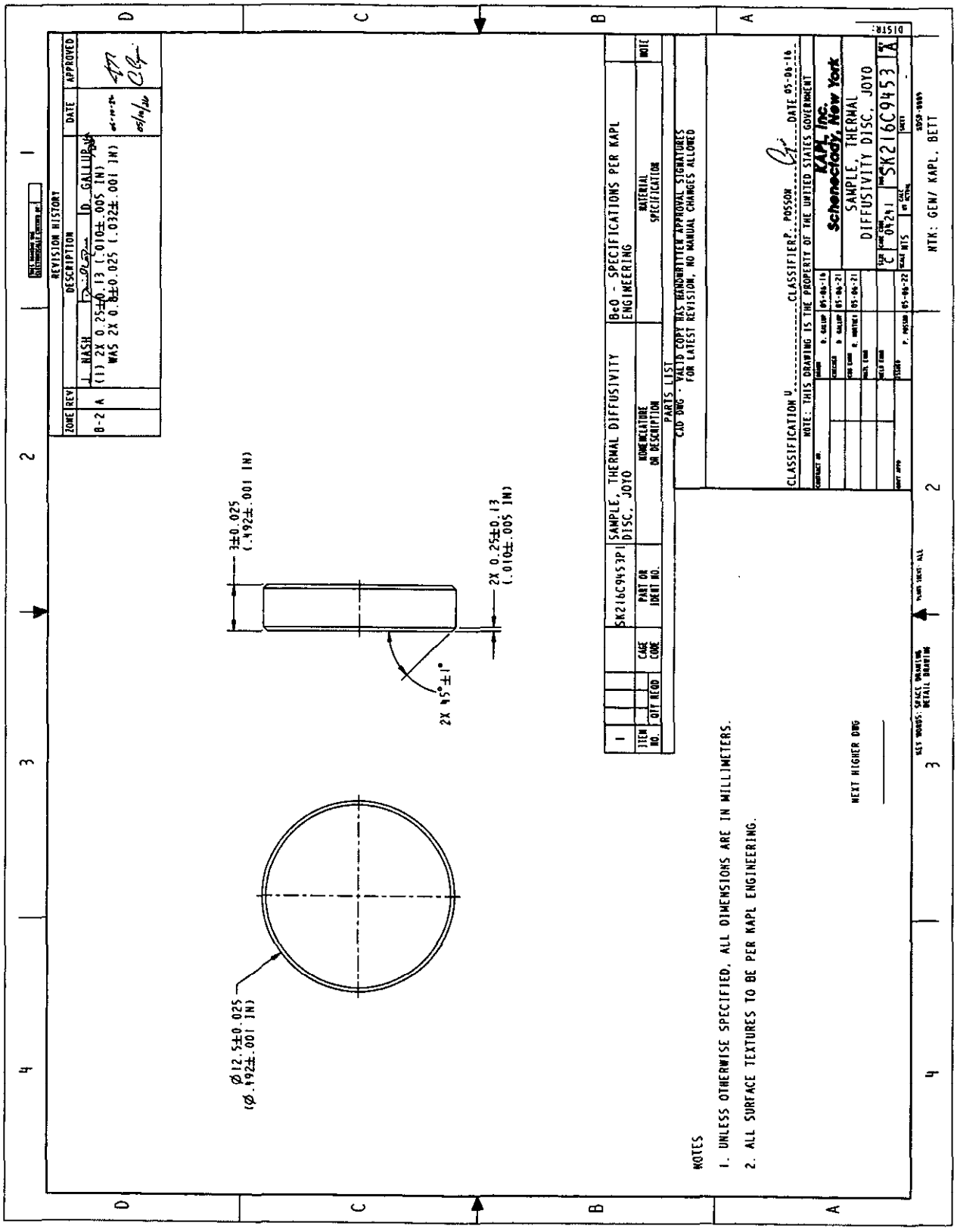
REVISION HISTORY
ZONE REV DESCRIPTION DATE APPROVED
B-2 A (1) 2X 0.25±0.13 (.010±.005 IN) WAS 2X 0.8±0.025 (.032±.001 IN) J. NASH D. GALLUP 05-06-16
PARTS LIST
ITEM NO. QTY REQD CAGE CODE PART OR IDENT NO. NOMENCLATURE OR DESCRIPTION MATERIAL SPECIFICATION NOTE
1 1 SK216C9453P1 SAMPLE, THERMAL DIFFUSIVITY DISC, JOYO BeO - SPECIFICATIONS PER KAPL ENGINEERING
CAD DWG - VALID COPY HAS HANDWRITTEN APPROVAL SIGNATURES FOR LATEST REVISION, NO MANUAL CHANGES ALLOWED
CLASSIFICATION: U CLASSIFIER: P. POSSON DATE 05-06-16
NOTE: THIS DRAWING IS THE PROPERTY OF THE UNITED STATES GOVERNMENT
KAPL, Inc. Schenectady, New York
SAMPLE, THERMAL DIFFUSIVITY DISC, JOYO
SK216C9453
SIZE A
SCALE NTS
SHEET
NTK: GEN/ KAPL, BETT
3±0.025 (.492±.001 IN)
2X 0.25±0.13 (.010±.005 IN)
2X 45°±1°
Ø12.5±0.025 (Ø.492±.001 IN)
NOTES
1. UNLESS OTHERWISE SPECIFIED, ALL DIMENSIONS ARE IN MILLIMETERS.
2. ALL SURFACE TEXTURES TO BE PER KAPL ENGINEERING.
NEXT HIGHER DWG

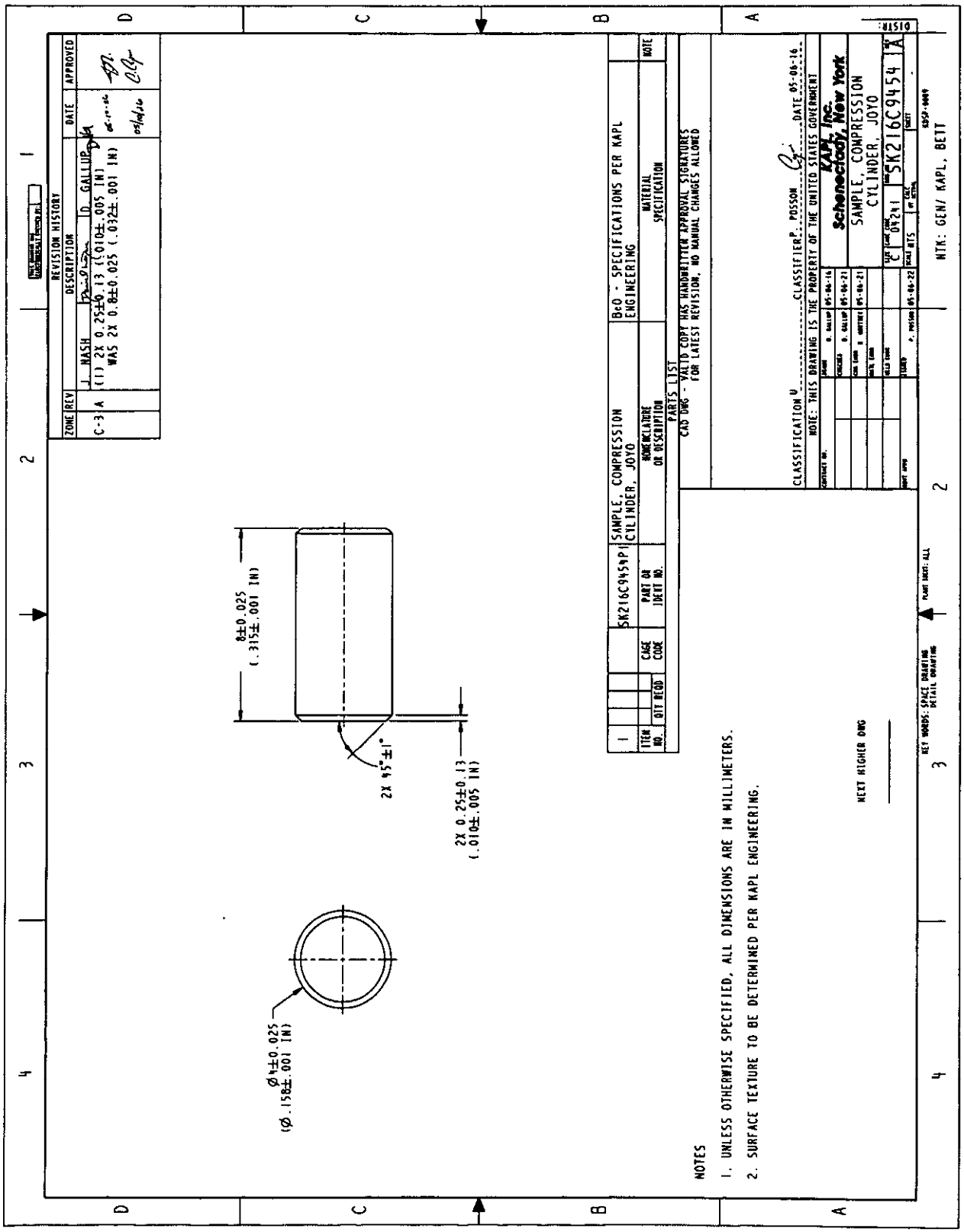
REVISION HISTORY
ZONE REV DESCRIPTION DATE APPROVED
C-3 A J. NASH D. GALLUP
(1) 2X 0.25±0.13 ((.010±.005 IN)
WAS 2X 0.8±0.025 (.032±.001 IN)
8±0.025
(.315±.001 IN)
2X 45°±1°
2X 0.25±0.13
(.010±.005 IN)
Ø1±0.025
(Ø.158±.001 IN)
SK216C9454P1
SAMPLE, COMPRESSION
CYLINDER, JOYO
B&O - SPECIFICATIONS PER KAPL
ENGINEERING
PARTS LIST
CAD DWG - VALID COPY HAS HANDWRITTEN APPROVAL SIGNATURES
FOR LATEST REVISION, NO MANUAL CHANGES ALLOWED
CLASSIFICATION U
CLASSIFIER P. POSSON
DATE 05-06-16
NOTE: THIS DRAWING IS THE PROPERTY OF THE UNITED STATES GOVERNMENT
KAPL, Inc.
Schenectady, New York
SAMPLE, COMPRESSION
CYLINDER, JOYO
SK216C9454
NOTES
1. UNLESS OTHERWISE SPECIFIED, ALL DIMENSIONS ARE IN MILLIMETERS.
2. SURFACE TEXTURE TO BE DETERMINED PER KAPL ENGINEERING.
NEXT HIGHER DWG
NTK: GEN/ KAPL, BETT

Attachment C to Enclosure 2 to MDO-723-0046/B-MT(SPME)-23:

Brush Ceramic Products Material Data Sheet
Isopressed Ceramics CDI-20, Rev. E

Brush Ceramic Products
Tucson, AZ
www.brushceramics.com

This Page Intentionally Left Blank

BeO

BRUSH CERAMIC PRODUCTS

Isopressed Ceramics CDI-20, Rev. E

1.0 General Provisions

1.1 Brush Ceramic Products, Inc. will provide written Certification of Compliance to this specification upon request.

1.2 Normal inspection is performed in accordance with ANSI/ASQ Z1.4-1993.

1.3 The term "Lot" is defined to include parts formed from the same powder batch and fired in the same kiln firing.

1.4 Visual defects are defined according to ASTM F-109.

1.5 All dimensions are interpreted per ASME Y14.5 M 1994.

1.6 The products produced to this specification are required to meet all the values listed in Section 2, 3, 5, 6 & 7. The properties tested in Section 4 are offered as typical properties of the ceramic and are not evaluated on a lot-to-lot basis, unless otherwise noted.

1.7 For areas not covered by this specification ASTM F-356-91 applies. (Standard Specification for Beryllia Ceramics for Electronic and Electrical Applications).

1.8 Unless otherwise stated on the purchase order, all Isopressed Ceramic will be manufactured and inspected to Dimensional Class 3 as per Section 7.0 and Visual Level 3 as per Section 6.0.

2.0 Chemical Composition

(Powder Batch)

2.1 Beryllium Oxide (BeO) is usually described as 99.5% minimum. The 99.5% minimum is defined to be 100 percent minus the total percentage of metallic impurities. The metallic impurity content is determined by emission spectroscopy.

3.0 Test Conditions

3.1 All physical, mechanical and electrical testing are performed at room temperature, except where noted.

4.0 Typical Properties

Property	Test Method	Value
4.1 Chemical		
4.1.1 BeO Content	Spectrographic by difference	99.5% min.
4.2 Thermal		
4.2.1 Coefficient of Thermal Expansion	ASTM E-228-95	(25-1000 deg. C), 9.0 x 10^{-6}/°C
4.2.2 Conductivity	Laser Flash Method	@ 25 deg. C 285 W/mK @ 100 deg. C 220 W/mK @ 150 deg. C 180 W/mK
	Axial Rod Method (Ref. ASTM C-408-88)	@ 25 deg. C 251 W/mK @ 100 deg. C 188 W/mK @ 150 deg. C 150 W/mK
4.2.3 Specific Heat	ASTM C-351-92b	0.25 cal./(gm. C)
4.3 Electrical		
4.3.1 Dielectric Constant	ASTM D-150-95 ASTM D-2520-95	@ 1 MHz 6.76 @ 9.3 GHz 6.67
4.3.2 Dissipation Factor	ASTM D-150-95 ASTM D-2520-95	@ 1 MHz 0.0004 Max. @ 9.3 GHz 0.004 Max.
4.3.3 Volume Resistivity	ASTM D-257-93	>10^{14} ohm-cm
4.3.4 Dielectric Strength	ASTM D-116-86	¼" (6.35 mm) thick 230V/mil
4.4 Physical		
4.4.1 Density	ASTM C-373-88	2.85 g/cm³, Minimum Average
4.4.2 Hardness	ASTM E-18-96	Rockwell 45N 60 min.
4.4.3 Average Grain Size**	Linear Intercept Method (Ref. ASTM E-112-96)	15 to 25 microns (standard parts) 20 to 40 microns (massive parts)
4.4.4 Impenetrability, Liquid	ASTM E-165-95 or Other Dye Penetrants	Impervious
4.5 Mechanical		
4.5.1 Flexural Strength**	ASTM F-417-78	(15-25 µm Grain Size) 30,000 psi Min. Average (15-25 µm Grain Size) 25,000 psi Min. Average
4.5.2 Modulus of Elasticity	ASTM C-623-92	50 x 10^6 psi
4.5.3 Poisson's Ratio	ASTM C-565-93	0.26
4.5.4 Tensile Strength	ASTM C-565-93	18,000 psi
4.5.5 Compressive Strength	ASTM C-773-88	225,000 psi
4.6 Gas Impenetrability	He-Mass Spectrometer	10^{-8} cc/sec. Helium

** *Due to geometry and size of specific parts, the grain size and flexural strength may vary from nominal values.*

4.7 Large Parts

Parts which require especially long firing cycles due to their size have coarser grains and lower mechanical strength. Such parts typically include machining stock or parts whose dimensions exceed one inch (25.4 mm).

There may be variation of properties within large parts. The outgoing quality of the large parts is required to conform to the bulk or sampled properties set forth below. Variation within the large parts not detected in the above tests is considered normal to this product and is not cause for return or rejection.

On the basis of bulk testing or limited sampling of material near the surface, the large parts shall meet the following properties:

- *Bulk Density 2.85 g/cc min.*
- *Grain Size 15 to 40 µm average*
- *Flexural Strength 25,000 psi minimum average.*

5.0 As-Fired Dimensional Tolerances

Dimensional Tolerances	Class 1 Machined Before Firing	Class 2 As Pressed	Class 3 As Pressed
5.1 Tubes and Rods			
5.1.1 Outside diameter	±1% NLT 0.005" (0.127 mm)	±2% NLT 1/16" (1.5875 mm)	±6% NLT 1/8" (3.175 mm)
5.1.2 Inside diameter	±1% NLT 0.003" (0.0762 mm)	±1½% NLT 0.005" (0.127 mm)	±2% NLT 0.010" (0.254 mm)
5.1.3 Length	±1% NLT 0.005" (0.127 mm)	±4% NLT 1/16" (1.5875 mm)	±6% NLT 1/8" (3.175 mm)
5.1.4 Concentricity	±1% NLT 0.005" (0.127 mm)	±5% NLT 0.010" (0.254 mm)	±10% NLT 0.025" (0.635 mm)
5.1.5 Camber, Max.	0.001 in/in	0.003 in/in	0.006 in/in
5.1.6 Ellipticity (roundness)	Within dimensional tolerances		
5.2 Bars, Plate, Blocks			
5.2.1 Width & Thickness	±1% NLT 0.005" (0.127 mm)	±4% NLT 1/16" (1.5875 mm)	±6% NLT 1/8" (3.175 mm)
5.2.2 Length	±1% NLT 0.005" (0.127 mm)	±4% NLT 1/16" (1.5875 mm)	±6% NLT 1/8" (3.175 mm)
5.2.3 Flat & Parallel	Within dimensional tolerances		
5.2.4 Bolt Pattern	±0.020" (0.508 mm)	±0.020" (0.508 mm)	±0.020" (0.508 mm)

Note 1. Bars, Plates & Blocks have 1/8" (3.175 mm) nominal radius.
Note 2. For extreme thin sections, some exceptions may be required.

6.0 Visual Defect Criteria

Visual Defects ASTM F-109	Machined Level 1 Max.	Machined Level 2 Max.	As Fired Blank Level 3 Max.
6.1 Blemish	None	0.030" (0.762 mm)	0.100" (2.54 mm)
6.2 Blister	None	0.015" (0.381 mm)	0.030" (0.762 mm)
6.3 Burr, Fin Flash	None	None	Within Dimensional Tolerances
6.4 Chip (open or closed) Chip length unlimited			
6.4.1 Parts up to 0.5" (12.7 mm) length or diameter	0.015" W x 0.015" D (0.381 mm W x 0.381 mm D)	0.020" W x 0.020" D (0.508 mm W x 0.508 mm D)	Within Dimensional Tolerances
6.4.2 Parts 0.5" to 1.0" (12.7 mm to 25.4 mm) length or diameter	0.020" W x 0.020" D (0.508 mm W x 0.508 mm D)	0.030" W x 0.030" D (0.762 mm W x 0.762 mm D)	Within Dimensional Tolerances
6.4.3 Parts 1.0" to 2.0" (25.4 mm to 50.8 mm) length or diameter	0.025" W x 0.025" D (0.635 mm W x 0.635 mm D)	0.040" W x 0.040" D (1.016 mm W x 1.016 mm D)	Within Dimensional Tolerances
6.4.4 Parts over 2.0" (50.8 mm) length or diameter	0.030" W x 0.030" D (0.762 mm W x 0.762 mm D)	0.050" W x 0.050" D (1.27 mm W x 1.27 mm D)	Within Dimensional Tolerances
6.5 Cracks & Lamination	None	Less than 0.015" (0.381mm) into part	Within Dimensional Tolerances
6.6 Grinding Marks	Within surface finish tolerance	Within surface finish tolerances	N/A
6.7 Inclusion	None	0.010" (0.254 mm)	0.030" (0.762 mm)
6.8 Pit, Pock, Hole, Porous Area	0.015" (0.381 mm)	0.025" (0.635 mm)	0.050" (1.27 mm)

7.0 Machined Dimensional Tolerances

Dimensional Tolerances	Class 1	Class 2	Class 3	Class 4
7.1 Length (outside)	±0.0005" (0.0127 mm)	±0.001" (0.0254 mm)	±0.005" (0.127 mm)	±0.010" (0.254 mm)
7.2 Diameter (outside)	±0.0005" (0.0127 mm)	±0.001" (0.0254 mm)	±0.005" (0.127 mm)	±0.010" (0.254 mm)
7.3 I.D. tubes	±0.0005" (0.0127 mm)	±0.001" (0.0254 mm)	±0.005" (0.127 mm)	±0.010" (0.254 mm)
7.4 Hole Diameter	±0.0005" (0.0127 mm)	±0.001" (0.0254 mm)	±0.005" (0.127 mm)	±0.010" (0.254 mm)
7.5 Hole Location	±0.001" (0.0254 mm)	±0.005" (0.127 mm)	±0.010" (0.254 mm)	N/A
7.6 Concentricity, TIR	0.001" (0.0254 mm)	0.005" (0.127 mm)	0.010" (0.254 mm)	N/A
7.7 Roundness	Within dimensional tolerance			N/A
7.8 Radius	±0.001" (0.0254 mm)	±0.005" (0.127 mm)	±0.010" (0.254 mm)	N/A
7.9 Angle, Degree	±½ degree	±1 degree	±2 degree	±5 degree
7.10 Flatness (plates)	0.0005" (0.0127 mm)	0.001" (0.0254 mm)	0.002" (0.0508 mm)	0.005" (0.127 mm)
7.11 Camber in/in max.	0.0005" (0.0127 mm)	0.001" (0.0254 mm)	0.0015" (0.0381 mm)	0.002" (0.0508 mm)
7.12 Parallelism, TIR	0.0005" (0.0127 mm)	0.001" (0.0254 mm)	0.002" (0.0508 mm)	0.005" (0.127 mm)
7.13 Surface Finish Ra Max.	32	64	64	N/A

Note 3. Tighter tolerances may be held for additional costs.

Where tolerances are not specified, standard tolerances will be used as follows:

Three decimal places	*± 0.005" (0.127 mm)*
Two decimal places	*± 0.010" (0.254 mm)*
Fractions	*± 1/64" (0.3962 mm)*
Angles	*± 1 degree*

Health and Safety

Handling beryllium oxide ceramics in solid form poses no special health risk. Like many industrial materials, beryllium-containing materials may pose a health risk if recommended safe handling practices are not followed. Inhalation of airborne beryllium may cause a serious lung disorder in susceptible individuals.

The Occupational Safety and Health Administration (OSHA) has set mandatory limits on occupational respiratory exposures. Read and follow the guidance in the Material Safety Data Sheet (MSDS) before working with this material.

For additional information on safe handling practices or technical data on beryllium oxide ceramics, contact Brush Ceramic Products' Sales Group at 520-746-0251.

International Sales Centers

Europe
Tel: 33-1-60-92-42-53
Fax: 33-1-60-92-41-30

Japan
Tel: 81-3-3230-2961
Fax: 81-3-3230-2908

www.brushwellman.com

Original Issue: September 24, 1971 • Rev. E August 16, 2011

B502 • 8/11

6100 S. Tucson Blvd. • Tucson, AZ 85706 • Phone: 520-746-0251 • Fax: 520-294-8906

Attachment D to Enclosure 2 to MDO-723-0046/B-MT(SPME)-23:

Beryllium Oxide Grain Size Reduction Experiments

Author:
James Nash

Reviewed by:
Barri Gurau

This Page Intentionally Left Blank

1. Introduction

Grain size of beryllium oxide (BeO) can be correlated to irradiation performance of BeO. Historical data indicates that finer grain size material swells less than larger grain size material (Reference (a)). Much of the data used for swelling correlations presented in Enclosure 2 and Reference (b) was obtained from fine grain size (nominally 5 μm) BeO specimens. In an effort to utilize historical data and minimize irradiation swelling, experimental efforts were taken to reduce the grain size of BW-1000 material (Brush Ceramic Products) from 10 μm to 5 μm (nominal grain size). Experimental material from Brush Ceramic Products (BCP) is herein referred to as BW-1000K material. It should be noted that other variables may influence swelling (e.g. sintering aid composition, impurities and processing). They were not considered in detail, and should be considered in future studies.

2. BW-1000 Brush Ceramics BeO

2.1 Processing and Sample Fabrication

Brush Ceramic Products produces two grades of BeO – Thermalox 995 and BW-1000 (Table 1). The primary difference between the two materials is the reduced grain size of BW-1000. The reduced grain size of the BW-1000 BeO relative to Thermalox 995 is due primarily to sintering additives and the sintering profile of the two materials. The finer grain sizes yield higher flexural strengths for BW-1000 but the sintering additives used in BW-1000 lower the thermal conductivity (References (c) and (d)). The maximum size for fired BW-1000 parts is 25.4 mm x 25.4 mm x 203 mm (1" x 1" x 8") while for Thermalox 995 the maximum size part is 127 mm x 127 mm x 508 mm (5" x 5" x 20"). These size limitations were expected to make reflector manufacturing more difficult by requiring many more parts per slider or drum (based on design assumptions).

Table 1: Material Properties Thermalox 995 vs. BW-1000 (References (c) and (d))

Property	Unit	Test Method	Thermalox 995	BW-1000
BeO content	Weight %	Spectrographic by difference	99.5 (min)	99.5 (min)
Nominal Density	g/cm^3 %theoretical	ASTM C-373	2.85 (95%)	2.85 (95%)
Hardness		ASTM E-18	60 min (Rockwell 45N)	60 min (Rockwell 45N)
Grain Size	microns	ASTM E-112	9-25 (15 typical)	9-12 (10 typical)
Flexural Strength	MPa	ASTM F-417	220 (min)	260 (min)
Thermal Conductivity	W/m-K (at T_{room})	Laser Flash	285	275
Mean Coefficient of Thermal Expansion	10^{-6} /°C	ASTM E-228	9.0 (T_{room} – 1273K)	9.0 (T_{room} – 1273K)

The starting BeO powder for BW-1000 material is urea derived oxide (UOX) powder from Brush Wellman (Reference (e)). Average starting particle size of the powder is 0.5 – 0.6 µm (0.65 µm max). Sintering aids are added to the starting powder and the powder is spray dried. Following spray drying the material is isopressed. Powder is contained in a flexible mold which is then immersed in water and the vessel is sealed. The chamber is pressurized to 29,500 psi and held at pressure for 3 minutes. Because pressure is the same on the mold from all directions (isostatically) the density is more uniform which reduces the internal stresses in the green state and eliminates cracks, strain and laminations. Additionally, the green strength is usually higher which allows for pre-firing machining. Isopressed parts are then sintered in a tunnel kiln as follows:

- Bake out: 454K – 725K over ~9 hrs
- Ramp up: 725K – 1798K over ~12 hrs
- Hold temperature: 1798K for ~5 hrs
- Ramp to room temperature: 1798K – 296K in ~18 hrs

Actual heat work done in a given kiln cycle can vary over time. The firing cycle is verified with test pieces sent through first. Grain size is measured and kiln adjustments are made if necessary to achieve the 9 – 12 µm (10 µm average) grain size. Normal density of fired BW-1000 BeO is ~2.89 g/cm^3 (approximately 96% theoretical density).

Table 2: Elemental Analysis of BW-1000*

Element	wt%, ppm
BeO	balance
B	< 1
Al	25
Cr	5
Fe	40
Mg	1400
Mn	< 2
Ni	5
Ti	< 2
Na	125
Ag	< 1
Ca	< 30
Co	< 1
Cu	< 2
Mo	< 3
Pb	< 2
Si	1900
Zn	< 20

*Block 83

2.2 Grain Size

Brush Ceramic Products performed grain size measurements on BW-1000 material. Grain size measurements ranged from 9 – 12 µm with an average of 10 µm. Grain size was measured

using the standard linear intercept method. Measurements were taken on both cylinder and disk samples at three different locations: surface, 25% through thickness and center. Results are presented in Table 3 and Figure 1. No differences were observed in the grain size at the center of the specimen versus the surface of the specimens. Additionally, note that no differences were observed in grain size between the cylinder and disk specimens taken from different blocks of material (no differences were expected).

Table 3: Grain Size Results from BW-1000 Cylinder and Disk Specimens

(All Grain Size Measurements are in μm)

Part	Location			Average
	Surface	25% thickness	Center	
cylinder 83A	12	10	10	
cylinder 83B	11	10	10	
cylinder 84A	10	10	10	
cylinder 84B	10	10	10	
cylinder 85A	10	10	10	
cylinder 85B	10	10	10	
cylinder 86A	9	10	10	
cylinder 86B	10	10	10	
Average (cylinders)	**10**	**10**	**10**	**10**
disk 27A	9	9	9	
disk 27B	9	10	9	
disk 51A	10	10	10	
disk 51B	10	9	10	
disk 62A	9	10	9	
disk 62B	9	9	9	
disk 87A	10	10	10	
disk 87B	11	10	10	
Average (disks)	**10**	**10**	**10**	**10**
Average	**10**	**10**	**10**	**10**

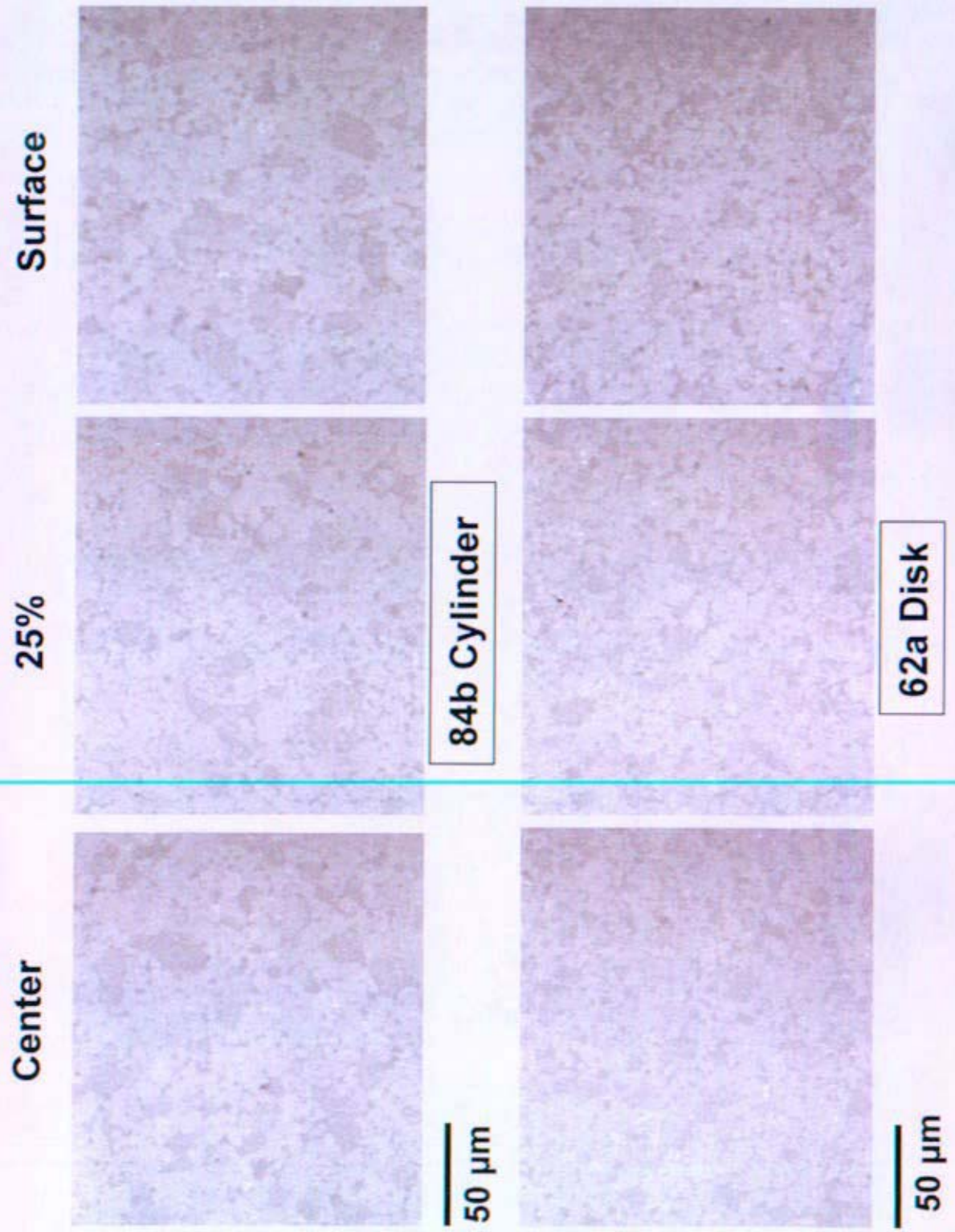

Figure 1: Optical Microscopy of BW-1000 Cylinder and Disk Specimens

3. Grain Size Reduction Runs (BW-1000K)

As previously discussed, BCP was contracted to perform three, sequential grain size reduction runs, utilizing lessons learned from each run. The primary goal of the grain size reductions runs was to reduce the average grain size of BW-1000 from 10 µm to 5 µm.

3.1 Run 1: BW-1000K-1

For the first grain size reduction experiment (BW-1000K-1) the sintering profile of BW-1000 was altered. Standard BW-1000 material is sintered at 1798K for ~5 hrs in a tunnel kiln. For BW-1000K-1, the sintering profile was altered and the material was fired at 1723K for 1 hr in a periodic kiln. This profile was selected through an iterative experimental process in which BCP kept reducing time and temperature until the density of the material began to decrease. No changes were made to the starting powder composition. Specimens fired were 20 mm x 20 mm x 200 mm bars. Average grain size of BW-1000K-1 was 9 µm with a density of 2.87 g/cm^3. Optical microscopy images of BW-1000K-1 material at three locations are shown in Figure 2.

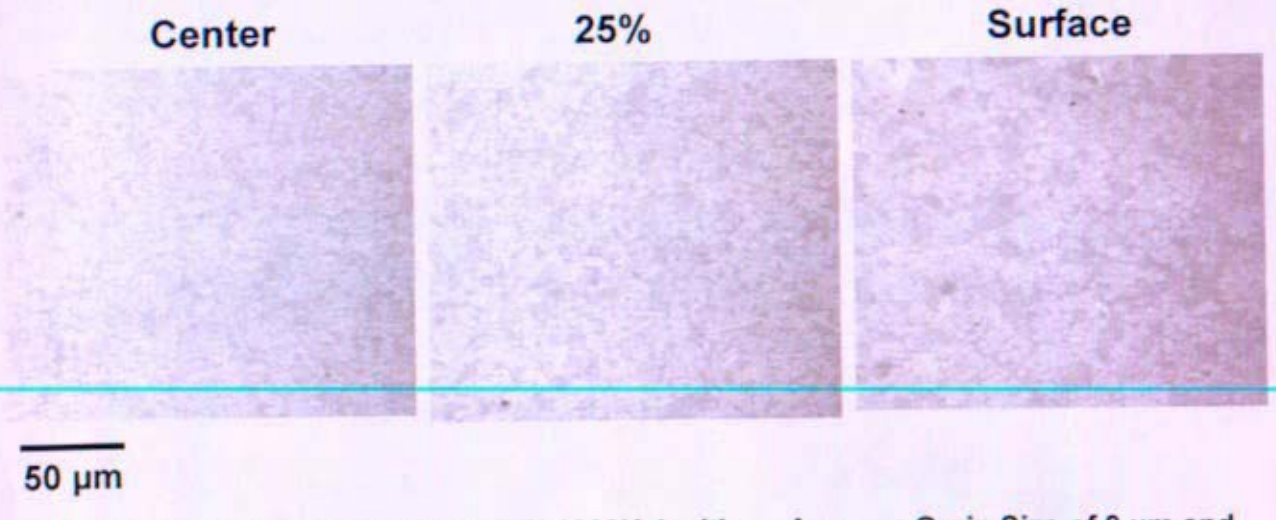

Figure 2: Optical Microscopy of BW-1000K-1 with an Average Grain Size of 9 µm and Density of 2.87 g/cm^3

3.2 Run 2: BW-1000K-2

The second grain size reduction run (BW-1000K-2) combined the sintering profile determined in Run 1 with a reduced starting average BeO particle size. For BW-1000 material the average BeO starting particle size is 0.5 – 0.6 µm (0.65 µm max). For BW-1000K-2 the starting BeO powder was "over-milled" to an average BeO particle size of 0.25 µm (0.5 µm max). BeO powder was wet milled until the desired particle size was achieved. The "over-milled" powder was pressed and 20 mm x 20 mm x 200 mm specimens were fired in the periodic kiln at 1723K for 1 hr. Average grain size of BW-1000K-2 was 9 µm with a density of 2.87 g/cm^3. Optical microscopy images of BW-1000K-2 material at three locations are shown in Figure 3. (Lines on the micrographs are from grain size measurements.)

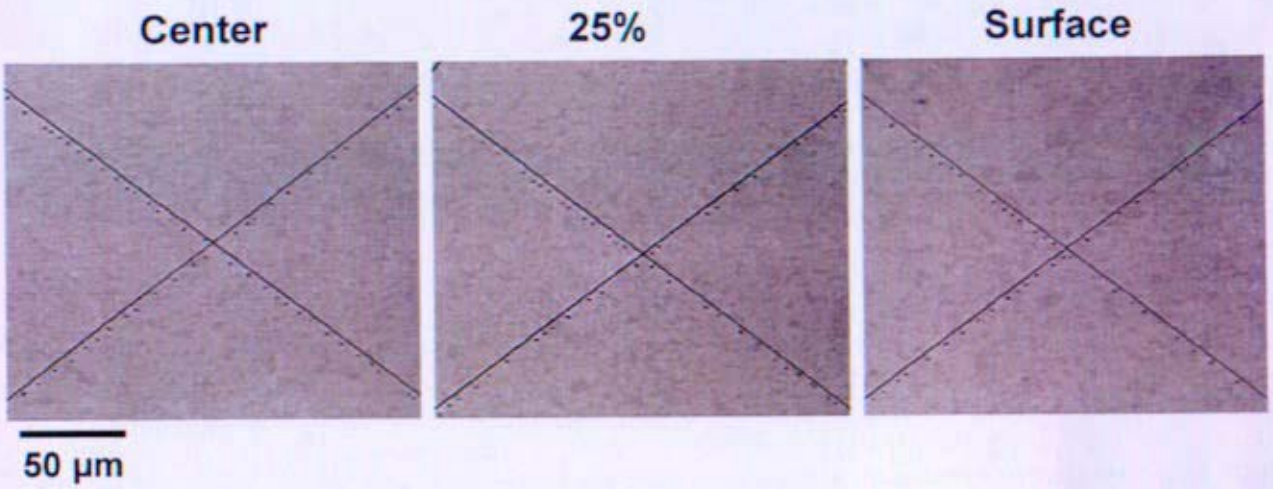

Figure 3: Optical Microscopy of BW-1000K-2 with an Average Grain Size of 9 µm and Density of 2.87 g/cm^3 (Lines on the micrographs are from grain size measurements.)

3.3 Run 3: BW-1000K-3

The final grain size reduction (BW-1000K-3) run re-visited the adjustments to the sintering profile. Based on the results of Run 2, it was determined that reducing the starting BeO particle size did not result in a reduced grain size. Standard BW-1000 BeO powder (0.5 – 0.6 µm particle size) was pressed and 20 mm x 20 mm x 200 mm specimens were fired in the periodic kiln at 1698K for 1 hr. Average grain size of BW-1000K-3 material was 7 µm with a density of 2.86 g/cm^3. Optical microscopy images of BW-1000K-3 material at three locations are shown in Figure 4. Elemental analysis was also performed on BW-1000K-3 and is presented in Table 4 compared to BW-1000 material. No changes were made to chemistry, however slight variations were observed.

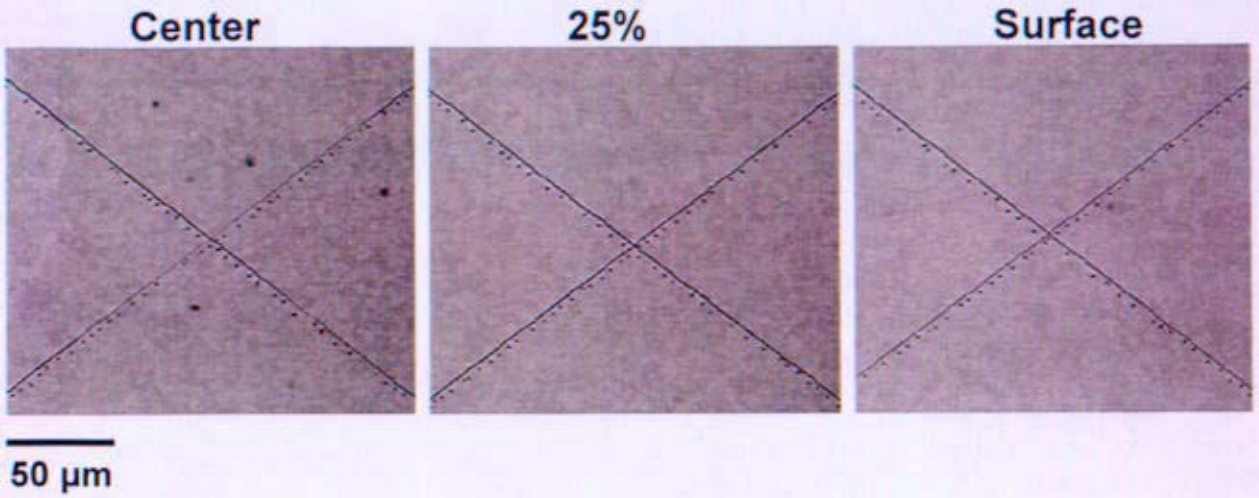

Figure 4: Optical Microscopy of BW-1000K-3 with an Average Grain Size of 7 µm and Density of 2.86 g/cm^3 (Lines on the micrographs are from grain size measurements.)

Table 4: Elemental Analysis of BW-1000 Material and BW-1000K-3 Material

Element	BW-1000, wt% ppm	BW-1000K-3, wt% ppm
BeO	Balance	Balance
B	< 1	<1
Al	25	45
Cr	5	4
Fe	40	40
Mg	1400	1240
Mn	< 2	<2
Ni	5	4
Ti	< 2	<2
Na	125	160
Ag	< 1	<1
Ca	< 30	<30
Co	< 1	<1
Cu	< 2	4
Mo	< 3	<3
Pb	< 2	<2
Si	1900	2200
Zn	< 20	<20

4. Discussion

The goal of this research study was to reduce the grain size of BW-1000 material from 10 µm to 5 µm to improve irradiation properties and leverage historical BeO data. Altering the sintering profile (BW-1000K-1 and BW-1000K-3) provided the most significant reduction in grain size (10 µm reduced to 7 µm) with minimal change in density (2.89 g/cm^3 reduced to 2.86 g/cm^3) and

composition. Reducing the starting particle size of the BeO powder (BW-1000K-2) did not result in a significant reduction in grain size. A 30% decrease in grain size was achieved in this limited grain size reduction study. With more study, grain size could potentially be further reduced and the target of 5 µm grain size achieved. A summary of all grain size reduction runs is provided in Table 5. Optical micrographs of BW-1000, BW-1000K-1, BW-1000K-2 and BW-1000K-3 are compared in Figure 5.

The strategy for the final grain size reduction run (BW-1000K-3) built upon the results of the first 2 grain size reduction runs. Because there was a slight decrease in grain size in Run 1 with very little decrease in density, it was determined that the sintering profile could be further altered for the final run. It is expected that as the sintering temperature is decreased (at constant sintering time), the grain size of the material should decrease, accompanied by a decrease in density. This trade-off between density and grain size with their impacts on the lifetime swelling performance would need to be investigated with regard to reactor design and the neutronics of a Prometheus type reflector.

Initial brainstorming sessions identified starting BeO chemistry (i.e., sintering aids) as a possible route to reducing grain size. However, given the limited number of experimental runs and questions about the effectiveness of altering the sintering aids (investigation of the phase diagram indicated no further advantage could be gained by altering the ratio of sintering aids currently used), this option was not selected. This method may warrant investigation by future researchers interested in reducing BeO grain size. Further, a detailed literature review of processing methods that produced the original 5 µm BeO should be performed.

Table 5: Summary of Grain Size Reduction Runs

	BW-1000	BW-1000K-1	BW-1000K-2	BW-1000K-3
Ave. Grain Size	10 µm	9 µm	9 µm	7 µm
Density (%theoretical)	2.89 g/cm^3 (96%)	2.87 g/cm^3 (95%)	2.87 g/cm^3 (95%)	2.86 g/cm^3 (95%)
Ave. BeO Particle Size	0.5 – 0.6 µm	0.5 – 0.6 µm	0.25 µm	0.5 – 0.6 µm
Sintering Time	~5 hrs	1 hr	1 hr	1 hr
Sintering Temperature	1798K	1723K	1723K	1698K

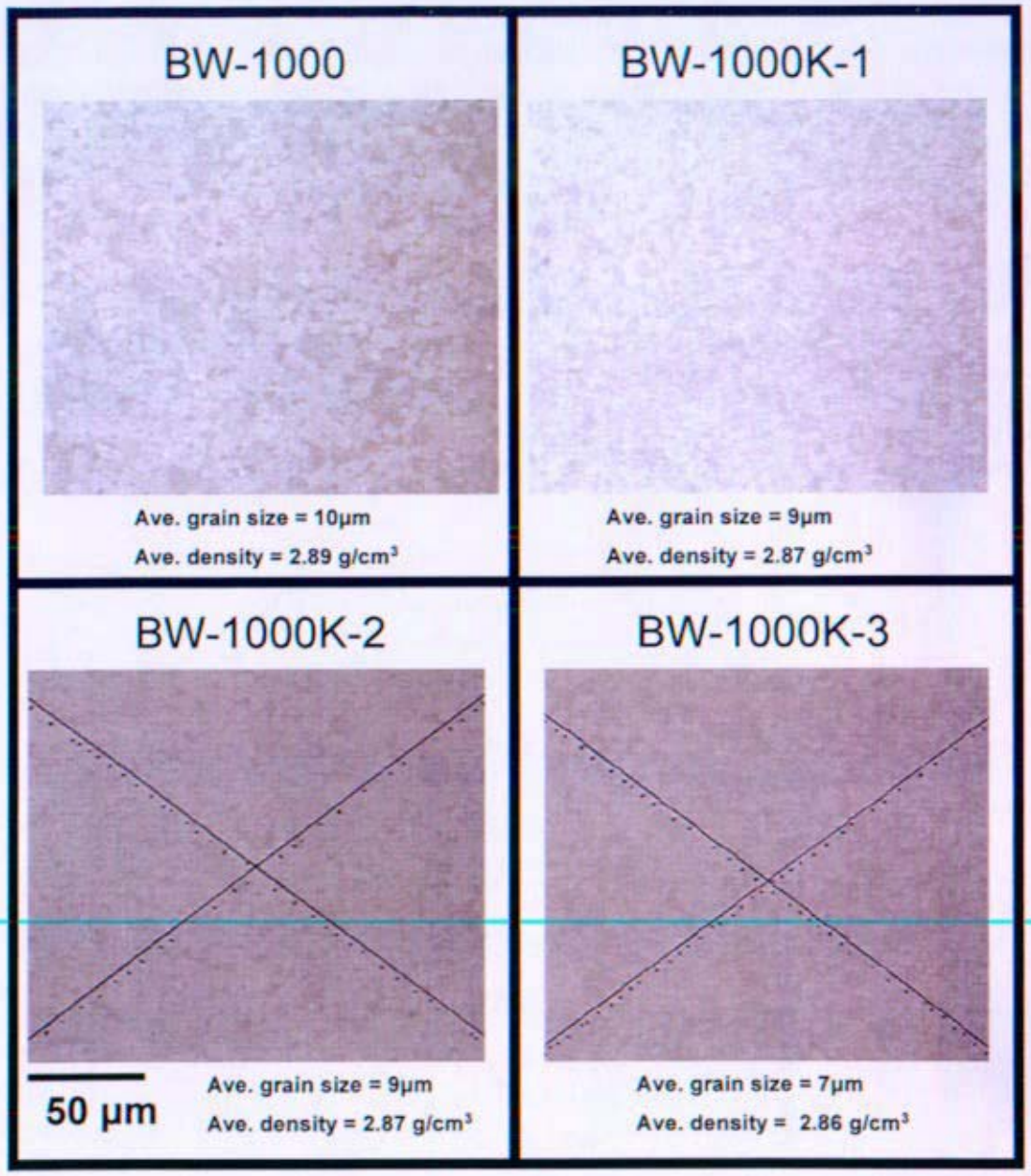

Figure 5: Comparison of BW-1000 Material to the Experimental Runs (BW-1000K-1, BW-1000K-2 and BW-1000K-3) (Lines on the micrographs are from grain size measurements.)

5. Conclusions

- Beryllium oxide grain size was reduced from 10 µm (BW-1000) to 7 µm (BW-1000K-3) with minimal impact on density by altering the sintering profile.
- Maximum dimensions of pressed and fired BW-1000 and BW-1000K parts currently is 25.4 mm x 25.4 mm x 203 mm (1" x 1" x 8"). Future effort is required to scale up the size

of pressed and fired BW-1000 and future BW-1000K (reduced grain size) parts, while maintaining the same material properties and grain size.

- The NRPCT judged that with further study, BeO grain size could potentially be reduced to 5 μm.

6. References

(a) Plumlee, D.E., "BeO Performance Lessons Learned" Martin Marietta Report DOE/SF/16006-T1216 (1994).
(b) KAPL Letter, MDO-723-0042, "Reflector and Shield Material Properties for Project Prometheus", dated November 2, 2005.
(c) Brush Ceramic Products, Product Guide, Dry Pressed Ceramics As-Fired or Machined CDDP-10, Rev. F (2001).
(d) Brush Ceramic Products, Product Guide, Isopressed Ceramics CDI-20, Rev. E (2001).
(e) Brush Wellman Specification, UOX Beryllium Oxide Powder, November 8, 1983.

Attachment E to Enclosure 2 to MDO-723-0046/B-MT(SPME)-23:

Material Property Testing of Brush Ceramic Products BW-1000 Beryllium Oxide

Author:
James Nash

Reviewed by:
Barri Gurau

This Page Intentionally Left Blank

1. Introduction

Unirradiated material property testing of Brush Ceramic Products (BCP) BW-1000 beryllium oxide (BeO) material was conducted by BCP. Properties tested included density (ASTM C-373-88), specific heat (ASTM C-351-92b), thermal diffusivity (ASTM E-1461-01), thermal expansion (ASTM E-228-95) and compressive strength (ASTM C-773-88). With the exception of compressive strength, these properties were tested over the temperature range T_{room} to 1250K. Compression testing was performed at T_{room} and 650K. Higher temperature (850K, 1050K and 1250K) compression testing was attempted and produced questionable results. All testing was planned to be complimentary to the JOYO irradiation test (Enclosure 2). Test specimens were fabricated from isopressed BW-1000 material with a nominal grain size of 10 µm. Specimens were machined out of larger BeO pieces representative of the material expected for use in a Prometheus reflector application.

2. Results

2.1 Density

Room temperature density measurements were performed on five BeO specimens in accordance with ASTM C-373-88, which is based on the Archimedes principle (Reference (a)). The five specimens were from five different blocks of material. Elemental analysis of Block 83 is presented in Table 1. Using average thermal expansion data in Section 2.4, room temperature density values were extrapolated to 1273K (assumes isotropic expansion). Extrapolated density data is presented in Table 2 and Figure 1. The theoretical density of BeO is 3.01 g/cm^3 (Reference (b)) and the percent theoretical density (%TD) is included in Figure 1.

Table 1: Elemental Analysis of BW-1000 BeO Block 83

Element	wt%, ppm
BeO	balance
B	< 1
Al	25
Cr	5
Fe	40
Mg	1400
Mn	< 2
Ni	5
Ti	< 2
Na	125
Ag	< 1
Ca	< 30
Co	< 1
Cu	< 2
Mo	< 3
Pb	< 2
Si	1900
Zn	< 20

Table 2: Room Temperature and Extrapolated Density Data Table for BeO

Density Values (g/cm^3)

Temperature (K)	Block 27	Block 51	Block 62	Block 83	Block 86
296 (T_{room})	2.89	2.89	2.88	2.90	2.89
373	2.88	2.88	2.88	2.90	2.89
473	2.88	2.88	2.87	2.89	2.88
573	2.87	2.87	2.87	2.88	2.88
673	2.87	2.86	2.86	2.88	2.87
773	2.86	2.86	2.85	2.87	2.86
873	2.85	2.85	2.85	2.86	2.85
973	2.84	2.84	2.84	2.85	2.84
1073	2.83	2.83	2.83	2.84	2.84
1173	2.82	2.82	2.82	2.83	2.83
1273	2.81	2.81	2.81	2.82	2.82

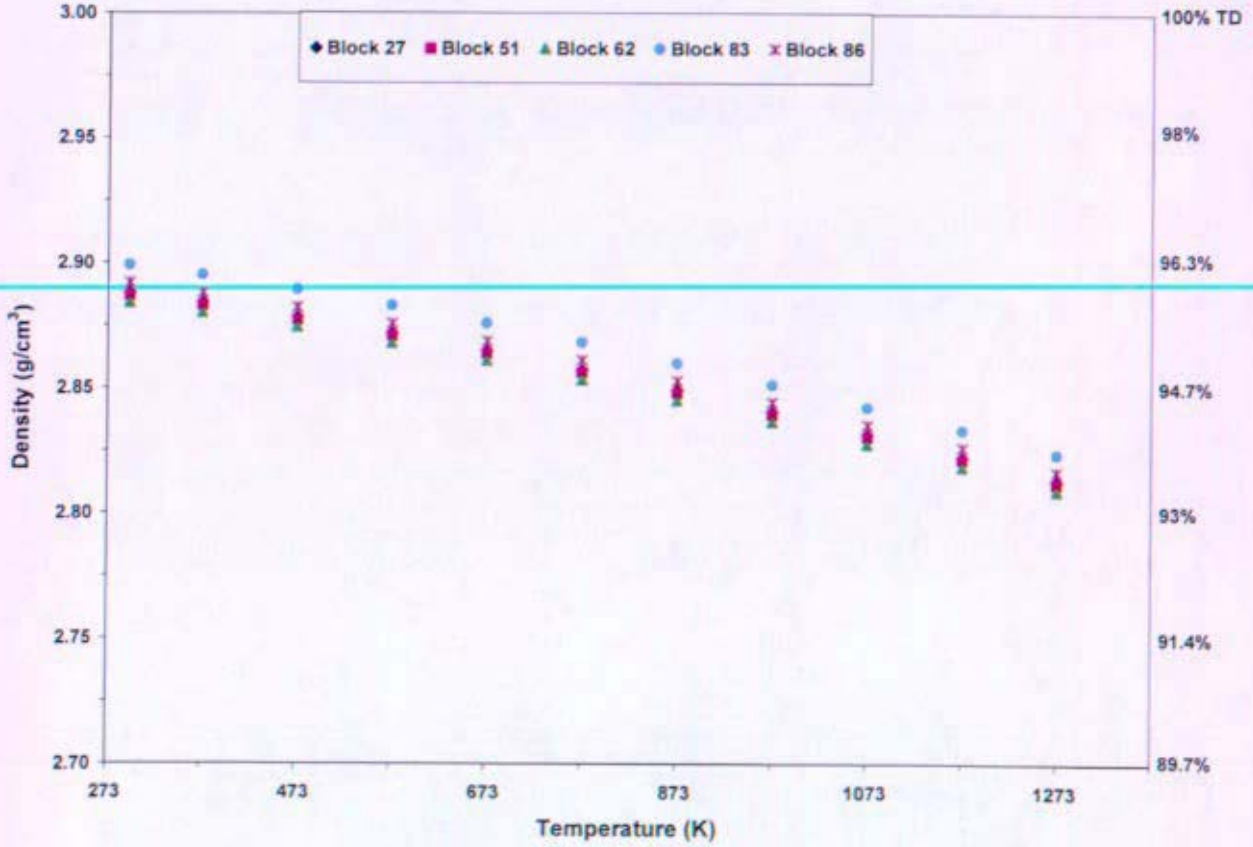

Figure 1: Room Temperature and Extrapolated Density Data for BeO

2.2 Specific Heat

Specific heat measurements were performed in accordance with ASTM C-351-92b from 323K to 1273K. Room temperature values of specific heat were extrapolated. Measurements from 323K to 573K were performed with a Perkin-Elmer calorimeter and at higher temperatures (623K – 1273K) were performed with a Netzch calorimeter. Disks used for specific heat measurements were 5.84 mm in diameter and 1.52 mm thick. Specific heat data is presented in Table 3 and Figure 2. Note that the 5 samples tested do not correlate with the 5 blocks tested for density in Section 2.1 or the 5 samples tested for thermal diffusivity (Section 2.3) and thermal expansion (Section 2.4). Error associated with specific heat measurements was reported as ± 2%.

Table 3: Specific Heat Data Table for BeO

Specific Heat (J/kg-K)

Temperature (K)	Sample 1	Sample 2	Sample 3	Sample 4	Sample 5
296	986	973	977	990	996
323	1088	1087	1083	1085	1091
348	1179	1182	1171	1174	1176
373	1254	1259	1245	1250	1250
398	1321	1328	1312	1318	1320
423	1380	1388	1371	1378	1380
448	1432	1442	1425	1431	1433
473	1479	1490	1471	1481	1483
498	1522	1553	1513	1525	1531
523	1560	1573	1552	1566	1564
548	1592	1610	1589	1610	1601
573	1618	1642	1622	1643	1634
623	1697	1701	1700	1692	1694
673	1734	1752	1738	1728	1744
723	1784	1790	1782	1779	1775
773	1809	1822	1809	1798	1819
823	1843	1856	1842	1841	1856
873	1855	1877	1872	1856	1867
923	1874	1903	1882	1876	1879
973	1896	1922	1901	1898	1892
1023	1915	1940	1918	1922	1916
1073	1941	1959	1937	1943	1938
1123	1967	1978	1972	1977	1970
1173	1992	2001	2000	1990	1998
1223	2020	2018	2014	2012	2012
1273	2045	2042	2030	2029	2034

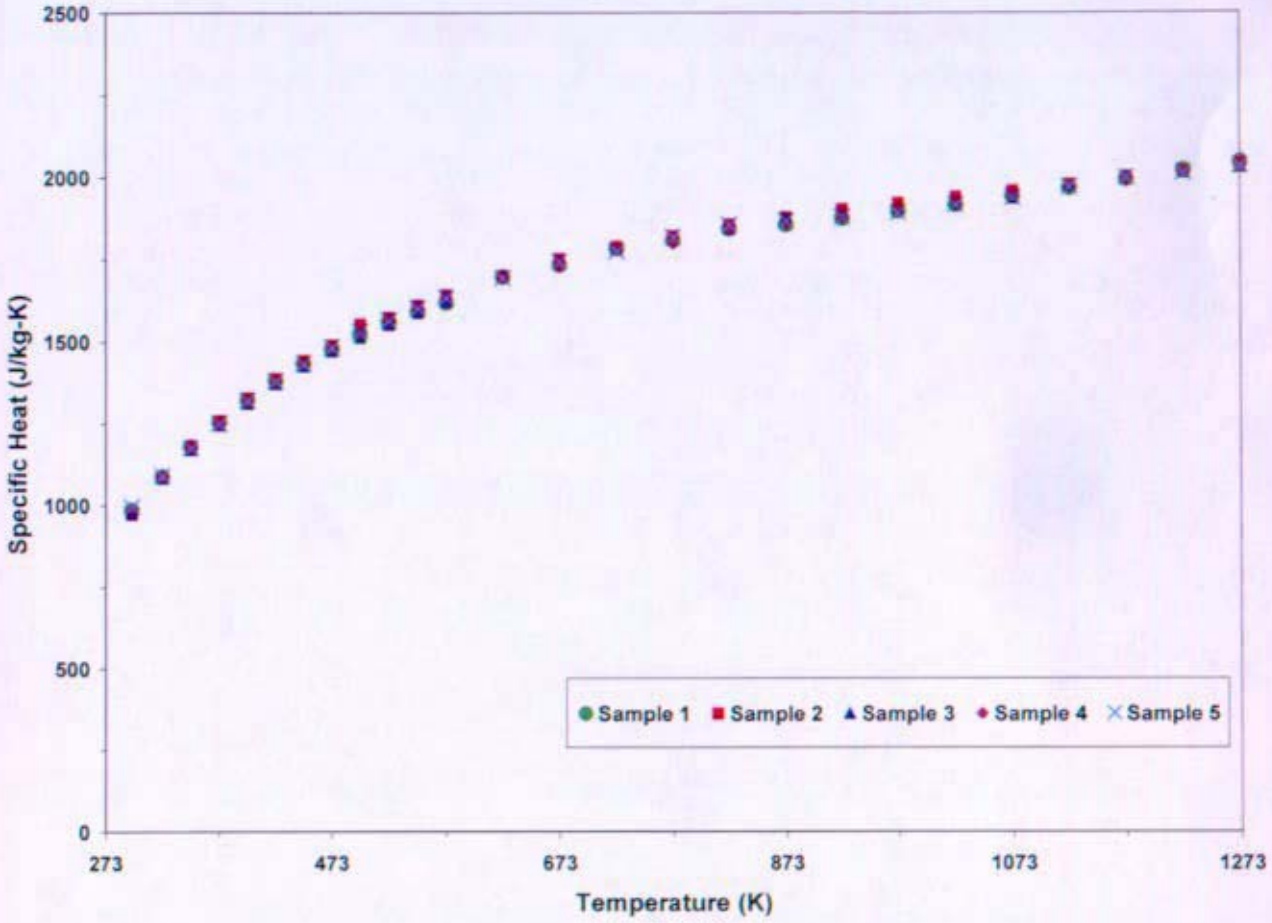

Figure 2: Specific Heat Data for BeO

2.3 Thermal Diffusivity/Thermal Conductivity

Thermal diffusivity measurements were performed via the laser flash method in accordance with ASTM E-1461-01. Samples tested were 12.7 mm diameter x 2.78 mm thick disks. Thermal diffusivity data is presented in Table 4 and Figure 3. The front face of the diffusivity test specimens were coated with silicon carbide (SiC) because the BeO was partially transparent to the laser. Error associated with thermal diffusivity measurements was reported as ± 2%. Given that the room temperature value obtained for Sample 1 in Table 4 was ~10% below the average diffusivity values for samples 2-5, the vendor reported accuracy of ±2% is considered suspect, but not necessarily in error. However, sufficient time was not available to fully explore this inconsistency.

Table 4: Thermal Diffusivity Data Table for BeO

Thermal Diffusivity (cm^2/s)

Temperature (K)	Sample 1	Sample 2	Sample 3	Sample 4	Sample 5
296	0.838	0.933	0.914	0.923	0.940
323	0.642	0.730	0.724	0.728	0.730
373	0.495	0.520	0.526	0.526	0.521
473	0.304	0.327	0.326	0.332	0.327
573	0.222	0.231	0.229	0.232	0.229
673	0.163	0.169	0.175	0.172	0.173
773	0.130	0.136	0.135	0.134	0.135
873	0.105	0.109	0.107	0.108	0.111
973	0.085	0.088	0.087	0.089	0.088
1073	0.071	0.073	0.072	0.072	0.073
1173	0.060	0.061	0.062	0.062	0.062
1273	0.052	0.053	0.054	0.054	0.054

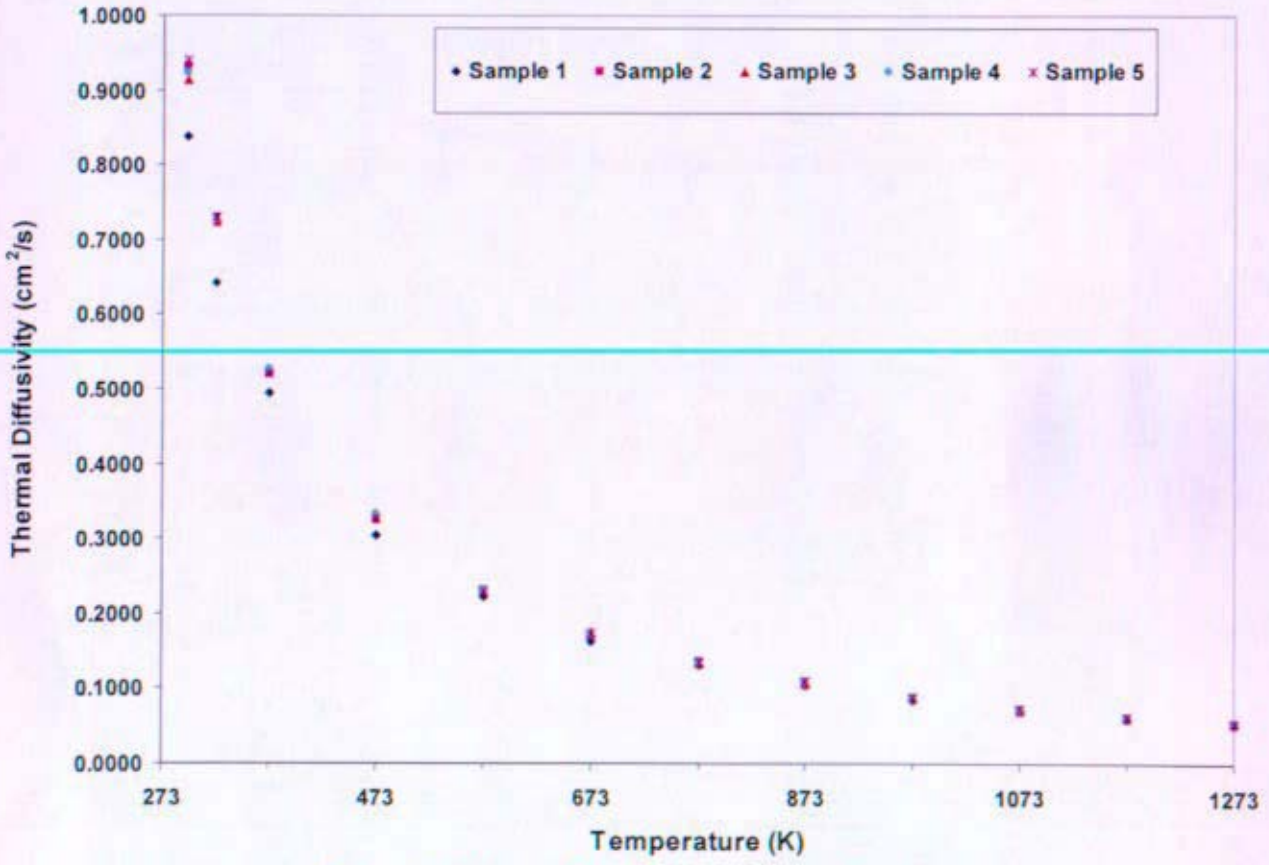

Figure 3: Thermal Diffusivity Data for BeO

Thermal conductivity was calculated from thermal diffusivity measurements based on the following equation:

$$\lambda = \alpha \cdot C_p \cdot \rho$$

where
λ = thermal conductivity, W/cm-K
α = thermal diffusivity, cm^2/s
C_p = specific heat, J/g-K
ρ = density, g/cm^3

Average values of specific heat and density were used for the thermal conductivity calculation because specific heat, density and thermal diffusivity measurements were performed for different samples from different blocks of material. The average density and specific heat from the five blocks/samples at each temperature was used and thermal conductivity calculated for each diffusivity measurement. Average values used in the thermal conductivity calculation are presented in Table 5. Calculated thermal conductivity data is presented in Table 6 and Figure 4.

Table 5: Average Density and Specific Heat Values Used in the Thermal Conductivity *Calculation*

Temperature (K)	Density (g/cm^3)	Specific Heat (J/g-K)
296	2.89	0.984
323	2.89	1.087
373	2.89	1.252
473	2.88	1.481
573	2.87	1.632
673	2.87	1.739
773	2.86	1.811
873	2.85	1.865
973	2.84	1.902
1073	2.83	1.944
1173	2.82	1.996
1273	2.81	2.036

Table 6: Calculated Thermal Conductivity Data Table for BeO

Thermal Conductivity (W/m-K)

Temperature (K)	Sample 1	Sample 2	Sample 3	Sample 4	Sample 5
296	238.4	265.4	260.0	262.6	267.4
323	201.6	229.3	227.4	228.7	229.3
373	178.8	187.8	190.0	190.0	188.2
473	129.6	139.5	139.0	141.6	139.5
573	104.1	108.3	107.4	108.8	107.4
673	81.3	84.3	87.3	85.8	86.3
773	67.3	70.4	69.9	69.4	69.9
873	55.8	58.0	56.9	57.4	59.0
973	46.0	47.6	47.0	48.1	47.6
1073	39.1	40.2	39.7	39.7	40.2
1173	33.8	34.4	35.0	35.0	35.0
1273	29.8	30.4	30.9	30.9	30.9

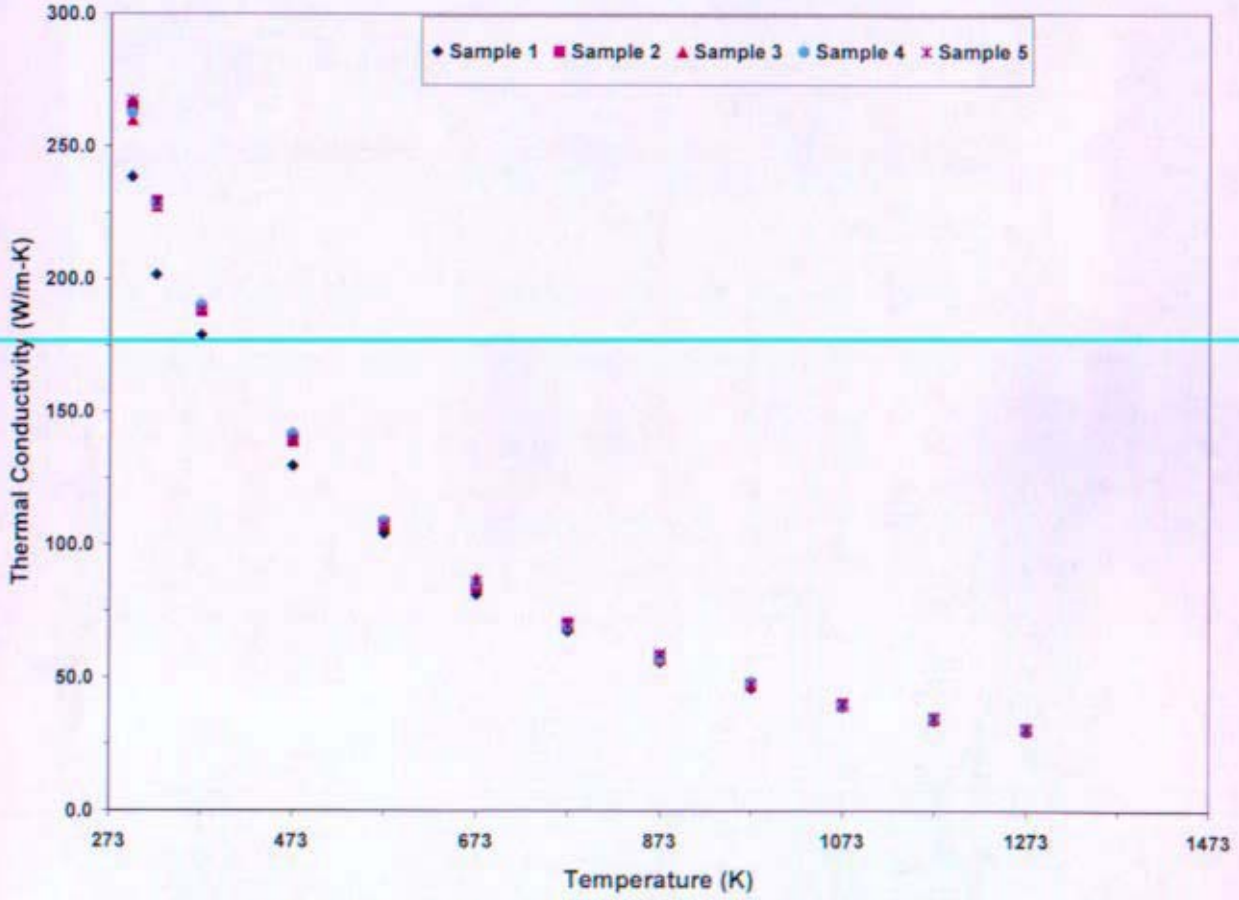

Figure 4: Calculated Thermal Conductivity for BeO

2.4 Thermal Expansion

Thermal expansion was measured in accordance with ASTM E-228-95 using an Innovative Thermal Systems dilatometer, model 3916. Samples tested were rectangular bars 4.2 mm x 4.2 mm x 26.5 mm. Linear expansion was measured for each specimen. Using the definition below, the mean coefficient of thermal expansion (CTE) was calculated. It should be noted that interpolation was used in some cases to report a CTE value at the selected temperatures in Table 7.

$$\Delta L = L \cdot \alpha_{mean} \cdot \Delta T \quad \text{or} \quad \alpha_{mean} = \frac{\Delta L / L}{\Delta T}$$

where
α_{mean} = mean coefficient of thermal expansion, K^{-1}
L = original specimen length
$\Delta L = L_{experimental} - L$
$\Delta T = T_{experimental} - T_{reference}$ (where $T_{reference} = 296K$)

Mean coefficient of thermal expansion data is shown in Table 7 and Figure 5. Note that the five samples tested do not correlate with the five blocks tested for density in Section 2.1 or the five samples tested for specific heat (Section 2.2) and thermal diffusivity/conductivity (Section 2.3).

Table 7: Mean CTE Data Table for BeO (All CTE Values are K^{-1})

Temperature (K)	CTE (K^{-1}) Sample 1	Temperature (K)	CTE (K^{-1}) Sample 2	Temperature (K)	CTE (K^{-1}) Sample 3
360	5.79E-06	367	5.92E-06	373	5.95E-06
373	5.89E-06	373	5.94E-06	473	6.29E-06
473	6.23E-06	473	6.25E-06	573	6.69E-06
573	6.61E-06	573	6.64E-06	673	7.09E-06
673	7.02E-06	673	7.04E-06	773	7.48E-06
773	7.42E-06	773	7.44E-06	873	7.84E-06
873	7.79E-06	873	7.80E-06	973	8.19E-06
973	8.15E-06	973	8.07E-06	1073	8.51E-06
1073	8.47E-06	1073	8.36E-06	1173	8.81E-06
1173	8.75E-06	1173	8.66E-06	1273	9.09E-06
1273	9.02E-06	1273	8.93E-06		

Temperature (K)	CTE (K^{-1}) Sample 4	Temperature (K)	CTE (K^{-1}) Sample 5
373	5.82E-06	367	5.92E-06
473	6.18E-06	373	6.02E-06
573	6.60E-06	473	6.34E-06
673	7.02E-06	573	6.70E-06
773	7.41E-06	673	7.13E-06
873	7.81E-06	773	7.49E-06
973	8.14E-06	873	7.88E-06
1073	8.43E-06	973	8.26E-06
1173	8.61E-06	1073	8.57E-06
1273	8.88E-06	1173	8.85E-06
		1273	9.10E-06

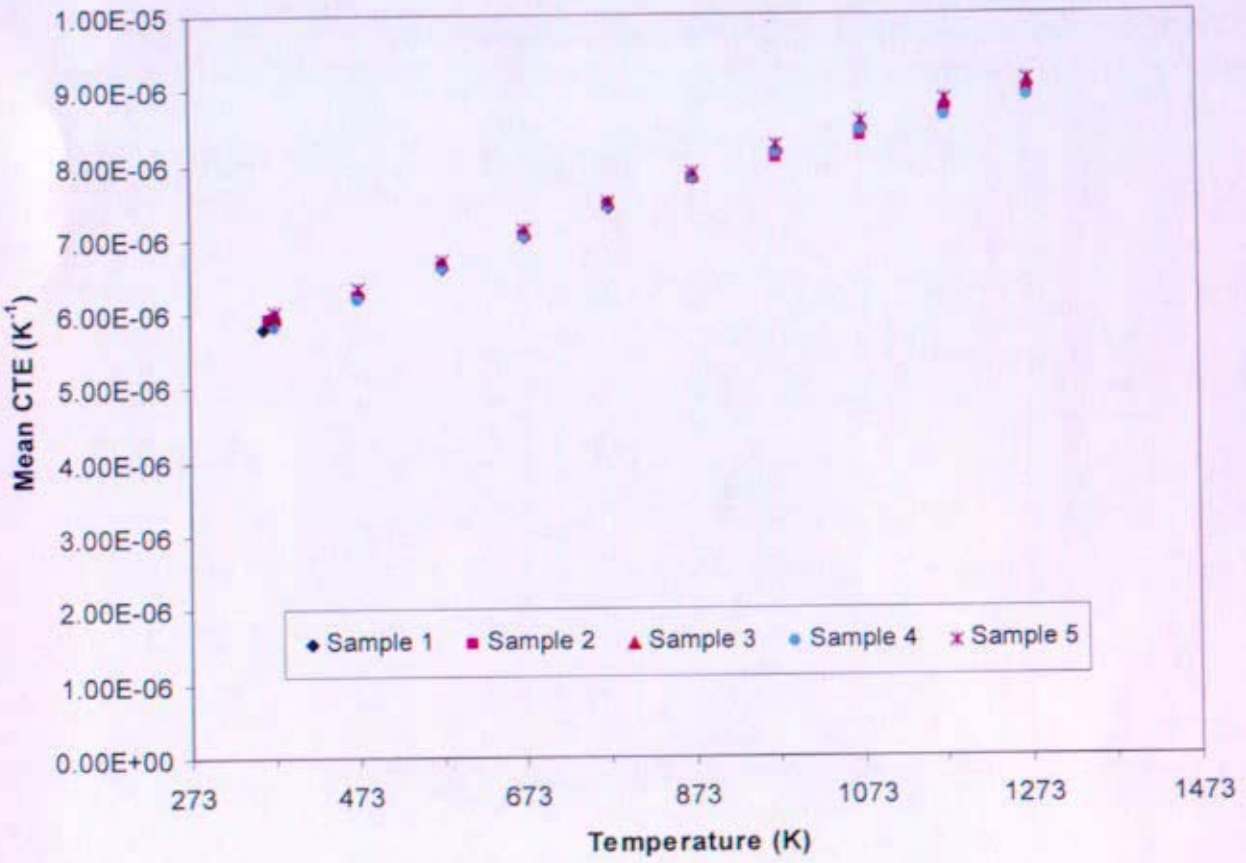

Figure 5: Mean CTE Data for BeO

2.5 Compressive Strength

Compressive strength testing of BeO was conducted by BCP in accordance with ASTM 773-88. Test specimens were right circular cylinders with a 12.7 mm (0.5") diameter and 38.1 mm (1.5") length. Load rate for compression testing was 0.1 mm/min (0.005 in/min). Compression testing was to be performed at T_{room}, 650K, 850K, 1050K and 1250K. Due to equipment failure, high temperature (850K, 1050K and 1250K) testing was not completed at the time of issuance of this report (a single data point is included for 850K and 1250K). Complete results can be found in Reference (c).

There were complications associated with the room temperature and 650K tests. BCP stated that "no meaningful data" resulted from compression testing based on unexpected failure of the test specimens. Failure modes included shearing near the edges (Figure 6) and shattering of the BeO specimens. The ultimate load and failure mode was reported for the tested specimens (Table 8). Using the area of the load bearing surface of the specimens, the compressive strength was calculated. For comparison, the room temperature compressive strength of BeO has been shown to be ~1420 MPa (206,000 psi) for 95% dense BeO (Reference (b)). While some of the room temperature data is near this value, there is large scatter in the data (Weibull modulus is ~2). This data is considered preliminary. Further investigation is required to

understand the fundamental failure mode of BeO. Until BeO failure in compression is understood, more data should be obtained to reduce uncertainty associated with compression testing.

Figure 6: Shearing Failure of BeO Compression Specimens

Table 8: Compression Testing Results as Reported for BeO

Temperature (K)	Ultimate Load (lbf)	Compressive Strength (MPa)	Failure Mode
296	-	1420	Typical compressive strength from literature (Reference (b))
296	42860	1504	Edge Shear
296	44970	1578	Edge Shear
296	16730	587	Edge Shear
296	33040	1160	Shattered
296	23080	810	Edge Shear
296	9245	324	Edge Shear
296	25840	907	Shattered
296	50040	1756	Shattered
296	40980	1438	Edge Shear
296	40640	1426	Shattered
650	26830	942	Shattered
650	26550	932	Shattered
650	29400	1032	Shattered
650	29480	1035	Shattered
650	29270	1027	Shattered
650	28340	995	Shattered
650	26110	916	Shattered
650	24800	870	Shattered
650	22650	795	Shattered
650	27330	959	Shattered
850	17210	604	-
1250	12480	438	-

3. Discussion

Material property testing conducted by BCP was compared to the literature review on BeO (Reference (b)). Density, specific heat and thermal conductivity results were consistent with literature. While it was not possible to perform a density, specific heat and thermal diffusivity measurement for a single sample, there was little variation in the calculated thermal conductivity of the material. Figure 7 shows the BW-1000 thermal conductivity data gathered from this study compared to the curve fit to historical data. It is observed that the BW-1000 BeO closely matches the historical grades. Thermal expansion measurements were slightly lower than reported for previous grades of BeO in the literature. The mean CTE of BW-1000 BeO compared to historical data is shown in Figure 8. It was undetermined if these results are representative of the isopressed material tested (BW-1000) versus historical data (e.g. other grades may be anisotropic or contain impurities). Further investigation of the current test results and test conditions are necessary to clarify this discrepancy. All of the raw data for density, specific heat, thermal expansion and thermal diffusivity will be included in Reference (c).

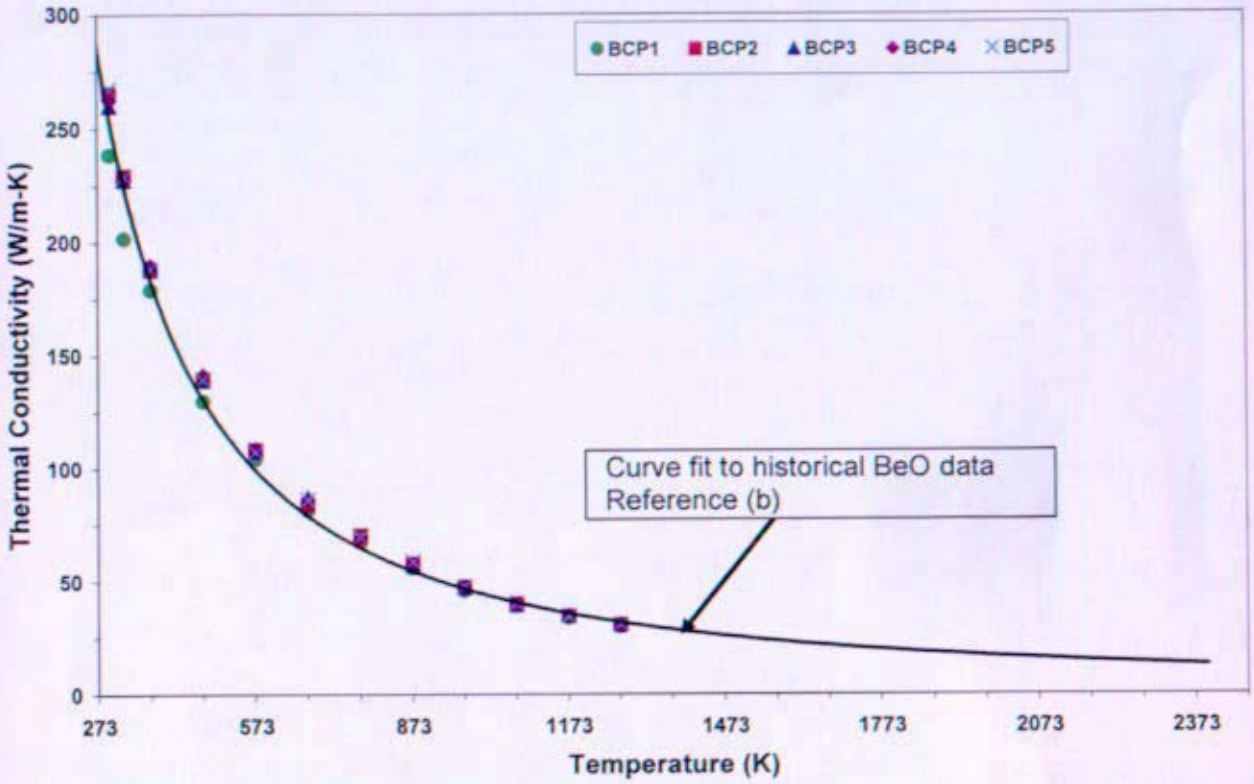

Figure 7: Comparison of BW-1000 BeO Thermal Conductivity Results and Curve Fit to Historical Data (Reference (b))

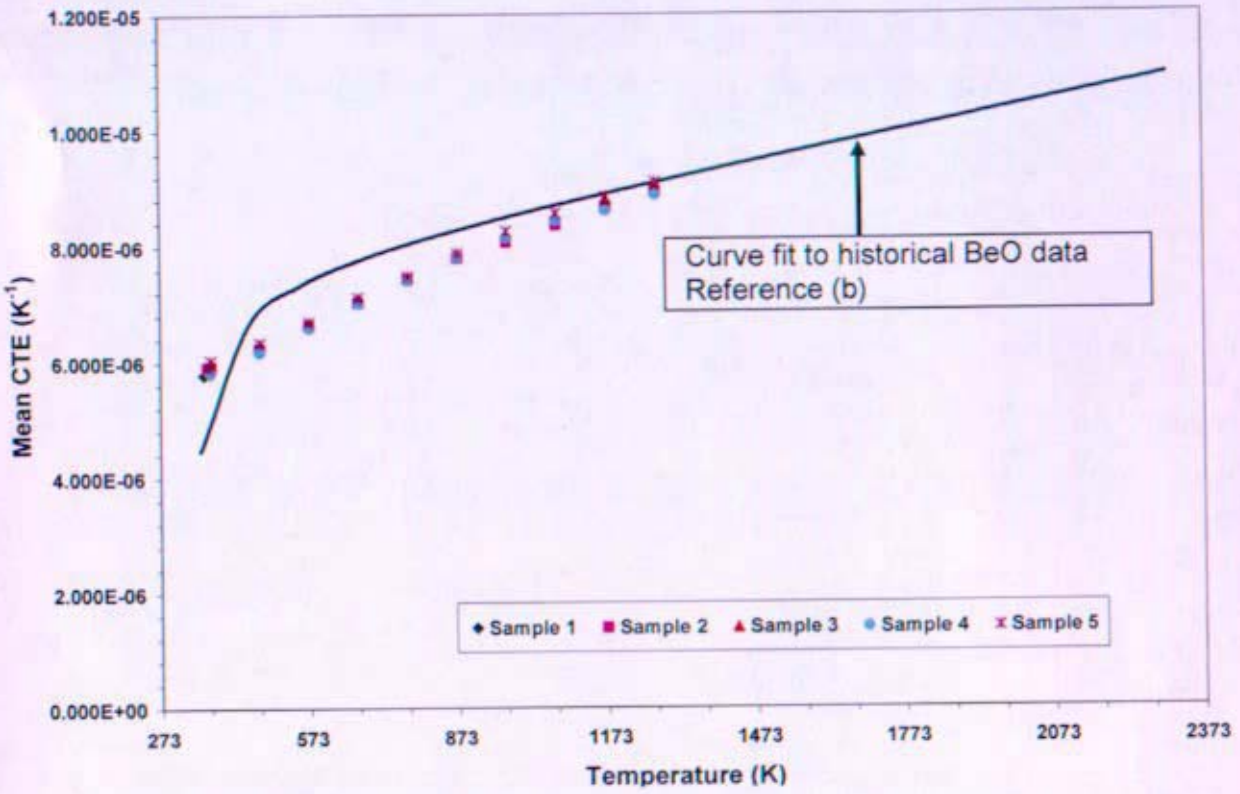

Figure 8: Comparison of BW-1000 BeO Mean CTE Results and Curve Fit to Historical Data (Reference (b))

Based on the results from compression testing, more work is required to fully characterize the compressive strength of BeO. Limited BeO compression data was located in the literature (Reference (b)). Additionally, many of the modern applications for BeO do not require in depth knowledge of compressive strength and therefore little developmental work has been conducted on testing BeO (the majority of applications are because of the high thermal conductivity of the material). Figure 9 shows the BW-1000 compressive strength data compared to literature. It was theorized that due to lack of compression testing experience, experimental conditions and methods may have contributed to scatter in the data. Initial tests at room temperature exhibited more scatter (Weibull modulus is 2) compared to tests at 650K taken at a later time (Weibull modulus is 12). Future studies could minimize this effect by using randomization in experimental design. Other potential reasons for large scatter in the compression test data, which have not been verified or dismissed, include but are not limited to:

- Machining flaws in the specimens
- Improper sample size (L/D ratio was originally specified as 2 and this was changed due to testing limitations to 3)
- Un-parallel sample faces resulting in un-even loading
- Mis-calibrated equipment resulting in un-even loading
- Improper load rate
- Improper experimental setup

- Lack of experience in testing dense ceramics in compression

More work is required to fully understand compression testing and the compressive strength of BeO.

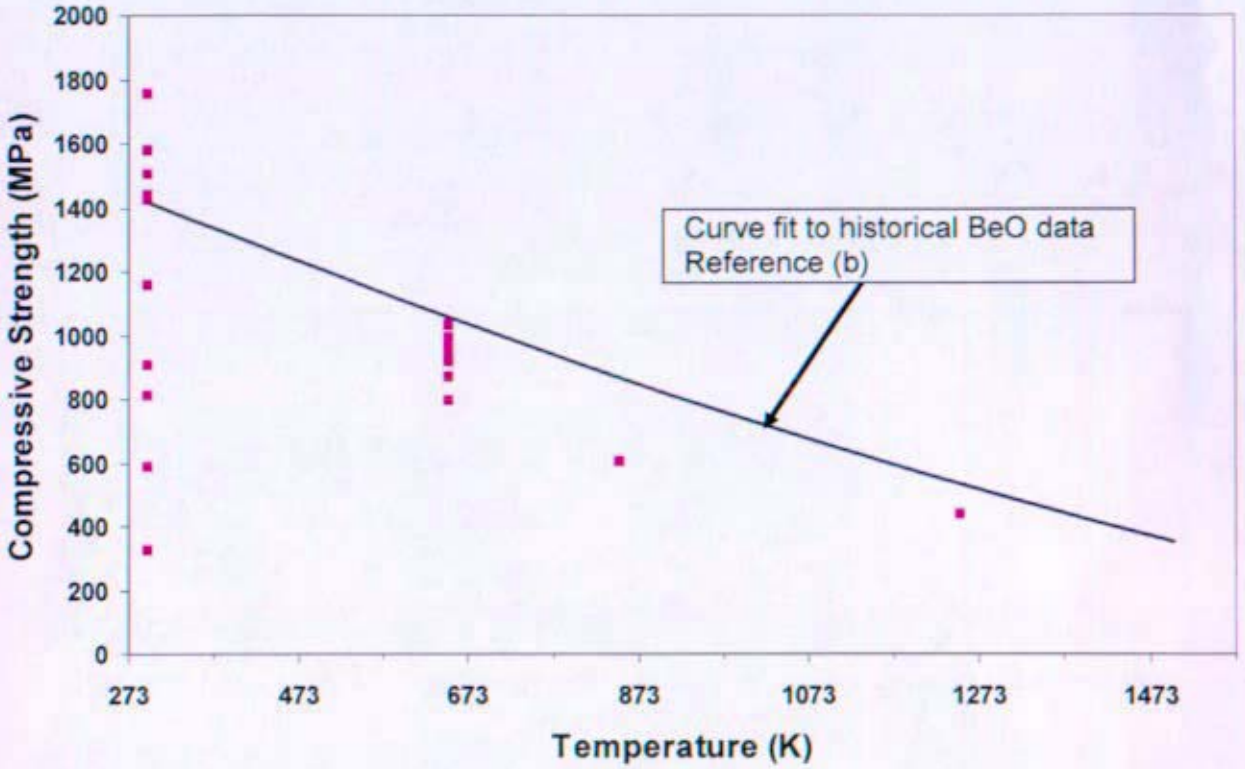

Figure 9: Comparison of BW-1000 BeO Compressive Strength Results and Curve Fit to Historical Data (Reference (b))

4. Conclusions

- Un-irradiated material properties of BeO have been largely characterized over the estimated operating range of a Prometheus type reactor.
- Density, specific heat and thermal conductivity of BW-1000 BeO, closely match the historical data.
- Mean CTE data for BW-1000 BeO differs slightly from the historical data.
- More work is required to determine the compressive strength of BeO.

5. References

(a) Halliday, D., R. Resnick and J. Walker, *Fundamentals of Physics Extended 5th Edition*. New York: John Wiley & Sons, Inc 1997.

(b) KAPL Letter MDO-723-0042, "Reflector and Shield Material Properties for Project Prometheus", dated November 2, 2005.

(c) KAPL Letter MDO-723-0032, "Transmittal of Final Vendor Report of Beryllium Oxide Grain Size Reduction Experiments and Material Property Testing", to be issued.

Enclosure 3 to MDO-723-0046/B-MT(SPME)-23

Assessment of Alumina, Spinel and Magnesia as Reflector Materials

Authors:
Laura L. Stimely
Vicente Munne

Reviewed by:
Wayne L. Ohlinger

This Page Intentionally Left Blank

1.0 Introduction

This enclosure provides technical information regarding the availability, physical properties and effectiveness of alumina, magnesia, and spinel as possible reflector materials.

1.1 Background

With Naval Reactors (NR) approval of the Naval Reactors Prime Contractor Team (NRPCT) recommendation to develop a gas cooled reactor directly coupled to a Brayton power conversion system as the Space Nuclear Power Plant (SNPP) for Project Prometheus (References (a) and (b)), alternative reflector materials have been proposed to eliminate the ES&H issues and associated costs related to manufacturing Be and BeO, the primary reflector material candidates (Reference (c)). Materials under consideration are alumina, magnesia, and spinel ($MgAl_2O_4$), all of which are non-moderating reflector materials. The alternative materials are about as effective because they do not moderate the neutron energy as strongly as the moderating beryllium reflectors. Moderation in the reflector causes an increase in the parasitic neutron absorption in structural materials having cross sections that increase as the neutron energies are lowered (e.g. rhenium) when the moderated neutrons return to the core, which in part negates the better reflecting properties of BeO. The alternative materials present a mass penalty relative to Be and BeO because their mass densities are higher. However, given their large manufacturing base, availability, lower cost, and non-hazardous nature, they present viable alternatives to Be and BeO.

1.2 Discussion

The main issues regarding potential reflector materials are their effectiveness as a reflector, density (mass), and irradiated material properties. Initially only BeO and beryllium metal were considered as reflector materials but calculations made on reflector effectiveness showed that alumina, magnesia and spinel could also potentially be used. These alternative reflector materials are not hazardous, and, therefore, do not share the ES&H, handling and processing issues associated with the beryllium materials. Moreover, these materials have a wider availability and vendor base. An initial assessment of the physical properties, neutronics, and vendor base of alumina, magnesia, and spinel is presented as a foundation for any future research. No experimental plans were developed or executed.

2.0 Alternate Reflector Materials

Beryllium (Be) and beryllia (BeO) are leading candidate reflector materials given their excellent neutronic properties (high atom density, high scattering and low absorption cross-sections, etc.) and low densities (Reference (d)). The use of Be and/or BeO is complicated by the difficulty in manufacturing components from these materials. Both materials have a sole source vendor leading to high cost and long lead times for manufacturing components. In addition, beryllium and beryllium compounds are hazardous substances requiring significant safeguards to avoid potential personnel health problems when handling powders or generating (e. g., in machining or grinding) particulate material. Given the above short-comings, lower-cost, readily-available alternative materials were considered for the reflector. Neutronic studies and other materials properties indicate that alumina (Al_2O_3), magnesia (MgO), and spinel ($MgAl_2O_4$) could be viable candidates pending satisfactory resolution of several issues including mass penalties, differences in neutronic characteristics, and a lack of irradiated materials data potentially impacting testing costs and the program schedule. Further

study of these non-moderating materials would be necessary before making a final decision for the reflector material.

Physical properties of the proposed reflector materials are listed below in Table 1 (Reference (e) unless otherwise noted). Unless otherwise noted, the values provided are at approximately 900K, the estimated working temperature for the reflector.

Table 1. Physical properties of proposed reflector materials (at approximately 900K unless otherwise noted)

		Be	BeO	Al_2O_3	MgO	$MgAl_2O_4$
Theoretical Density [b]	($g\ cm^{-3}$)	1.85	3.01	3.96	3.58	3.60
Thermal conductivity	($W\ m^{-1}\ K^{-1}$)	95 [a]	58.3 [b]	9.3 [b]	11.5 [c]	7.4 [b]
Coeff. of thermal expansion	($x10^{-6}\ K^{-1}$)	20.0	9.6	8	13	7.6 – 8.8
Tensile strength	(MPa)	150 [d]	124	285 – 550	105	83 – 220
Modulus of elasticity	(GPa)	287	300	390	250 – 300	240 – 260
Fracture toughness	($MPa\ m^{1/2}$)	9 – 13	3.68	2.0 – 3.0	1.3 – 2.0	1.9
Poisson's ratio		0.032	0.32	0.26	0.18	0.27
Knoop or Vickers hardness	(GPa)	5.5	11 – 13	18 - 23	5.5 – 6.0	8
Specific heat	($kJ\ kg^{-1}\ K^{-1}$)	2.92 [a]	1.9	1.2	1.25	1.2

[a] Reference (d) [b] Reference (f) [c] Reference (g) [d] vacuum hot-pressed block

2.1 Aluminum Oxide (Al_2O_3)

2.1.1 Physical Properties

See Table 1 (above).

2.1.2 Neutronics

Neutronic studies indicate that alumina is a viable candidate for a reflector material from the standpoint of the excess reactivity level that can be achieved. It has a relatively high neutron scattering cross-section and a relatively low neutron absorption cross-section. Questions regarding how well alumina will perform at elevated temperatures in long-term service and the radiation environment remain to be resolved.

BeO has a high atom density, high temperature capability, and along with its good moderating characteristics and (n,2n) reaction, it is considered to be the leading candidate and was used for the design of the reflectors in all of the core concepts studied. Mass penalties are a concern for all of the alternative reflector materials. Both the material density and reflector thickness will affect the total mass of the reflector. Figure 1 (Reference (c)) provides a comparison of each material's effectiveness as a function of its thickness for one of the notional reactor concepts studied by the NRPCT using axially translating reflector segments (sliders). The estimated thickness of the sliders for both beryllia

and alumina, minimizing mass, is 11cm. The estimated reactor mass penalty for alumina is approximately 8% relative to beryllia, or 2073kg versus 1923kg (Δ = 150kg). With this preconceptual reactor's material and geometric configuration, for reflectors of 11 to 13cm or more thickness, alumina, spinel, and magnesia are all equally or more effective than beryllia, and hold a significant advantage over beryllium. One of beryllium's distinct advantages is its relatively low density, making it the lowest mass option (~1792kg) (References (c) and (d)); however, its irradiation performance requires further evaluation. Cracking and breakage have been reported at fluences comparable to those estimated for the Prometheus reflector in applications such as the Advanced Test Reactor (ATR) reflector, albeit, at lower temperature (Reference (h)). Generally, differential swelling could be expected based on local variations in temperature and fluence (References (d) and (i)) for all candidate materials, potentially inducing substantial stresses in brittle materials (including embrittled Be). If breakage allowed relocation of the reflector material within canning, or loss of material if the reflector were not canned, the ability to accurately index the reflector position could be lost. This may be unacceptable for the pre-conceptual reactor concepts, where it is estimated that reflector position must be known and controlled to within less than one millimeter.

Figure 1. Reflector Effectiveness vs. Thickness for a Preconceptual Reactor Materials and Geometric Configuration

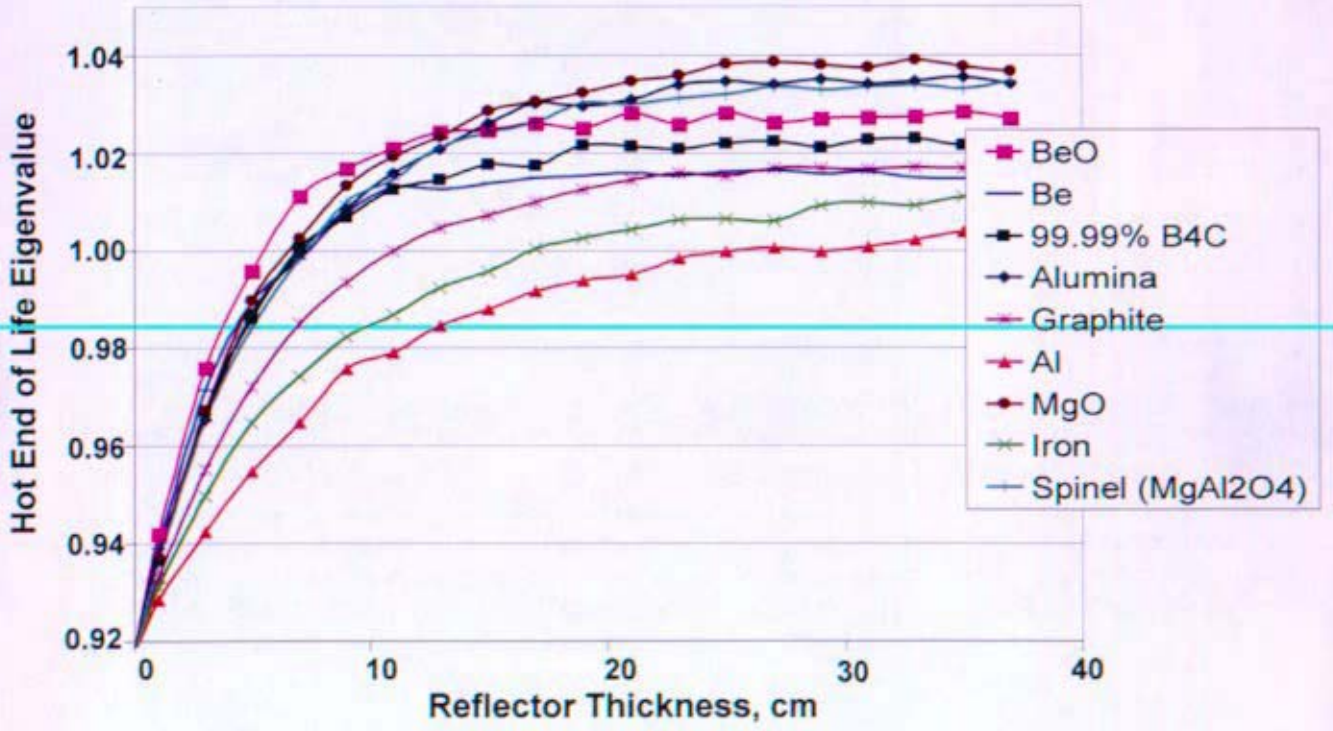

Alumina has been found to swell 1.2 – 3% under neutronic irradiation with fluences around 10^{22} n/cm^2 (References (j), (k), (l)). From preconceptual reactor design evaluations, it is anticipated that the reflector will experience a peak fluence of approximately 10^{21} n/cm^2 (E>1.0MeV) and therefore some swelling is to be expected. There is also some very minor anisotropic lattice expansion that would lead to internal stresses in the polycrystalline alumina. It is, however, inconsequential compared with the macroscopic swelling.

It has been well-documented that alumina experiences extensive grain boundary microcracking under high neutron irradiation (~10^{22} n/cm^2). (References (j), (k), (l)) One study observed extensive fracture in polycrystalline alumina samples exposed to doses above $3x10^{21}$ n/cm^2 but virtually no fracturing with doses less than $2x10^{21}$ n/cm^2. Young's modulus of polycrystalline alumina was reduced by 3% after irradiation to $3x10^{22}$ n/cm^2 at 350K. As the fluence and temperature go up, the study showed a shift from transgranular to intergranular fracture (Reference (m)). Testing would be required to understand how the microcracking will affect alumina's employment as a reflector material (Reference (n)).

2.1.3 Current Vendor Base

Alumina is the most widely used fine ceramic material. As such, alumina powders and finished products are available in a broad range of purities from multiple vendors including Coors, Alcoa, Vesuvius, and numerous others. Material quality for commercially available bulk powders is on the order of 99.9+%, with higher or lower qualities available as cost and application dictate. Alumina does not exhibit the toxicity concerns of BeO and is amenable to various standard manufacturing processes. The extensive commercial availability, vendor base, and lack of processing complication (toxicity) should lead to substantially lower final costs for alumina reflectors as compared with BeO. Those savings could, however, be overwhelmed by irradiated materials testing costs and program delays.

2.2 Magnesium Oxide (MgO)

2.2.1 Physical Properties

See Table 1 in Section 2.0 - Physical properties of proposed reflector materials.

2.2.2 Neutronics

No literature reports have been found on magnesia's properties and behavior under neutron irradiation at expected fluence values. See Figure 1 in Section 2.1.2 for a discussion of estimated reflector thickness requirements.

The mass penalty associated with use of magnesia versus beryllia is the least of the three alternative materials evaluated for one of the preconceptual reactor material and geometric configurations. The estimated penalty is approximately 4%, or 2006kg versus 1923kg (Δ = 83kg) (Reference (c)).

2.2.3 Current Vendor Base

Magnesia is a commonly used refractory material in the iron and steel industry. Thus, a vendor base exists, but the ability to readily obtain the extremely high quality material required for the reflector application must be verified. Martin Marietta Magnesia Specialties and Rohm & Haas both provide high purity magnesium oxide powders for technical refractories applications. New Castle Refractories, Vesuvius, ANH Refractories, and Refco, Inc. all manufacture magnesia based refractory shapes.

It should also be noted that magnesia, in common with other alkaline earth oxides (CaO, SrO and BaO) is prone to formation of a stable hydroxide on exposure to typical ambient humidity levels. It is

assumed that some degree of caution would need to be exercised in processing, fabrication and handling to avoid problems. Detailed understanding of the severity of this problem requires further evaluation. There is also an overwhelming lack of irradiated materials data that would lead to costly testing and program delays.

2.3 Spinel ($MgAl_2O_4$)

2.3.1 Physical Properties

See Table 1 in Section 2.0 - Physical properties of proposed reflector materials.

2.3.2 Neutronics

Spinel exhibits exceptional stability under irradiation at elevated temperatures. Little to no damage in the form of volumetric swelling, thermal conductivity changes, and visible defects have been observed for fluence values up to 10^{22} n/cm^2 in the temperature range of interest. Defects recombine easily during irradiation at elevated temperature, leading to essentially constant structural properties even at very high fluences. Spinel retains structural properties better than any other reflector material considered for the combination of fluence and temperature envisioned during service (References (o) and (p)).

The mass penalty associated with use of spinel versus beryllia is intermediate between magnesia and alumina for the preconceptual reactor material and geometric configuration evaluated. The estimated penalty is approximately 5%, or 2025kg versus 1923kg (Δ = 102kg) (Reference (c)).

2.3.3 Current Vendor Base

Spinel powders and finished products are available in a range of stoichiometries from multiple vendors including Coors, Linde, Ceradyne, and numerous others. Material quality for commercially available bulk powders is on the order of 99.9+%, with higher or lower qualities available as cost and application dictate. Spinel does not exhibit the toxicity concerns of BeO and is amenable to standard ceramic manufacturing processes. The greater commercial availability, vendor base, and lack of processing complexity (toxicity) should lead to substantially lower final costs for spinel reflectors as compared with BeO. As with the other alternatives, these savings could, however, be overwhelmed by irradiated materials testing costs and program delays.

3.0 Conclusions

A discussion of the potential merits of alumina, magnesia, and spinel as reflector materials was presented identifying these materials as viable alternatives to beryllium and beryllium oxide and worthy of in-depth evaluation. Basic materials properties and availability were discussed and compared with the BeO and beryllium metal properties. While use of any of the three alternative materials will likely incur a mass penalty relative to either Be or BeO, the tradeoff of ~85 to 150kg mass (relative to BeO) for elimination of ES&H concerns in fabrication and processing, as well as possible inadvertent reentry concerns, reduced cost and ready availability from numerous vendors is potentially attractive.

4.0 References

a. NR Letter I#05-01228, "Space Nuclear Power - Reactor Coolant and Power Conversion System Concept - Approval Of, "dated April 20, 2005
b. Bettis Letter B-SE-0077/KAPL Letter SPP-67110-0005, "Space Nuclear Power Plant Concept Selection, For NR Approval," dated March 4, 2005
c. NRPCT Letter SPP-67410-0013/B-SE(RE)-0003, "Project Prometheus Space Reactor Pre-conceptual Design Report," January 27, 2006.
d. KAPL Letter MDO-723-0042, "Reflector and Shield Material Properties for Project Prometheus", dated November 2, 2005.
e. Metals Handbook Desk Edition, ASM, 1985.
f. Touloukian, Y. *et al.*, Thermal Conductivity, Thermophysical Properties of Matter, Volume 1, IFI/Plenum, New York, 1970
g. Smithells, C. J. and Brandes, E. A., Metals Reference Book, 5th Ed., Butterworths, Woburn MA, 1976.
h. Beeston, J. M., "Properties of Irradiatied Beryllium – Statistical Evaluation," Idaho National Engineering Laboratory, Report TREE-1063, EG&G Idaho, Inc., October 1976.
i. Bettis Letter B-SE(RE)THD-0007, "Pressure Vessel and Reflector Temperature Sensitivity Studies," dated October 31, 2005.
j. Wu, W. Y., Chin, B. A., and Zee, R. H., "Radiation induced mechanical stresses in polycrystalline alumina insulators," 16th Radiation Symposium.
k. Yano, T., "Neutron irradiated damage in aluminum oxide and aluminum nitride ceramics up to very high fluences," Bull. Res. Lab. Nuclear Reactor, Vol. 25, 2001, p. 95-96.
l. Youngman, R. A. et al., "High dose neutron irradiation damage in alpha alumina," J. of Materials Research, Vol. 6, No. 10, Oct 1991, p. 2178-2187.
m. Pells, G. P., "Radiation damage effects in alumina," J. American Ceramic Society, Vol. 77 [2], 1994, p. 368-77.
n. Keilholtz, G. W. and Moore, R. E., "Irradiation damage to aluminum oxide exposed to $5x10^{21}$ fast neutrons/cm^2," Nuclear Applications Vol. 3 November 1967, p. 686-691.
o. Li, Z. et. al., "Elastic stability of high dose neutron irradiated spinel," J. of Nuclear Materials 219 (1995), p. 139-142.
p. Yano, T., "Effects of neutron irradiation on the mechanical properties of magnesium aluminate spinel single crystals and polycrystals," J. American Ceramic Society, Vol. 82 [12], 1999, p. 3355-65.

Enclosure (4) to
MDO-723-0046/
B-MT(SPME)-23

Enclosure 4 to MDO-723-0046/B-MT(SPME)-23:

Annotated Bibliography

Authors:
James Nash

Reviewed by:
Beth Lugert
Barri Gurau

1.0 Beryllium (Be)

Author: Billone, M.
Title: Recommended Design Correlations for S-65 Beryllium
Reference: Proceedings 2nd IEA International Workshop on Beryllium Technology for Fusion pp 348-363
Date: September 6-8, 1995
Key Words: Beryllium, Be, material properties, irradiation swelling

Summary

This paper focuses on the use of beryllium (Be) as a plasma-facing component (PFC) material. However, the correlations presented can also be used to describe the performance of Be in other radiation environments. Correlations are provided for S-65 grade Be (Brush Wellman). The properties for Be are divided into two categories: properties which do not change when the bulk of the material has radiation damage; properties which are degraded by neutron irradiation. Irradiation independent properties include specific heat, thermal expansion and elastic constants. Irradiation dependent properties include thermal conductivity, yield strength, ultimate tensile strength, tensile elongation, creep strength and swelling.

Author: Chaouadi, R., F. Moons and J.L. Puzzolante
Title: Tensile and Fracture Toughness Test Results of Neutron Irradiated Beryllium
Reference: Proceedings 3rd IEA International Workshop on Beryllium Technology for Fusion pp 241-253
Date: October 22-24, 1997
Key Words: Beryllium, Be, tensile properties, fracture toughness, neutron irradiation, Brush Wellman, S-65, S-65H, S-200, S-200FH

Summary

Report of tensile and fracture toughness test results for 4 grades of Be (S-65, S-65H, S-200F and S-200FH). Specimens were irradiated in the BR2 material test reactor at fluences ranging from $0.65 - 2.45 \times 10^{21}$ n/cm^2 (E>1 MeV) and temperatures ranging from 458 – 878K. Unirradiated specimens were thermally aged to determine possible thermal effects on material properties. It was reported that the tensile properties of different grades of Be behave similarly under irradiation conditions. In general, irradiation strengthened the material and resulted in a loss of ductility and decrease of fracture toughness. Beryllium test specimen geometries and test methods were also discussed.

Author: Dalle Donne, M., F. Scaffidi-Argentina, C. Ferrero and C. Ronchi
Title: Modeling of Swelling and Tritium Release in Irradiated Beryllium
Reference: Journal of Nuclear Materials Volume 212-215 pp 954-960
Date: 1994
Key Words: Beryllium, Be, irradiation swelling, ANFIBE, helium generation, tritium release

Summary

This paper reviews important effects of neutron irradiation on Be including swelling, embrittlement and tritium retention. A computer code was developed capable of describing the helium and tritium behavior in Be. The resulting code, ANFIBE (ANalysis of Fusion Irradiated BEryllium), is a modification to an existing code available for the modeling of fission gas behavior in UO_2 irradiated in fission reactors. ANFIBE allows the calculation of gas distribution, induced swelling and helium and tritium release from Be. Good agreement between the ANFIBE

code and experimental data are given in addition to volumetric swelling curves for Be irradiated to various fluences at various temperatures.

Author: Dombrowski, D.E., E. Deksnis and M.A. Pick
Title: Thermomechanical Properties of Beryllium
Reference: Brush Wellman Report TR-1182
Date: 1995
Key Words: Beryllium, Be, Brush Wellman, material properties, S-65, S-200F, S-65H, S-200FH, Be powder metallurgy

Summary

This review summarizes many properties of beryllium (physical, thermal and mechanical) at temperatures of interest to its application as a plasma-facing component. The different grades of Be are examined and a description of the powder metallurgy associated with Be processing is given. The majority of the properties and data reported are for unirradiated Be grades. These properties include specific heat, density, viscosity, vapor pressure, thermal conductivity, thermal expansion, electrical resistivity, elastic modulus, Poisson's ratio, ultimate tensile strength, yield strength, elongation, reduction in area, creep, fatigue and fracture toughness. A summary is included which outlines gaps in the unirradiated and irradiated property data and future needs for Be use in nuclear applications. Safety and handling experience associated with Be is also *included with airborne and surface contamination limits.*

Author: Gelles, D.S., G.A. Sernyaev, M. Dalle Donne and H. Kawamura
Title: Radiation Effects in Beryllium Used for Plasma Protection
Reference: Journal of Nuclear Materials Volume 212-215 pp 29-38
Date: 1994
Key Words: Beryllium, Be, irradiation swelling, compressive yield strength

Summary

This document is a review of the literature on Be, with emphasis on the effects of irradiation on the material properties. Neutron irradiation swelling and embrittlement experiments are described as a function of temperature, fluence and neutron spectrum. These experiments are quantified where possible. Data and correlations are given for neutron irradiation swelling of Be. Some mechanical properties (hardness and compressive yield strength) are also discussed for various neutron irradiation conditions. Additionally, the effects of impurity content are reported, from which optimum composition specifications can be defined.

Author: Hickman, B.S
Title: Radiation Effects in Beryllium and Beryllium Oxide
Reference: Studies in Radiation Effects, Series A Physical and Chemical Volume 1
Date: 1966
Key Words: Beryllium, Be, irradiation swelling, helium, tritium, mechanical properties

Summary

This source provides a general discussion of Be and the effect of irradiation on the material. Irradiation swelling and the effect of irradiation on mechanical properties are discussed. Computed helium and tritium quantities are given for various doses. The nucleation and growth of the helium bubbles are also discussed in reference to swelling. Predicted swelling curves versus helium bubble diameter are calculated at 873K. A summary of available irradiation data is also included for various fluences and temperatures.

Author: Moons, F.
Title: Beryllium Characterization: Tensile Tests on Neutron Irradiated and Reference Beryllium
Reference: SCK CEN Progress Report FT/Mol/96-03 ITER Task 23 – OSTI ID 615166
Date: 1996
Key Words: Beryllium, Be, neutron irradiation, tensile properties
Summary
This report is a study of the irradiation embrittlement characteristics of Be grades manufactured by Brush Wellman (S-65, S-65H, S-200F and S-200FH). Three batches of Be were tested: a neutron irradiated group, a thermal control group and a reference group. Testing of the Be specimens consisted of swelling determination by immersion density, tensile testing, fracture toughness, helium and tritium analysis and microstructural examinations. Test procedures and specimen drawings are included with the raw data.

Author: Scaffidi-Argentina, F., G.R. Longhurst, V. Shestakov and H. Kawamura
Title: Beryllium R&D for Fusion Applications
Reference: Fusion Engineering and Design Volume 51-52 pp 23-41
Date: 2000
Key Words: Beryllium, Be, thermal properties, mechanical properties, irradiation swelling, design correlations
Summary
This paper represents a database of unirradiated material property correlations for Be in both plasma facing material and neutron multiplication for fusion applications. Thermal and physical properties discussed include: density, vapor pressure, specific heat, thermal conductivity and thermal expansion. Mechanical properties discussed include elastic modulus, yield strength and ultimate tensile strength. Limited creep data is also included. Neutron irradiation swelling is discussed in addition to helium and tritium generation. The correlations given are fits to the data referenced and in many cases the actual data is not given. However, this source does provide a good overview of unirradiated Be properties and the effects of irradiation on Be.

Author: Snead, L.L. and A.T. Nelson
Title: Candidate Materials for Space Reactor Shielding Applications
Reference: ORNL/LTR/NR-PROM 1/05-15
Date: July 2005
Key Words: Beryllium, Be, material properties, irradiation swelling
Summary
This is a comprehensive summary report for beryllium containing materials and their use in nuclear applications. This report includes a summary of Be processing (vacuum hot pressed and hot isostatic pressed grades) and the current Be commercial infrastructure. Mechanical and thermal properties, both unirradiated and irradiated, are reported for Be with emphasis on the low ductility resulting from irradiation. Design conclusions for Be are included for various irradiation conditions. Additionally, there is a discussion of Be safety and a comparison of modern grades of Be to historical grades and the difference in impurity content.

2.0 Beryllium Oxide (BeO)

Author: Busboom, H.
Title: Material Properties for Beryllium Oxide (BeO)
Reference: GE Specification 23A3186
Date: 1989
Key Words: Beryllium Oxide, BeO, beryllia, material properties, irradiation swelling, SP-100
Summary
BeO was considered as a potential reflector material at the high temperatures envisioned for SP-100 design. This document represents a compilation of material properties for BeO including general information, physical, mechanical and thermal properties. Design curves are given for unirradiated BeO. Much of the data used to generate the equations was obtained from the Thermophysical Propeties of Matter series. Additionally, radiation induced swelling of BeO is summarized with a set of equations. Overall, there is little discussion of the data used and the primary focus of the document is to provide recommended equations for various material properties.

Author: Collins, G.
Title: Radiation Effects in BeO
Reference: Journal of Nuclear Materials, Volume 14 pp 69-86
Date: 1964
Key Words: Beryllium Oxide, BeO, beryllia, irradiation swelling, grain size, helium bubble
Summary
Irradiation swelling data of BeO for neutron irradiation dosages up to 1.5×10^{21} n/cm^2 (E≥1 MeV) is reported at temperatures from 100° - 1200°C. BeO of various grain sizes (5-100 μm) and grades (AOX and UOX grade BeO powder) were used in the experiments. Maximum swelling observed was approximately 6%. The data presented represents a large portion of the swelling data available and is the basis for swelling correlations. A detailed discussion of the kinetics of volume expansion in BeO is included. Additionally, there are limited discussions on the effect of irradiation on other material properties including thermal expansion, elastic constants and strength.

Author: Gurau, B.
Title: Trip Report – Brush Ceramic Products, Discuss Possible Sample Fabrication to Support Irradiation Testing
Reference: KAPL Letter SM-7232-0003
Date: June 2005
Key Words: Beryllium Oxide, BeO, beryllia, Brush Ceramic Products, Brush Wellman, ESH
Summary
This trip report provides a summary of the Be/BeO health and safety controls in place at Brush Ceramic Products (BCP). It includes OSHA, DOE and Brush Wellman airborne control limits for Be/BeO particulate. Additionally, there is a discussion about Brush Wellman and Brush Ceramics. BCP's two main grades of BeO (Thermalox 995 and BW-1000) are described with respect to grain size and processing methods and limitations. Plans for fabricating the JOYO test specimens were included along with other processing ideas to reduce the grain size of the BeO (i.e. HIP'ing and rate controlled sintering).

Author: Hickman, B.S.
Title: Radiation Effects in Beryllium and Beryllium Oxide
Reference: Studies in Radiation Effects, Series A Physical and Chemical Volume 1
Date: 1966
Key Words: Beryllium Oxide, BeO, beryllia, material properties, irradiation swelling, thermal conductivity

Summary

This source provides a general discussion of BeO and the effect of irradiation on the material. This includes a summary of low temperature (373K) irradiation thermal conductivity studies and predictions for high temperature irradiations (673 – 1073K). High temperature thermal conductivity predictions are reported with reference to the onset of microcracking in the material. Irradiation swelling of BeO is examined and Hickman presents an alternate kinetic rate equation similar to Collins (1964). Prediction curves for swelling at 373 – 1073K are provided for a range of flux and fluence conditions including a discussion of defects and defect structure.

Author: Hickman, B.S. and A.W. Pryor
Title: The Effect of Neutron Irradiation on Beryllium Oxide
Reference: Journal of Nuclear Materials, Volume 14 pp 96-110
Date: 1964
Key Words: Beryllium Oxide, BeO, beryllia, defect structure, thermal conductivity, irradiation swelling

Summary

Neutron irradiation test results are reported to doses of 1.4×10^{21} n/cm^2 (E>1MeV) at temperatures 348 – 973K for polycrystalline BeO. Various processing methods were used (hot pressing and cold pressing) to produce a range of grain sizes and densities. Information on the defect structure of BeO is reviewed and related to the observed property changes. Irradiation induced cracking and powdering of BeO due to irradiation is reviewed and related to the grain size of the starting material. Irradiation swelling is examined and an alternate kinetic rate equation is presented, similar to Collins (1964). Predictions for irradiation swelling and irradiated thermal conductivity of BeO are also included.

Author: Keilholtz, G.W., J.E. Lee Jr. and R.E. Moore
Title: Irradiation Damage to Sintered Beryllium Oxide as a Function of Fast-Neutron Dose and Flux at 110, 650 and 1100°C
Reference: Nuclear Science and Engineering Volume 26 pp 329-338
Date: 1966
Key Words: Beryllium Oxide, BeO, beryllia, irradiation swelling, microcracking, powdering

Summary

This is a summary of an irradiation test program for BeO with a primary objective of establishing the limits of stability of sintered BeO of various grain sizes and densities toward fast neutrons and determination of the mechanisms of damage. Specimens were irradiated at 383, 923 and 1373K to fast neutron doses up to 4.7×10^{21} n/cm^2 (E>1 MeV). Both long and short term irradiations were performed to determine the effect of flux on irradiation damage (i.e. swelling). BeO specimens had varying densities (2.7 – 2.95 g/cm^3) and grain sizes (17 – 74μm). A summary of the gross damage to BeO specimens irradiated at various temperatures, fluxes and fluences is included and identifies fracturing and powdering limits of the samples tested.

Author: Nash, J. M. and R. Lewis
Title: Beryllium Oxide and Beryllium Irradiation Data and JOYO Reflector Material Test Plan Summary (U), For Information
Reference: KAPL Letter SM-7231-0009
Date: 2005
Key Words: Beryllium Oxide, BeO, beryllia, thermal conductivity, compressive strength, irradiation swelling, JOYO, Beryllium, Be

Summary

This document presents information on past irradiation testing of BeO and the planned testing of BeO in the JOYO test reactor. The JOYO test matrix is included for the BeO specimens. Samples were selected to test irradiation swelling, thermal conductivity and compressive strength. A brief discussion is included on each of the parameters that effect irradiation swelling (grain size, temperature, fluence, flux and theoretical density). Predicted irradiation swelling curves for the JOYO BeO specimens and the predicted Prometheus operating conditions are given in relation to the existing data. Additionally, there is a brief discussion of beryllium (Be) and the existing irradiated material database.

Author: Nash, J. M.
Title: Trip Report – Brush Ceramic Products, Discuss Cleaning, Handling and Packaging Procedures for BeO Specimens
Reference: KAPL Letter SM-7232-0004
Date: 2005
Key Words: Beryllium Oxide, BeO, beryllia, Brush Ceramic Products, Brush Wellman, ESH, JOYO

Summary

This trip report to Brush Ceramic Products (BCP) summarizes the post machining process for samples planned for irradiation in the JOYO test reactor (i.e. cleaning, bakeout, contamination testing and packaging). Handling concerns of BeO specimens at Naval Reactors Prime Contractor Team (NRPCT) facilities resulted in a detailed plan for the cleaning and packaging of BeO specimens at BCP prior to shipment. Surface contamination limits from DOE and KAPL were discussed. The NRPCT identified a loose BeO surface contamination limit of 0.25 $\mu g/100cm^2$. Both wet and dry swipe testing were discussed as a method of detecting loose BeO contamination.

Author: Paxton, D. M.
Title: Irradiation and Examination of Beryllium Oxide Pellets from the SP-100 Special Purpose Materials Test
Reference: WHC-SP-1007
Date: 1993
Key Words: Beryllium Oxide, BeO, beryllia, SPM test, SP-100, neutron irradiation

Summary

Multiple types of specimens were irradiated as part of the Special Purpose Materials (SPM) test in the Experimental Breeder Reactor-II (EBR-II) to obtain the irradiation effects on materials in support of the design of SP-100 components. As part of the SPM test, BeO pellets were irradiated at low ($0.8x10^{22}$ n/cm^2) and high ($6.0x10^{22}$ n/cm^2) fluence. Irradiation temperatures ranged from 1200 to 1800K and a total of 40 BeO specimens were irradiated. Two densities of BeO pellets were tested, 85% and 95% theoretical density. However, irradiated data was limited

due to the fact that only 4 of the BeO pellets designated for post irradiation examination were recovered from the sample holders.

Author: Plumlee, E
Title: BeO Performance Lessons Learned, SP-100 Program
Reference: Martin Marietta Report DOE/SF/16006-T1216
Date: 1994
Key Words: Beryllium Oxide, BeO, beryllia, irradiation swelling, swelling correlation, SPM test, SP-100

Summary

This report documents what were considered the major lessons learned with respect to BeO performance during the SP-100 program. Lessons learned included BeO performance data established in previous literature and new data generated as part of the SP-100 program. The general irradiation behavior of BeO is summarized with reference to prior testing. Correlations are included to predict the irradiation swelling of BeO based on temperature, flux and fluence. These correlations are somewhat limited in that they are based on data covering a narrow range of fluxes and fluences at limited temperatures (373, 873 and 1273K). The data generated from the Special Purpose Materials (SPM) test and future test data requirements are summarized (only four of the irradiated BeO specimens were recovered).

Author: Snead, L.L. and A.T. Nelson
Title: Candidate Materials for Space Reactor Shielding Applications
Reference: ORNL/LTR/NR-PROM 1/05-15
Date: July 2005
Key Words: Beryllium Oxide, BeO, beryllia, material properties, processing

Summary

A comprehensive summary report for beryllium containing materials and their use in nuclear applications. This report includes a summary of BeO processing and the current BeO commercial infrastructure. Mechanical and thermal properties, both unirradiated and irradiated, are reported for BeO. Design conclusions for BeO are included for various irradiation conditions and identify that complete material property test data is required for BeO irradiated $>1x10^{20}$ n/cm^2 (E>0.1 MeV).

Distribution to
MDO-723-0046
B-MT(SPME)-23

CONCURRENCE/DESIGN CHECK FORM FOR DOCUMENT NO. MDO-723-0046 B-MT(SPME)-23 **Date:** 1/31/06

DOCUMENT TITLE: Space Reflector Materials for a Prometheus Application

REFERENCES MDO-723-0042
B-SE(RE)-0003/SPP-67410-0013

ENCLOSURES: (1) Beryllium (Be)
(2) Beryllium Oxide (BeO)
(3) Assessment of Alumina, Spinel and Magnesia as Reflector Materials
(4) Annotated Bibliography

1. ADSARS: PERMANENT RECORD: Yes X No ___ Repository MFLIB Corporate Author: KAPL NR PROGRAM 08S

Key Words:	Reflector	Prometheus	Be	BeO	Al_2O_3	MgO		
Need to Know Categories	REP							
Available Sites:	PRNR							
Design File Location(s)								

2. DESIGN CHECK

Type of Check	Signature(s)	Comments: (Including Reference to Check Document If Appropriate)
A. No check considered necessary		
B. Check vs. previous results/issues		
C. Checked calculations made	for Barri Guram per telecon 1/26/06	BSG for cover letter, Enc. 1, 2, Att. A-E
D. Checked computer input and/or output		
E. Computer Programs approved/qualified		
F. Performed independent audit		
G. Spot checked significant points	for Barri Guram per telecon 1/26/06	BSG for cover letter, Enc. 1, 2, Att. A-E
H. Reviewed methods used		
I. Reviewed results for reasonableness	for Barri Guram per telecon 1/26/06	BSG for cover letter, Enc. 1, 2, Att. A-E
J. Comparison with test data		
K. Reviewed vs. drawings		
L. Verified procedures		
M. Technical content reviewed	for Barri Guram per telecon 1/26/06	BSG for cover letter, Enc. 1, 2, Att. A-E
N. Management verification of adequate review by others	B Clayton	W. Ohlinger primary reviewer for Enc 3
O. Performed Lessons Learned Search		
P. Used Measurement Uncertainty Methods		
Q. Other Checks (Describe)		

3. CONCURRENCE REQUIREMENTS: Indicate signatures required by X:

W. Ohlinger	ARP MANAGER		NCSG		FLUID DYNAM
	NUCLEAR ENGINEERING		ADVANCED CONCEPTS		STRUC. ENGRG
	REACTOR TH/MECH DESIGN		NOISE & ELEC. TECH.		DRAFTING
	REACTOR EQUIPMENT		SHIELDING		QA
	POWER PLANT MECHANICAL		REACTOR SAFETY		OTHER
	POWER PLANT ELECTRICAL		TO	X B Campbell for	BETTIS J. Hoch per telecon
	FINANCE		RSO		BPMI
	NEW SHIP PROGRAMS		FSO	X D Gill 1/31/06	ADMIN REVIEW
	PROGRAM COORDINATION		MDO		

Cognizant Manager _____
(Must Be Subsection or Higher for External Letters)

4. AUTHORIZED CLASSIFIER: Reviewed By: B. Campbell B Campbell CLASSIFICATION: UNCL

5. RELATED SUBJECTS:

UTRS Implication (Y/N)	N	Commitment Made (Y/N)	N	Commitment Complete (Y/N)	N
Safety Council Review (Y/N)	N	Design Basis Info. (Y/N)	N	UTRS Doc. #	
		Design Review (Y/N)	N		

6. Distribution:

NR

DI Curtis, 08S, For NR Information
JD Yoxtheimer, 08S/8034
JP Mosquera, 08C/8017
ST Bell, O8I/8024
CH Oosterman, 08C/8017

PNR

JF Koury**
JA Andes**

SNR

D Potts, 065
D Clapper, 065
GM Millis, 065
H Miller, 065

BETTIS

J Bowman**
C Eshelman**
JE Hack**
W Ohlinger**
V Munne**
L Stimely**
R Baranwal**

KAPL

SA Simonson**
J Ashcroft**
BC Campbell, 092
W Gideon**
DF McCoy**
JM Nash, 092
M Trbovich**
J Witter**
H Schwartzman**
D Hjelmar**
S Samuell**
D Poeth**
PF Baldasaro**
MJ Wollman**
G Newsome**
Y Ballout**
L Kolaya**
R Najafabadi**
G Dansfield**
R Grossman**
SM File
ADSARS

**Electronic Copy Only